

HARMFUL ALGAL BLOOMS IN THE  
GULF OF MEXICO:  
BREVETOXIN DEGRADATION AND DERIVATIVE  
FORMATION VIA PHOTOCHEMICAL PROCESSES

Ron C. Hardman

A Thesis Submitted to the  
University of North Carolina at Wilmington in Partial Fulfillment  
of the Requirements for the Degree of  
Master of Science in Marine Science

Center for Marine Science Research  
University of North Carolina at Wilmington  
2002

Approved By

Advisory Committee

Dr. Jeff Wright    Dr. William Cooper

Dr. Daniel Baden  
Chair

Accepted By

---

Dean, Graduate School

## TABLE OF CONTENTS

TABLE OF CONTENTS.....	III
ABSTRACT.....	V
ACKNOWLEDGEMENTS.....	VI
DEDICATION.....	VII
LIST OF TABLES.....	VIII
LIST OF FIGURES.....	IX
LIST OF ABBREVIATIONS.....	X
INTRODUCTION.....	1
Background on Harmful Algal Blooms.....	1
Research Overview.....	3
History of Gulf of Mexico HAB's.....	5
Bloom Dynamics in the Gulf of Mexico.....	6
Nutrients.....	8
Non-Regional Brevetoxin Related Blooms.....	9
HAB Management.....	10
Summary.....	12
BREVETOXIN AND PHARMACOLOGICAL ACTIVITY.....	13
Chemistry.....	13
Physiological Effects.....	18
Therapeutics.....	20
EXPRIMENTAL OVERVIEW.....	21
Background.....	21
Sea Surface Microlayer (SSML).....	22
Photochemical Processes.....	23
MATERIALS AND METHODS.....	24
Chemicals.....	24
Equipment.....	24
Toxin purification.....	25
Samples.....	25
Experimental Design.....	26
Procedure.....	27
PRELIMINARY WORK AND RESULTS.....	28
RESULTS.....	29
Overview of Findings.....	29
By-Product Formation.....	30
Quantification Overview.....	36

Quantification of By-Product Formation .....	38
Quantification of PbTx2 Degradation .....	41
By-Product Characterization .....	50
Analysis of HPLC-MS Peak Ions .....	51
Characterization of Peaks 8, 9 and 10 .....	57
Characterization of Peak 5 .....	63
Characterization of Peak 11 .....	64
Characterization Summary .....	66
PbTx2 Recovery .....	68
PbTx2 Spike Purity .....	69
DISCUSSION .....	74
Temperature Effects .....	74
Mass Balance .....	74
Theoretical Considerations .....	75
<i>K. brevis</i> Production- Polyketide Synthesis of Brevetoxins .....	75
Metabolites .....	79
Photochemistry .....	79
The Environment .....	83
Aerosolized Brevetoxin .....	84
Caveats and Recommendations .....	84
Sea Surface Microlayer .....	85
CONCLUSION .....	86
REFERENCES .....	89

## ABSTRACT

Harmful algal blooms (HAB's) of the dinoflagellate *Karenia brevis* (*Gymnodinium breve*) are recurring events in the Gulf of Mexico (GOM) which have significant adverse human health, environmental and economic impacts. Brevetoxins (PbTx), produced by *K. brevis*, are potent neurotoxins and during HAB events are responsible for mass morbidity and mortality in fish, birds and marine mammals and the causative agent(s) of Neurotoxic Shellfish Poisoning (NSP) in humans. Brevetoxin exposure (inhalation or oral) results in systemic distribution of the toxin to all bodily tissues with a variety pathophysiological sequelae. Current evidence suggests that, in addition to the known acute toxicological effects on cardiovascular, neuromuscular, and respiratory systems, chronic brevetoxin exposure may result in immunosuppression and toxicity to the hemopoietic and thermoregulatory systems. Brevetoxin (PbTx1) has recently been shown to be teratogenic in fish embryo studies.

While acute effects of brevetoxin exposures have been studied over the last two decades, far less is known about the effects of chronic/repeated brevetoxin exposure on humans and marine wildlife and little is understood about the transport and fate of brevetoxins in the environment (water, air, sediments, and selected biota). In order to apply effective risk assessment and develop accurate and reliable detection methodologies, greater knowledge of the transport and fate of brevetoxins in the environment are needed. These findings suggest solar radiation plays a significant role in the mediation of brevetoxin (PbTx2) degradation and brevetoxin derivative formation. Hence, it suggested that photochemistry may play a critical role in the transport and fate of brevetoxin(s) in the environment.

## ACKNOWLEDGEMENTS

Certainly I must acknowledge the help of my graduate committee, thanks to Dan Baden, Bill Cooper and Jeff Wright for their knowledgeable input. In addition, I would like to extend a thanks to the professors who I have had the opportunity to study under here in the Marine Science program at the University of North Carolina at Wilmington (UNCW), the Center for Marine Science Research (CMSR) and the Bermuda Biological Station for Research (BBSR). I have to say it has been a thoroughly enjoyable and educational experience, so thanks to Joan Wiley, Jack Manock, Lewis Abrams, Nancy Grindlay, Carmelo Tomas, Larry Cahoon and Don Olson out of the University of Miami. Additional thanks to Paul Hosier and Bill Cleary, Peter Wells of Environment Canada, Richard Owen and Megan at BBSR, Michael Depledge of the University of Plymouth, James Butler of Harvard University and Eric Dewailly of Laval University, Québec.

I must also thank everyone in the HABLAB for their assistance and camaraderie. Additionally, I cannot go without extending a warm thanks to my friends here in the Oceans and Human Health program, those who have made this sojourn a fine one, so warm thanks' and thoughts to them and my Bermudan comrades; Mark Taylor, Jake Asher, Michelle Gomperts, Eszter Gulácsy, Tara MacPherson, Megen Miller, Bob Golembeski, Thomas Molesky, Suzanne Sexton, Ashley Skeen, Jed Smith, Bryan Bishop, Kevin Yates, Matt Head, Shauna Slingsby and Susie Holzt.

Lastly, a tip of the hat to the Swizzle Inn and White Horse in the Queen's country, where stresses were allayed and enjoyments had, to the fine men and women of those establishments, for their song and for their merriment. To the Piper Maru and Pappa Pinky and that fine captain of the Weatherbird, Rob Chadwell.

## DEDICATION

I would like to dedicate this work to Deborah Triplett, who, through her unbridled support and giving made graduate school possible.

## LIST OF TABLES

Table 1: EC50's In Receptor Binding Protocols for Brevetoxins.....	17
Table 2: By-Product Formation .....	43
Table 3: Average By-Product Formation and PbTx2 Degradation.....	44
Table 4: Average PbTx2 Reduction.....	49
Table 5: HPLC-MS Results for Six By-Products .....	56
Table 6: Summary Characterization Data For Each Isolate.....	67
Table 7: Spiking Solution Check: .....	72
Table 8: Electromagnetic Spectrum Measurements.....	81

## LIST OF FIGURES

Figure 1: Brevetoxins.....	15
Figure 2: Chromatograms - Effects of Solar Radiation on PbTx2 By-Product Formation.....	31
Figure 3: Chromatograms - PbTx2 Spiked Samples Subjected to Dark Conditions .....	32
Figure 4: Chromatogram - Solar Radiation vs. Dark Conditions.....	33
Figure 5: Chromatograms - Control and PbTx2 Spiked Samples.....	35
Figure 6: PbTx Standards and By-Products Formed .....	37
Figure 7: Chromatograms – By-Product Peak Identification.....	39
Figure 8: Chromatogram –8hr Exposures.....	40
Figure 9: Charting of PbTx2 Profile Changes (24hr Exposures).....	42
Figure 10: PbTx2 Degradation.....	45
Figure 11: PbTx2 Reduction – Solar Exposed vs. Dark Conditions.....	47
Figure 12: PbTx2 Reduction - Solar Exposed versus Dark Conditions (Averages).....	48
Figure 13: Theoretical Modifications to H-ring, J-ring and K-ring Side Chain. ....	52
Figure 14: Correlation of Proposed Structural Modifications to Mass Ions .....	54
Figure 15: Peaks (8), (9) and (10) [83:17, ACN:H <sub>2</sub> O].....	58
Figure 16: <sup>1</sup> H-NMR (400 MHz) Spectra - By-Product P1.....	61
Figure 17: <sup>1</sup> H-NMR (400 MHz) Spectra – Isolate ACN 5.8.....	62
Figure 18: <sup>1</sup> H-NMR (400 MHz) Spectra - Peak 11.....	65
Figure 19: Purity Check of PbTx2 Spike.....	70
Figure 20: PbTx2 Spike Purity – Comparison Chart.....	73
Figure 21: <i>Karenia brevis</i> Culture Room Experiments .....	77
Figure 22: Electromagnetic Energy Profiles.....	82



## LIST OF ABBREVIATIONS

CDOM	Chromophoric Dissolved Organic Matter
CMSR	Center for Marine Science Research
CSCS	Coastal Zone Color Scanner
ECOHAB	Ecology and Oceanography of Harmful Algal Blooms
GEOHAB	Global Ecology and Oceanography of Harmful Algal Blooms
GOM	Gulf of Mexico
HAB	Harmful Algal Bloom
HABLAB	Harmful Algal Bloom Laboratories (CMSR)
NIH	National Institute of Health
NRC	National Research Council
MMAD	Mass Median Aerodynamic Diameter
SSML	Sea Surface Micro Layer
VGSC	Voltage Gated Sodium Channel
UNCW	University of North Carolina at Wilmington
PAR	Photosynthetically Active Radiation
ELISA	Enzyme-Linked Immunosorbent Assay

## INTRODUCTION

### Background on Harmful Algal Blooms

Harmful algal blooms (HAB's) are one of the most scientifically complex and internationally significant coastal issues facing the world today; they pose a substantial challenge to coastal management and public health authorities due their wide ranging impacts on human health, fisheries, marine wildlife, aquaculture and tourism. Such impacts often result in significant economic losses to the areas in which they occur (Anderson et al, 2000; Shumway, 1990; Viviani, 1992). HAB's are a growing concern to coastal communities worldwide given they are unpredictable, cannot be prevented and are inherently difficult to detect and manage (Anderson and Garrison, 1997; GEOHAB, 1998; Boesch et al, 1997; Smayda, 1990).

Though opinions differ as to the exact cause of the increase, there is a general consensus in the scientific community that, over the last 30 years, HAB events and their associated impacts have been increasing worldwide in frequency, duration and geographic distribution (Anderson, 1989; Harvell et al, 1999; Hallegraeff 1993, Smayda, 1990; CENR, 2000; HEED, 1998). HAB's and their deleterious impacts are now known to occur in every ocean but the Antarctic.

Mirroring the worldwide increase in bloom events, an HAB in the Gulf of Mexico (GOM) is a growing concern here in the U.S. where blooms of the dinoflagellate *Karenia brevis* (*Gymnodinium breve*) are occurring on nearly an annual basis (Steidinger and Tomas, 1999). *K. brevis* produces brevetoxin, a highly potent neurotoxin, responsible for mass morbidity and mortality among marine wildlife such as fish, birds, marine mammals and invertebrates (Steidinger et al, 1998; CENR, 2000) and the causative agent of Neurotoxic Shellfish Poisoning (NSP) in humans. Blooms of *K. brevis* result in a significant increase in the environmental

concentration of brevetoxin, an event not dissimilar to a natural chemical spill, as such, humans and marine wildlife are at an increased risk of exposure.

Brevetoxin exposure may result from a variety of pathways; fish and shellfish may uptake waterborne toxin after cell lysis or exudation and filter feeders such as sponges, zooplankton, and bivalves may directly ingest toxic *K. brevis* cells. Crustaceans, gastropods, fish, birds, turtles, and mammals may consume food/prey that have bioaccumulated the toxin or toxic cells and aerosolized brevetoxin may be inhaled by mammals, turtles and birds. Humans acquire NSP by the ingestion of bivalves, such as oysters and scallops, which, as filter feeders, have bioaccumulated the toxin in their tissues via uptake of free toxin in the water column or the uptake of *K. brevis* cells. Cases of NSP have been reported from the GOM, Florida's east coast, North Carolina, northern Spain, Japan and New Zealand (Baden et al,1995)

Biotoxins such as brevetoxin may deleteriously impact other members of their community as the toxin moves through the environment and food web affecting the viability, growth, fecundity and recruitment of a variety of organisms with which they may be competing (Smayda, 1993; Plumely, 1997).

Brevetoxins are potent ichthyotoxins; fish mortalities associated with *K. brevis* blooms are common, widespread and impact hundreds of species. Typical kills during bloom events are around 100 tons per day with cumulative losses over the years in the billions. A 1998 bloom resulted in excess of 21 million fish washing ashore Texas beaches (CENR, 2000). Brevetoxin has been implicated as the direct or proximate cause of mass mortalities of bottlenose dolphins (Wilson et al, 1999), manatees (Bossart et al 1998; O'Shea, 1991), water fowl (Forrester et al 1977; Krueder et al, 1998), sea turtles and benthic species (FMRI).

The economic costs of HAB events are not fully known, though estimates are significant. The range of impacts of HAB's on human health, wildlife, tourism, aquaculture and fisheries, have resulted in estimated economic losses of \$18-\$24 million per event (Anderson et al, 2000). A 1987-88, *K. brevis* HAB in North Carolina (exported from the GOM to the North Carolina

coast via the Loop and Gulf Stream currents) resulted in an NSP outbreak and closure of 365,000 acres of scallop fisheries for an entire year, with a resulting economic loss of \$25 million (Tester et al, 1991).

In summary, HAB events result in a wide range of impacts on human health, marine wildlife and fisheries. The biological, physical and chemical factors that initiate and regulate blooms remain poorly defined, as such, HAB's have proven difficult to predict and manage and their impacts pose a significant challenge for current and future public health and coastal management authorities worldwide.

#### Research Overview

While acute effects of brevetoxin exposures have been studied and observed over the last two decades, far less is known about the effects of chronic/repeated brevetoxin exposure on humans and marine wildlife. Little is understood about the transport and fate of brevetoxins in the environment (water, air, sediments, and selected biota). Currently it is not known how long brevetoxins may persist in the environment upon the demise of a bloom and it has become apparent that metabolic processing results in structural changes to the toxin(s) in vivo as it is transported through trophic levels, which in turn modifies toxin potency and residence times in tissues (Poli et al, 2000; Plakas et al, 2001).

Brevetoxins (designated as PbTx) are a suite of at least 10 distinct chemical entities, with more pharmacologically active derivatives, some of them natural antagonists, currently being characterized. Not all brevetoxins possess the same potency, metabolic stability or exert the same pharmacological affects (Baden, 1989; Rein et al, 1994; Gawley et al, 1995; Hua and Cole, 2000; Purkerson-Parker et al, 2000; Poli et al, 2000; Plakas et al, 2001). There are synthetic brevetoxin derivatives that act as antagonists, preventing or markedly diminishing the toxicity of sister toxins (Purkerson-Parker et al, 2000). Similarly, a naturally occurring brevetoxin derivative currently being characterized has also demonstrated antagonistic activity (Baden and Bourdelais, verbal

communication). Among the synthetic derivatives are toxins which mimic all of the natural toxin effects, some which demonstrate no toxicity and some which possess a subset of the natural toxin characteristics (Baden et al, 1996). In short, the brevetoxins are a suite of polyether neurotoxins, with varying toxicities, binding affinities and metabolic stabilities, all characteristics which may be modified by metabolic or environmental biochemical processes, as well as modifications (as this paper will suggest) via photochemical processes.

Current evidence suggests that, in addition to the known acute toxicological effects on cardiovascular, neuromuscular, and respiratory systems (Baden et al, 1984; Huang et al, 1984; Ishida and Shibata, 1985; Koley et al 1995; Borison et al, 1980; Deshpande et al, 1993), chronic brevetoxin exposure may result in immunosuppression and toxicity to hemopoietic (Bossart et al 1998) and thermoregulatory systems (Gordon et al, 2001). Brevetoxin (PbTx1) has also been shown to be teratogenic in fish embryo studies (Kimm-Brinson and Ramsdell, 2001).

A complete etiology of acute and chronic brevetoxicosis remains poorly defined. Our lack of understanding the transport and fate of brevetoxin in the environment and the processes of assimilation, metabolism and depuration among the varying taxa that uptake the toxin(s) poses limitations to the development of toxin detection methodologies and public health risk assessment. Similarly, there is no clear correlation between the observed pathologies in humans and marine wildlife with the type of brevetoxin, or suite of toxins, to which the organism was exposed. Similarly lacking is a correlation, if there is one, describing the duration and route of exposure to observed pathologies. How these factors are correlated remains to be elucidated.

In light of these recent findings and given the increase of HAB events in the Gulf of Mexico and the resulting increased exposure of humans and marine wildlife to brevetoxins, of concern are the effects of chronic and sublethal exposures, of which there is little information to date (Steidinger and Tomas, 1999; Flemming and Baden, 1998). This research considered the possible photochemical degradation and/or photochemical by-products of brevetoxin (PbTx2), the predominate brevetoxin in the environment. PbTx2 exists free in water column and is known to

accumulate in the sea surface microlayer during HAB events. The intensity of solar radiation and the duration of exposure in the natural environment provide ample opportunity for photochemical transformation of the toxin. Such photochemical processes may provide information useful to understanding the transport and fate of the toxin in the environment and aid in assessing the risk of acute and chronic exposure to the toxin(s).

#### History of Gulf of Mexico HAB's

Written reports from ships logs of Spanish explorers describe HAB events in Florida dating back to the 1500's and anecdotal reports of HAB's in the GOM describing noxious 'gases' and mass fish kills have occurred throughout the last century. While our observations of HAB's, or their impacts, date back over 400 years, harmful algal blooms were most likely occurring in the GOM long before human settlement.

The cause of the mass fish kills and noxious aerosols, a single celled phytoplankton, was eventually identified by C.C. Davis (1948) during a 1946 red tide outbreak. The dinoflagellate was named *Gymnodinium breve* and has since been reclassified into its own genus (2001), *Karenia brevis*. The soft-bodied dinoflagellate is indigenous to and found throughout the Gulf of Mexico and the U.S. South Atlantic Bight.

While the number of species of phytoplankton in the GOM that produce toxins exceeds 40 (Steidinger and Tomas, 1999), *Karenia brevis* is the most notorious in terms of GOM HAB's. Blooms of *K. brevis* are known to occur from the Yucatan in the south, along the Tamaulipas and Texas coasts, to Mississippi, Alabama, and Louisiana waters, although they are most frequent along the gulf coasts of Florida and Texas.

Through the early nineteenth hundreds blooms in the GOM, or their symptomatic fish kills, were observed only once every 3 to 5 years. Over the last 42 years there have been 28 red tides of  $>1 \times 10^4$  *K. brevis* cells  $l^{-1}$  (Walsh and Steidinger, 2002) and blooms, with their resulting impacts, now occur in the GOM on nearly an annual basis.

## Bloom Dynamics in the Gulf of Mexico

Bloom dynamics (initiation, transport and termination) are complex and are not yet clearly defined. The biological, chemical and physical factors that regulate blooms are interrelated and intimately tied to larger global climate patterns. However, based on observations over the last century it can be simplistically stated that bloom dynamics are governed by both local ecosystem parameters (chemical & biological) and large scale forcing. Large-scale forcing (processes associated with fronts, Loop Current intrusion into the GOM, spin-off eddies, coastal currents, winds and upwelling) tends to govern bloom initiation, transport and localization (Huh et al, 1981; Haddad, 1982; Steidinger and Haddad, 1981; Geesey and Tester, 1993; Tester and Steidinger 1997) while the more local parameters such as nutrient concentrations, variable PAR, grazing and viral/bacterial cell lysis tend to govern growth rates and bloom density (Shanley et al, 1993; Tester and Steidinger 1997; Liu et al, 2001; Lenos et al, 2001; Walsh et al, 2002).

Bloom initiation is typically, though not exclusively, offshore, around 18-74 km (Steidinger and Haddad, 1981). The toxic offshore blooms may persist for months and serve as an inoculum source as they may be, and often are, transported to (via physical processes) inshore coastal environments. Blooms may re-inoculate coastal areas several times throughout a bloom season. Why blooms do not initiate further inshore remains a topic of question.

Typical physical parameters associated with initiation are temperate to tropical waters (optimal temperatures of 22 to 28°C) and salinities > 24‰ (Steidinger and Haddad, 1981). However, *K. brevis* can tolerate temperatures from 10-33°C and salinities up to 37‰. Blooms usually, but not always, initiate in the late summer and autumn months (>70%), may persist for weeks to months and have been known to last for up to 1.5 years. Blooms can be expansive and may reach sizes covering an area of 30,000 km<sup>2</sup>, they can be found to extend to depths of 100 meters or more and are monospecific where *K. brevis* represents ~ 90% of the biomass during bloom events (Steidinger and Joyce, 1973). At one time blooms were thought to originate from

offshore “seed beds”, however, the existence of resting cysts of *K. brevis* has not been confirmed though laboratory observations have identified a benthic palmelloid stage in the life cycle that may alternatively serve as a seed population (FMRI).

Background (non-bloom) *K. brevis* cell concentrations in the GOM are typically  $< 10^3$  cells  $L^{-1}$  but may increase to  $10^7$  or  $10^8$  cells  $L^{-1}$  during bloom events. Toxin production per cell (organism) has been noted to be  $\sim 10$ - $20$  pg cell $^{-1}$  and cultured *K. brevis* yields  $\sim 0.45$  mg  $L^{-1}$  of toxin which roughly correlates to the brevetoxin/cell estimate. Hence, environmental concentrations of brevetoxin during bloom events may reach  $\sim 50$  mg  $L^{-1}$ , a highly toxic concentration given neuronal injury and death in rat studies occurs at EC<sub>50</sub>'s of 80 nM (Berman et al, 1999) and lethal dosages in mouse assays are  $10^{-9}$  to  $10^{-12}$  moles/kg. In human cases of NSP the brevetoxin concentrations present in contaminated clams have been reported to be 78-120 ug/100g. Given the potency of brevetoxin the risks of brevetoxin exposure may occur at cell concentrations well below  $10^7$  or  $10^8$  cells  $L^{-1}$ . Variable brevetoxin production among *K. brevis* strains has been noted (Greene et al, 2001) and fish mortalities have occurred at lower bloom concentrations  $< 2.5 \times 10^5$  cells  $L^{-1}$  (Tester and Steidinger, 1997). Hence, cell densities are not necessarily indicative of toxicity.

The toxicity of the organism itself may be regulated by environmental conditions. Nutrient conditions may serve as a governing factor in determining bloom toxicity. There is evidence that nutrient limiting conditions may actually enhance brevetoxin production in *K. brevis*. By lowering nitrate  $< 10$  uM, phosphate  $< 0.6$  uM, by substituting urea  $< 5$  uM, or by lowering irradiance (PAR), brevetoxin production was found to increase some 10 fold, from the production of  $10$ - $20$  pg cell $^{-1}$  under standard nutrient conditions to  $> 100$  pg cell $^{-1}$  (Greene et al, 2001).



## Nutrients

While anthropogenic forcing due to nutrient loading of coastal waters has been correlated with HAB events in other parts of the world and U.S. no correlation between *K. brevis* blooms in the GOM and anthropogenic forcing has been established. HAB's in Florida occurred prior to significant pollution from human population (Steidinger et al, 1998) and *K. brevis* blooms typically initiate in waters far from anthropogenic nutrient inputs. The offshore GOM waters where *K. brevis* blooms predominately initiate are oligotrophic with typical inorganic nitrate and phosphate concentrations of  $< 0.5$  and  $0.2$  mM, respectively and past studies reveal *K. brevis* as well adapted to oligotrophic conditions.

The organism effectively utilizes inorganic and organic phosphorus and nitrogen (urea, amino acids and dissolved organic matter) under varying amounts of PAR while exhibiting steady growth rates of 0.2-0.5 divisions per day (Shanley and Vargo, 1993; Steidinger et al, 1998). Blooms of the organism have been known to initiate when nitrate concentrations in the bloom area were below detectable levels (Baden and Mende, 1979; Shimizu and Wrensford, 1993; Tester et al, 1991; Steidinger et al, 1998).

In terms of nutrients the trace metal iron may figure as a significant player in *K. brevis* bloom dynamics and there may be a correlation between climactic variability (North Atlantic Oscillation, NAO) and HAB events in the Gulf of Mexico (HEED, 2000; Usup and Azanza, 1998). The eolian transport of dust from Africa to the western Atlantic and Caribbean basin is a well-documented, seasonal phenomenon (Prospero and Nees, 1986; Mbourou et al., 1997). Over the last decade Iron has been recognized as a significant limiting nutrient, a vital factor in all phytoplankton and cyanobacterium nutrient regimes and essential element for chloroplasts and nitrogen fixation. Analysis of over 35 years of historical HAB data suggests a correlation may exist between atmospheric iron deposition from Saharan dust events and large-scale *K. brevis* HAB's (Liu et al, 2001; Capone and Zehr, 1997; Lenos et al, 2001). Hayes et al

(2001) suggest that a sudden, large-scale increase in iron supply to the ocean has the potential to alter the nutrient limitation processes that hold opportunistic species in check. The delivery, via eolian input, of "new" iron in pulses to typically iron-poor regions of the oceans, such as the Gulf of Mexico, will reduce or remove the limits to rapid biological growth (*e.g.* blooms) (Smayda, 1990).

Blooms in the GOM of the iron limited cyanobacterium *Trichodesmium*, recognized as prolific nitrogen fixer, have been found to coincide with the atmospheric deposition of iron rich dust from Saharan dust storms. Once *Trichodesmium* blooms are established they may serve as a source of nitrogen for *K. brevis* via the excretion of amino acids and the bacterial degradation of excretory material and particulate matter. *Trichodesmium* typically releases ~ 15-20 uMoles of N/Kg of DON into the environment, 4x the background level in the GOM, after Saharan dust events (Lenes et al, 2001). This premise provides the basis for understanding a functional link between climate variability, such as NAO, and marine disturbances such as blooms of HAB species (Hayes et al, 2001), however, this relationship between *K. brevis* blooms, *Trichodesmium* and climate variability has not yet been clearly established.

In summary, while anthropogenic forcing via nutrient loading does not appear to be a factor in *K. brevis* bloom dynamics, oligotrophic conditions, iron deposition from Saharan dust events and the co-occurrence of *Trichodesmium spp.* in the GOM may be contributing factors that select for *K. brevis*, creating the necessary conditions that foster bloom type growth. The organism is well adapted to oligotrophic conditions, is able to utilize a variety inorganic and organic nutrient sources under variable conditions of PAR and is dominant as a HAB species over the 40 odd other potentially harmful algae that coexist in the GOM.

#### Non-Regional Brevetoxin Related Blooms

Though *K. brevis* is indigenous to the GOM, related dinoflagellate species producing brevetoxin like compounds are found in other parts of the world. *Chattonella marina* found in

Japan, New Zealand and Australia, *Chattonella antiqua*, found in Japan, *Fibrocapsa japonica*, found in Japan and *Heterosigma akashiwo*, found on both the east and west coasts of the U.S. and in Japan, have also been reported to produce this class of polyether toxin (Hallegraeef et al, 1998; Sagir et al, 1995; Khan et al, 1997). The toxins produced by these organisms, chemically similar to brevetoxin, may follow related pathways of transport and fate in the environment and in vivo. Hence, the associated risks of brevetoxin exposure and the impacts on human health, fisheries, marine wildlife and tourism may not necessarily be limited to the Gulf coast states.

### HAB Management

Harmful algal blooms are generally understood to be antithetical to the concept of 'health of the ocean'. However, phytoplankton blooms are natural phenomena, part of the ecosystem itself, and blooms of harmful species, from our anthropogenic perspective, should be understood as such. *K. brevis*, while accredited with mass morbidity and mortality events among a variety of marine taxa, may also account for ~40% of the primary production of Florida's west coast (Vargo et al, 1987). Overall, HAB's have exhibited negligible long term negative effects on marine ecosystems. However, HAB's do have significant public health and economic impacts, and they have resulted in acute episodic mass mortalities among marine wildlife.

HAB events are unpredictable and prevention of such events may never be feasible. Our current understanding of the biological, physical, and chemical processes that regulate HAB's renders management, mitigation and public health efforts difficult, however, current national and international efforts through joint research projects such as ECOHAB (ECOHAB, 1995) and GEOHAB (GEOHAB, 1998) promise to expand our understanding of HAB dynamics.

In the U.S. there has been little direct intervention in HAB's in coastal waters largely due to the fact that the remedies proposed for intervention have either posed a greater threat to the environment than the HAB itself or were ineffective. Several remedial techniques for bloom management have been explored in the past, including chemical treatment with copper sulfate

(toxic to a variety of organism) and flocculating clays to remove phytoplankton from the upper water column (ECOHAB, 1995; Steidinger and Tomas, 1999; Ewert et al, 2000; Zingone et al, 2000). But such strategies have either proven to be inefficient, or the chemicals or clays themselves, being non-selective in effect, pose their own environmental risks. Also explored are natural viral and bacterial pathogens to which *K. brevis* maybe susceptible. However, very few of these preventative techniques have been employed on a regular basis due to the inherent risks in each.

Toxin detection/screening in coastal waters and seafood during bloom events can be said to be the cornerstone of public health efforts. The toxicity testing methods currently employed in many countries include the US FDA-approved mouse bioassay and a variety of chemical, pharmacological, immunological and cell based assays. While the chemical, pharmacological and immunological assays are reliable and sensitive for many of the well known toxins, they generally constitute "high capacity, high throughput" detection, detecting only the presence of known compounds. These particular assays do not necessarily detect or imply toxicity nor do they provide conclusive evidence as to the specific toxin present (Baden et al, 1992; Poli et al., 1995; Van Dolah et al., 1997).

Given the variety of testing methodologies employed there are the expected discrepancies among them (Baden et al, 1995; Dickey et al, 1999; Poli et al, 2000). Such discrepancies arise due to metabolic variations among species of mollusks and the resulting changes to toxin profiles in vivo, as well as variations in the detection methodologies themselves. While discrepancies among explored detection methodologies exist and greater specificity in detection is called for, emerging methodologies such as ELISA (Baden et al, 1995; Naar et al, 2001) and cell based assays (Fairey et al, 1997; Kerr et al 1999), provide effective tools for toxin detection and HAB management efforts and may offer greater specificity in toxin detection in the future.

Prediction and tracking of HAB event in the GOM has, in the past, exceeded our capabilities. The use of satellite technologies such as Coastal Zone Color Scanner (CZCS) and

SEAWIFS in tracking ocean currents and blooms movements holds promise for possibly forecasting the occurrence and transport dynamics of a HAB event, however, current CZCS's resolutions only allow for the detection cell concentrations above  $10^6$  cells  $L^{-1}$ , or  $> 10\mu g$  Chl  $L^{-1}$  (Walsh et al, 2002), a resolution inadequate for thorough HAB monitoring and tracking given blooms of *K. brevis* are harmful at concentrations well below  $10^6$  cells  $L^{-1}$ . Shellfish beds are closed to harvesting at  $5 \times 10^3$  cells  $L^{-1}$  due to bioaccumulation of toxin and fish kills may occur at  $2.5 \times 10^5$  cells  $L^{-1}$ , both concentrations below current CZCS detection resolutions.

Though our past resources posed limits to HAB management, the technologies and knowledge base needed for the effective management of coastal resources and public health in regions where HAB's occur has improved markedly over the last decade. Monitoring programs for HAB species and their naturally occurring marine biotoxins will undoubtedly improve with advances in remote sensing, GIS technologies, real-time data acquisition and the development of substantial predictive models and toxin detection methodologies.

## Summary

Blooms of *K. brevis* are unpredictable, are not anthropogenically forced, occur and sustain under oligotrophic conditions and cannot be controlled. Modest increases in cell density result in significant increases in the environmental concentrations of brevetoxin which poses adverse risk to humans and marine wildlife. Currently there are no reliable predictive models of cell population development, transport, and toxin accumulation for any of the major harmful algal species in the United States, to include *K. brevis*, hence, the forecasting of HAB events and their behavior is beyond our current capabilities. As such, HAB's of *K. brevis* promise to continue unabated by man's efforts and figure as a significant concern for coastal management, human health and marine wildlife.

## BREVETOXIN AND PHARMACOLOGICAL ACTIVITY

### Chemistry

Why exactly a select few, some 60 out of ~5000 microalgae species produce toxins and how it is they do so without killing themselves are questions without definitive answers. Biotoxins are generally classed as secondary metabolites that may serve as allelopathic or antipredation agents, lending the organism a competitive advantage in their environment. It has also been suggested that the toxins may be precursors to other necessary intracellular compounds of undetermined function. In general, the definitive purpose of these intracellular toxins is not clear. Many algal species synthesize elegant chemicals of remarkable toxicity and in the case of brevetoxin, capable of adversely affecting the health of a variety of organisms, including humans. At least 100 species of marine animals are known to have been killed due to brevetoxin exposure (Martin and Martin, 1976).

*K. brevis* produces 2 types of lipid soluble toxins; hemolytic and neurotoxic. The neurotoxins (brevetoxins) are the some of the most potent non-macromolecular agents known (Appendix 4), toxic in nanomolar concentrations in receptor binding protocols (Table 1) (Poli et al, 1986), picomolar concentrations in nerve-muscle preparations (Baden et al, 1988) and capable of producing bronchioconstriction in animal models in femtomolar concentrations (Singer et al, 1998).

The brevetoxins (designated PbTx) are a suite of at least 10 structurally related toxins based on 2 distinct structural backbones (Lin and Risk, 1981; Baden, 1989), brevetoxin A (synonymous with PbTx1) and brevetoxin B (synonymous with PbTx2). Derivatives of the type-A and type-B parent structures (PbTx's 3, 5, 6, 7, 8, 9 and 10) vary in the K-ring (Type B) or J-ring (Type A)

side chains. All brevetoxins share common features; they are transfused polyether ladders, similar in length (~30Å) and overall structure (cigar shaped), with lactone ring ‘head’ and ether ring ‘tail’ regions which play vital roles in binding (to VGSC) and toxicity (Figure 1).

Neurotoxicity is due to their function as a sodium channel agonists (Catterall and Risk, 1985; Poli et al, 1986). Brevetoxins bind to receptor site 5 on voltage-gated sodium channel’s (VGSC) (Trainer et al, 1994) modifying the normal sodium ion flux across cell membranes. In essence they disrupt neural signaling, fouling the natural process of electrochemical communication. Their physiological effect is chronic sodium channel activation resulting in permanent membrane depolarization and eventual cell death. Several mechanisms are suggested, including inactivation of the process which allows VGSC’s to achieve their resting state (Jeglitsch et al, 1998), a shift of channel activation potential to more negative values where the channels open at normal resting potentials (Huang et al, 1984, Jeglitsch et al, 1998) and the induction of subconductance states (Schreibmayer et al, 1992, Jeglitsch et al, 1998).

Though all brevetoxins are believed to share the same pharmacophore they do not all demonstrate the same binding affinity or toxicity (Table 1). Binding affinities in synaptosome binding assays are PbTx1 >PbTx3 >PbTx2 >PbTx6 (Gawley et al, 1992; Baden et al, 1996). Hence PbTx1, PbTx2 and PbTx3 have been recognized as the most toxic. The conformation and length of the structure, functionality of the K- and J-ring tails and A-ring head regions largely determine binding affinity and toxicity. The A-ring lactone head region appears to be vital to binding affinity. The common model involves hydrogen bonding in the region of the A-ring carbonyl to a locus at site 5 of the VGSC (Baden 1994). Modifications to the A-ring and/or carbonyl group on the A-ring, or modifications to length of the molecule, significantly alter binding affinities and toxicity (Gawley et al, 1995). Similarly, functional group modifications to the K- and J- ring tails can markedly alter toxicity (Purkerson-Parker et al, 2000; Gawley et al, 1995; Singh et al, 2002). Reduction of the H-ring double bond and the proposed conformational

# BREVETOXINS

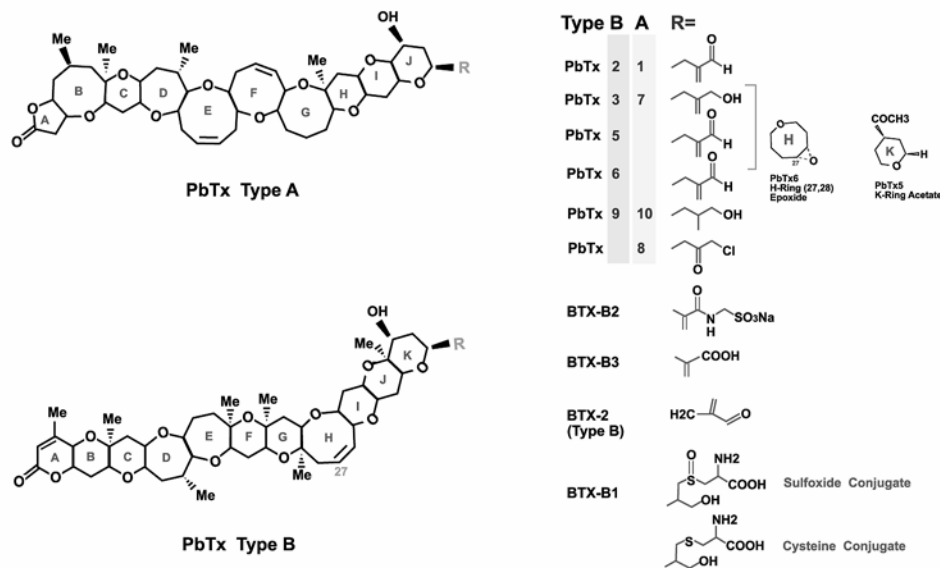


Figure 1: Brevetoxins

The conformation of the molecule, critical length and functionality of the K- and J-ring tails, H-ring and A-ring head regions determine binding affinity and toxicity. The A-ring lactone appears to be critical to VGSC binding affinity. Modifications to the A-ring and/or carbonyl group, or modifications to length of the molecule, significantly alter binding affinities and toxicity. Similarly, functional group modifications to the K- and J- ring tails can markedly alter toxicity. Reduction of the H-ring double bonds and the proposed conformational change of the H-ring from boat-chair to crown has also been shown to significantly reduce the binding affinity and toxicity of brevetoxin B. Numerous synthetic derivatives of the natural toxin have been generated via modifications to the K- and J- ring side chain, the H-ring and A-ring head region. Among them there are derivatives that mimic all of the natural toxin effects, some derivatives which have no effect on VGSC, some which demonstrate some but not all of the natural toxin attributes, and some which act as antagonists.



change of the H-ring from boat-chair to crown, has also been shown to significantly reduce the binding affinity and toxicity of brevetoxin B (Rein and Borrone, 1999).

Numerous synthetic derivatives of the natural toxin have been generated (Rein et al, 1994) via modifications to the K-and J-ring side chain, the H-ring and A-ring head region. Among them are derivatives that mimic all of the natural toxin effects, some derivatives which have no effect on VGSC, some which demonstrate a subset of the natural toxin attributes and some which act as antagonists (Baden, 1989). Further evidence of the critical role of K-ring functionality is the demonstration of brevetoxin derivatives that act as antagonist, inhibiting the neurotoxic activity of fellow congeners. Recently synthetic  $\alpha$ - and  $\beta$ -naphthoyl derivatives were shown to bind to, but not activate, VGSC's. The  $\alpha$ -Naphthoyl-PbTx-3 acted as a PbTx-3 antagonist, abolishing PbTx3 toxicity, and it did not demonstrate toxicity to VGSC's that were not exposed to PbTx-3 (Purkerson-Parker et al, 2000). Interestingly, while the  $\alpha$ -naphthoyl PbTx3 acted as an antagonist in vitro it exhibited a modest level of toxicity (LC50=142 vs LC50=15nM for PbTx3) in vivo. Similarly, a naturally occurring brevetoxin derivative that acts as a brevetoxin antagonist is currently being characterized (Baden and Bourdelais, verbal communication).

Hence, the brevetoxins are suite of chemically dynamic compounds whose binding affinities and toxicity are governed by functional groups at the K- and J-ring side chains, conformation, length and A-ring lactone modifications. These characteristics are in turn susceptible to environmental and/or metabolic transformations, and, as this paper will suggest, photochemical modification.

While there is variability among brevetoxins in their metabolic stabilities, binding affinities, toxicities and antagonistic activities, the primary backbones (Brevetoxin Type A and Type B) appear to be resilient as they are heat and acid stable, cannot be removed by food preparation procedures such as cooking or freezing (Baden et al, 1989) and are known to persist in bivalve tissues for up to seven days after uptake (Benson et al, 1999). How long they persist in the environment is unknown.

---

<b>BREVE TOXIN BINDING AFFINITIES</b>	
neuronal injury and death in rat neurons	
	<b>EC50</b>
PbTx-1	9.31 +/- 0.45 nM
PbTx-3	53.9 +/- 2.8 nM
PbTx-2	80.5 +/- 5.9 nM
PbTx-6	1417 +/- 32 nM

---

Table 1: EC50's In Receptor Binding Protocols for Brevetoxins

(From: Berman et al, 1999)

## Physiological Effects

There are three potential routes of exposure to brevetoxin in humans and wildlife: Inhalation of aerosolized toxin, ingestion of contaminated seafood and toxic seawater intake. Any of these three routes of exposure may result in systemic distribution of brevetoxin to all bodily tissues (Poli et al, 1990; Benson et al, 1999; Bossart et al, 1998) a growing concern given recent evidence that brevetoxin may accumulate in organ tissues (such as lung, liver and brain) upon chronic/repeated exposure (Bossart et al, 1998).

A variety of pathophysiological sequelae are related with brevetoxin exposure. Acute exposures result in toxicity to the cardiovascular, nervous, neuromuscular and respiratory systems (Bossart, 1998; Baden et al, 1984; Clare et al, 2000; Borison et al, 1985; Koley et al, 1995; Templeton et al, 1989). Most recent findings suggest brevetoxins may also be toxic to mammalian immune, hemopoietic (Bossart et al, 1998; ) and thermoregulatory systems (Gordon et al 2001) upon chronic or repeated exposure. In addition, brevetoxin (PbTx1) has been shown to be teratogenic in fish embryo studies (Kimm-Brinson and Ramsdell, 2001).

Brevetoxin bioaccumulates in filter feeding bivalves, such as clams, oysters, mussels, scallops and coquina, organisms commonly consumed as foods by man and marine wildlife. Ingestion of the toxic bivalves results in Neurotoxic Shellfish Poisoning in humans, the symptoms of which are severe gastrointestinal disturbance, numbness, tingling and hot/cold reversal and in severe cases, cardiovascular symptoms (Baden et al, 1995; Flemming and Baden, 1998).

Cardiovascular effects resulting from brevetoxin exposure include arrhythmia, sinus bradycardia, hypotension and peripheral vasodilation (Templeton et al, 1989; Ellis, 1985; Borison et al, 1980; Rodgers et al, 1984). Respiratory abnormalities such as apnea and hyperapnea, have been reported in experimental animals (Koley et al, 1995) and sufficient doses of brevetoxin may result in respiratory failure (Johnson et al, 1985). Marine mammal studies

from a 1996 manatee epizootic have shown brevetoxicosis to be responsible for rhinitis (inflammation of the mucous membrane of the nasal passages with profuse discharge of mucus), pulmonary hemorrhage (bleeding within the lung tissue) and hemosiderosis (a general increase in iron stores in tissues without tissue damage), indicating prolonged hemolytic anemia (Bossart et al, 1998). The histopathological observations from this particular manatee epizootic suggested brevetoxin's immunoreactivity in lymphoid tissue, indicating the toxin may be a potential immunosuppressant. Significant were indications that mortality resulting from brevetoxin exposure, as in the case of the manatees, may not be necessarily acute, but may occur after chronic exposure to the toxin (Bossart et al, 1998).

Aerosolized brevetoxin, generated from wind and wave action during Florida HAB events, results in one of the largest naturally recurring pulmonary exposure in United States. The aerosols are concentrated in brevetoxin (PbTx's 1, 2, 3 & 6) 25 to 50 fold over culture concentrations (Pierce et al, 1990) and, upon inhalation, have been shown to produce bronchioconstriction in femtomolar concentrations in animal models (Singer et al, 1998). Toxic aerosols of brevetoxin were suspected as the proximate cause of the significant (155) die-offs of endangered manatees during the above mentioned 1996 HAB event (Bossart et al, 1998).

The toxicological effects from brevetoxin exposure are clearly wide ranging. The rise in evidence of the potential adverse human health impacts resulting from HAB exposures has resulted in HAB events, such as the *K. brevis* bloom in the Gulf of Mexico, being classified as one of the "Emerging Disease" groups by the National Institute of Health and the National Academy of Sciences (NRC, 1999). To date there is little published literature or formal epidemiological studies on the human health effects of acute brevetoxin exposure and no existing statistics for the incidence of brevetoxin exposure (Fleming and Baden, 1998). Given recent findings demonstrating systemic distribution of brevetoxin upon acute exposure, the potential accumulation of brevetoxin in organ tissues upon chronic/repeated exposures and our incomplete

knowledge of brevetoxicosis etiology, it is clear that brevetoxin exposures, particularly chronic, may pose substantial unforeseeable risks to public health.

### Therapeutics

Voltage-gated sodium channels (VGSCs) are complex membrane proteins that are widely expressed throughout the body in neuronal, neuroendocrine, skeletal muscle and cardiac cells. They regulate a vast array physiological activities and better understanding their pharmacology and physiological regulatory functions promises to yield novel therapeutic treatments for VGSC associated diseases and pathologies. The indispensable roles of VGSCs in human health is well illustrated by the array of physiological/toxicological effects resulting from neurotoxic inhibition of their normal activity.

Compounds that modulate VGSCs, such as brevetoxin, have proven invaluable tools for probing ion channel function. Similarly, drugs that modulate VGSCs have proven of therapeutic value in local anesthesia, cardiac arrhythmia, pain and epilepsy (Clare et al, 2000). While brevetoxins are potent neurotoxins that have deleterious effects on human health and marine wildlife, they have also served as useful probes for elucidating ion channel function and may potentially help arrive at novel therapies for VGSC related pathologies. Current research employs synthetic brevetoxin derivatives that will serve as ion channel probes that may help to further elucidate sodium channel architecture and functionality (Baden, verbal communication).

## EXPRIMENTAL OVERVIEW

### Background

The purpose of this research was to investigate the effects of solar radiation on PbTx<sub>2</sub>, the predominate form of brevetoxin found in the environment. Specifically, to investigate possible photochemically induced by-products and/or derivatives of PbTx<sub>2</sub> and, if any, the chemical characterization of these by-products.

The relevance of this research is in addressing the fundamental need to understand the transport and fate of brevetoxin in the environment, due to the established and potential human health risks, described above, associated with acute and chronic exposure to brevetoxin exposure. Brevetoxin may be readily assayed in the environment, much less so once the toxin is in vivo. Understanding the environmental variables affecting brevetoxin speciation and its transport and fate in the environment is critical to identifying the nature of the toxin being ingested or inhaled. Further, photochemical and biochemical metabolic processes share similar mechanisms (redox, Michael addition) and information gained here on any photochemical processes (PbTx<sub>2</sub> degradation or derivative formation) may possibly be useful in further elucidating the transport and fate of the toxin in vivo.

Considered were possible variations in photochemically driven processes between sea-surface microlayer (SSML) and seawater. The chemistry of the SSML is suspected to differ from the chemistry of the water column as it involves numerous reactive species and processes due to the enrichment of organics, the sea-air interface and solar radiation, factors unique to the surface layer. Such factors suggest the potential for photochemical processes (both direct and indirect) to which brevetoxin may be disposed. PbTx<sub>2</sub> is the most ubiquitous species of brevetoxin, is found free (extracellular) in the environment during HAB events and, being lipophilic, brevetoxin tends to accumulate in the sea surface micro layer upon cell lysis (Rumbold and Snedaker, 1999).

Given such conditions there may be potential for photochemical degradation or by-product formation of PbTx2 in the surface waters or in aerosolized form. If either of these events occurs and whether such by-products are toxic is unknown.

#### Sea Surface Microlayer (SSML)

The sea-surface microlayer (SSML) is operationally defined as the top 1 to 1000  $\mu\text{m}$  of the ocean surface and comprises a series of sub layers; These include a thin surface nano-layer ( $\ll 1 \mu\text{m}$ ) enriched in surface-active compounds; the surface microlayer ( $\ll 1000 \mu\text{m}$ ) containing high densities of particles and microorganisms; and the surface millilayer ( $\ll 10 \text{ mm}$ ) inhabited by small life forms, the ova and larvae of fish and invertebrates. The microlayer concentrates a variety chemical substances, both anthropogenic and biotic; amino acids, proteins, fatty acids, lipids, phenols, halogens and an array of other organics and as well as anthropogenic chemicals and pollutants accumulate in the surface layer.

Due to the enrichment of chemicals and biota within the SSML it is widely held that the surface microlayer could act as a highly efficient and selective microreactor (GESAMP, 1995; Blough, 1996). Rapid photochemical, chemical, and biological reactions within the microlayer could produce a variety of reaction mechanisms, such as photochemical reactions which might destroy or produce surface-active species. How brevetoxins react within this matrix, with and without solar radiation is of question, and the purpose of this investigation.

It is the surface layer of the oceans that is entrained in winds and aerosolized. Toxic aerosols of brevetoxin are well recognized as a public health risk. Few studies have examined the brevetoxin profiles of these aerosols save Pierce et al (1990) where it was demonstrated that toxins concentrations are increased in aerosols some 20 to 50 fold, and a current NIEHS project studying the toxin profiles of Florida HAB aerosols (Baden, POI/ES/10594, DHHS, NIEHS).

Further examination of the photochemistry of SSML and the possible presence of brevetoxin derivatives could prove valuable in assessing the toxin profiles of aerosolized brevetoxin.

### Photochemical Processes

Two potential pathways exist by which photochemical processes may occur in solution. One, if the absorption wavelength/spectrum of the molecule is harmonic with the wavelength of incoming radiation the molecule may undergo photoreaction directly. Brevetoxins possess several susceptible reactive sites; double bonds, methylene and carbonyl groups those with most photochemically reactive potential. The absorption spectra for the A-ring lactone conjugated double bonds is 194nm (assigned to the  $\pi$ -  $\pi^*$  transition) and 239nm for the n-  $\pi^*$  transition, both well below ambient UV energy levels. The conjugated double bonds of the aldehyde functional group (PbTx2) located on the K-ring side chain has been shown to absorb at 208 nm ( $\pi$ -  $\pi$  transition), (Brousseau et al, 1998). Elsewhere aldehyde functional groups have been shown to absorb at 315 nm (n-  $\pi^*$  transition).

In the absence of direct excitation of reactive sites such as double bonds, brevetoxin may undergo indirect photoreaction via sensitizers. Solar energy may be absorbed by other substances which may react with a secondary substrate, such as brevetoxin, resulting in an indirect photochemical reaction. A variety of light reactive substances, potential sensitizers, exist in the microlayer which could be conducive to structural changes in PbTx2. The major photochemical intermediates in the sea water include oxygen radicals; singlet oxygen ( $^1\text{O}_2$ ), superoxide and hydroperoxide ( $\text{O}_2^-$  and  $\text{HO}_2$ ), peroxide ( $\text{H}_2\text{O}_2$ ) and hydroxyl ( $\text{OH}^-$ ) and peroxy radicals ( $\text{RO}_2$ ), (Zepp et al, 1985; Cooper, 1989). In addition, halogens, metals, ketones, amines and phenoxy radicals are all known to be present. Singlet oxygen  $^1\text{O}_2$  is formed primarily through energy transfer from the excited triplet states of CDOM (chromophoric dissolved organic matter) to ground state dioxygen,  $^3\text{O}_2$ , and wavelengths in the UV-A (315-400 nm) and UV-B (280-315 nm)



are most effective in its formation (Zepp et al., 1985). Such reactant species, conjoined with the complex chemistry of the sea surface microlayer and solar energy provide interesting possibilities in terms of brevetoxin degradation or by-product formation.

## MATERIALS AND METHODS

### Chemicals

HPLC grade Methanol, Acetone, Acetonitrile and Ethyl Acetate (Fischer Scientific, USA). Deionized water and HPLC grade water.

### Equipment

Chromatographic analyses of samples were performed on a Hewlett-Packard 1100 HPLC using Chemstation software. Chromatography specifications were as follows: An isocratic mobile phase of 85:15 (MeOH:H<sub>2</sub>O, C18 reverse phase column) with a flow of 1.4 mls/min. was used for standard analysis. Isocratic and gradient mobile phases (C18 reverse phase columns) using varying concentrations of 95:5 to 70:30 MeOH:H<sub>2</sub>O, or ACN:H<sub>2</sub>O, were used for the isolation of by-products. Detection - Diode ray wavelength of 215nm using a 360uM reference. Column - 5uM C18 column from Agilent Technologies.

Toxin (PbTx<sub>2</sub>) purification and crude analyses were performed on an HPLC comprised of a Waters 6000A Pump and Isco V4 absorbance detector. Chromatography specifications for the Waters/Isco HPLC were: Isocratic mobile phase of 85:15 (MeOH:H<sub>2</sub>O) with a flow of 1.4 mls/min. Detection - Deuterium light source using a detection wavelength of 215nm. Column - Microsorb 5uM C18 column.

Artificial sunlight exposures were made using a Spectral Energy LPS 256 SM and LH 1153 Solar Simulator generating a solar spectrum from 300nm to 700nm (Appendix 3). Exposures to natural sunlight were done at all hours of the day, sun-up to sundown, at the Center for Marine Science Research, Wilmington, NC (approx. 45°N latitude).

#### Toxin purification

PbTx2 (used for spiking) and brevetoxin standards were supplied in dried frozen form by Dr. Dan Baden (Center for Marine Science Research/HABLAB/University of North Carolina at Wilmington). The supplied PbTx2 was further purified by suspending the toxin in methanol (HPLC grade) and peak isolation via HPLC. The collected peak, purified, was dried under vacuum and stored frozen until use as a spiking agent.

#### Samples

Sea-surface microlayer was collected in pre-cleaned glass beakers using the glass plate technique described elsewhere (Hardy et al., 1985). This method consists of vertically dipping a glass-plate through the air-sea interface, withdrawing slowly (~3cm/sec), allowing it to drain for several seconds, then wiping off the adhering material (about 2-4 ml) into a collection vessel with a silicon squeegee. The depth collected by this method is estimated to be the top 30-55 mm of the surface layer.

Seawater samples were collected from a depth of ~0.5 m below the surface by submerging a sealed glass bottle and opening and closing it underwater. Both SSML and seawater samples were collected from the Intercoastal Waterway at the CMSR dock in Wilmington, NC.

Deionized water was from the DI water supply in the CMSR laboratories, the source of which is from a building (CMSR) wide deionization system.

## Experimental Design

The approach in design of these experiments was a more qualitative, as opposed to quantitative, assessment of the changes in the PbTx2 profile in natural waters due to photochemical processes. However, capturing enough data to allow for basic quantitative assessments of potential changes to the PbTx2 profile was considered and brought into the experimental design were methods that would allow for as much quantitative data as could be gained without sacrificing the range of detection. In essence, the design of this experiment was more of a screening and detection process, looking broadly at the possible by-products that may be forming due to photochemical processes.

To allow for preliminary quantitative assessments of possible changes to the PbTx2 profile methods were employed that allowed for collection of peak area data on all HPLC analyses. Quantitative measurements of PbTx2 used for spike preparation and recovered PbTx2 across assays was employed and regressions were generated using known PbTx standards to allow for quantitative estimates of PbTx2 degradation and by-product formation.

In summary, 20 ml to 100 ml samples of seawater, sea-surface microlayer and deionized water were spiked with equal quantities of purified PbTx2 and subjected to light (natural sunlight or solar simulator) and dark conditions for varying periods of time (0 to 36 hours). After a period of exposure samples were extracted with an organic solvent, ethyl acetate, at 0hrs, 2hrs, 4hrs, 8hrs, 24hrs and 36hrs. The collected organic layer (extract) was dried under vacuum and the remaining material suspended in methanol (HPLC grade) and assayed on a Hewlett-Packard 1100 HPLC. Peak area was captured for all samples and used for preliminary quantitative work. Methodology varied only in exposure time and PbTx2 spike concentration. A detailed description of this procedure follows.

## Procedure

PbTx2 spiking solutions consisted of purified PbTx2 (described above), typically 0.1mg to 10mg, suspended in methanol (HPLC grade, from 600ul to 1000ul). Spike solution concentrations were intentionally varied among assays to observe any effects PbTx2 concentration may have on by-product formation or PbTx2 degradation. All spike preparations were mixed thoroughly for uniformity and used within 20 minutes of preparation. Spike solutions were assayed (HPLC) immediately upon preparation and prior to spiking of samples to check for purity (discussed later under 'Spike Purity').

A PbTx2 spike was applied to samples of deionized water, seawater and sea-surface microlayer (glass beakers, 20mls to 100mls of media). All samples in a given assay received exactly the same quantity of PbTx2 spike. Controls were run in tandem with spiked samples and consisted of an identical sample of sea-surface microlayer, seawater or deionized water, without a PbTx2 spike applied, subjected to the same conditions as all spiked samples.

The PbTx2 spiked samples (sea surface microlayer, seawater, deionized water) were subjected to dark conditions at 23-28°C, natural sunlight and exposed under a solar simulator for up to 36 hours. After exposure to a light source or dark conditions all samples (spiked and controls) were extracted 1:1 with ethyl acetate using a separation funnel. The organic layer was collected and dried under vacuum in round bottom flasks. The dried material was resuspended in 400-600ul methanol (HPLC grade), transferred to 10ml scintillation vials and dried under a vacuum a second time, the dried substrate was suspended in 25ul to 100ul HPLC grade MeOH and assayed for by-products on a Hewlett-Packard 1100 HPLC using 5ul - 25ul injections. In the event any salt water sample was assayed, all samples were filtered using a 0.2 $\mu$  nylon membrane filter prior to HPLC analysis.

## PRELIMINARY WORK AND RESULTS

Preliminary investigations into the affects of solar radiation (300nm-700nm) on PbTx<sub>2</sub> degradation and by-product formation examined photochemical effects in seawater, sea surface microlayer and deionized water. The effect of solar radiation on PbTx<sub>2</sub> degradation and by-product formation was distinct and occurred in all three media, however, no significant variance between the three media was observed. While PbTx<sub>2</sub> degradation and by-product formation was consistent in all three media using the methodology employed, early work did reveal inconsistent PbTx<sub>2</sub> spike recovery in saltwater samples (at times 10%-30% less recovery of the PbTx<sub>2</sub> spike in SSML and seawater samples as opposed to deionized water samples). The lower recovery of PbTx<sub>2</sub> spike was attributed to, in part, the presence of a salts/organics matrix possibly binding and sequestering PbTx. Salts and some organic material were present after extraction with ethyl acetate and drying and with the methodology employed were insoluble.

Finding no significant variance between the three media in terms of PbTx<sub>2</sub> degradation and the by-products formed and given greater recovery and consistency of PbTx<sub>2</sub> spike recovery in the deionized water samples, further work, the bulk upon which these results are based, employed only deionized water.

Similarly, preliminary experiments were run employing both natural sunlight and simulated solar energy from an artificial light source and the results were the same, there was no observable difference between the natural or simulated solar radiation in terms of PbTx<sub>2</sub> degradation and by-product formation.

Given the above preliminary findings all final experiments were conducted using deionized water, natural sunlight and a solar simulator as light sources. The solar simulator was chosen as an alternate light source due to its output of the same spectrum and similar intensity of solar energy found in the natural environment (300-700nm) at sea level. Solar simulation also allowed

greater control over the solar energy intensity and exposure time. Try as I may, the weather is difficult to control.

While no significant variations between the SSML and deionized water samples were observed, it is premature to suggest that brevetoxin chemistry in the SSML and deionized water are not dissimilar. The methodology used here was by no means comprehensive as it was designed to detect brevetoxin like compounds. Only organic extracts were assayed, water soluble fractions were not tested, hence, water soluble by-products and by-products better detected at wavelengths other than 215nm may have gone unobserved. Further work will need to be done to assess any existing variance between the photochemistry of the three media in terms of PbTx<sub>2</sub> degradation and the resulting derivatives and/or by-products formed.

## RESULTS

### Overview of Findings

Results from this work suggest photochemistry plays a significant role in PbTx<sub>2</sub> degradation and by-product/derivative formation in the natural environment. The findings here suggest that solar radiation mediates the environmental degradation of PbTx<sub>2</sub> and the formation/generation of brevetoxin derivatives, demonstrating that photochemical processes may strongly regulate the brevetoxin profiles in natural waters. Further, these results may raise interesting questions as to which brevetoxins are produced *in vivo* by *K. brevis*, suggesting some brevetoxins may be environmental by-products, generated via photochemical processes, and may not necessarily be produced by the organism *in vivo*.

## By-Product Formation

The changes in the brevetoxin profile in PbTx<sub>2</sub> spiked aqueous solutions subjected to solar radiation differed markedly from PbTx<sub>2</sub> spiked aqueous solutions subjected to dark conditions. Numerous chemical entities (at least 18 by-products) were present in the solar exposed samples that were not detected in controls (those samples without a PbTx<sub>2</sub> spike applied) and either not detected or present in trace quantities in samples subjected to dark conditions. Chromatograms from a typical experiment (Figure 2) and (Figure 3) illustrate the affects of solar radiation on PbTx<sub>2</sub> degradation and by-product formation over time. Figure 2 is a chromatogram of a typical 8 hr experiment. The chromatograms are from a PbTx<sub>2</sub> spike solution (DiH<sub>2</sub>O) subjected to solar radiation, and its control, an identical sample of DiH<sub>2</sub>O but without a PbTx<sub>2</sub> spike. Evident in the chromatogram is the increase in concentration of by-products, those peaks between retention times of 3 minutes and 8 minutes. The bottom chromatogram in Figure 2 is the control sample, same exposure time (8hrs) and media (DiH<sub>2</sub>O), but with no PbTx<sub>2</sub> spike applied and no detected by-products. Evident in the control is the absence of any by-product formation.

Figure 3 is a typical chromatogram of a PbTx<sub>2</sub> spiked sample (DiH<sub>2</sub>O) subjected to dark conditions for an 8 hour period, consistently observed was the absence of the by-products found in the PbTx<sub>2</sub> spiked solar exposed samples over an 8 hour period. A comparison of typical chromatograms of PbTx<sub>2</sub> spiked samples subjected to solar radiation and dark conditions is seen in (Figure 4). Distinct is the difference between the PbTx<sub>2</sub> spiked solar exposed sample and PbTx<sub>2</sub> spiked sample subjected to dark conditions. Identical results, as presented here in Figures 2 through 4, were observed in all samples exposed for 4hrs, 24hrs and 36 hrs, with greater PbTx<sub>2</sub> degradation and by-product formation occurring as solar exposure time increased. The PbTx<sub>2</sub> spiked solar exposed samples consistently demonstrated significantly greater concentrations of by-product formation (n=17) over varying exposure times (from 2 to 36 hours) and varying concentrations of PbTx<sub>2</sub> spike (from 150ug/100mls to 0.45mg/100mls [bloom concentration]).

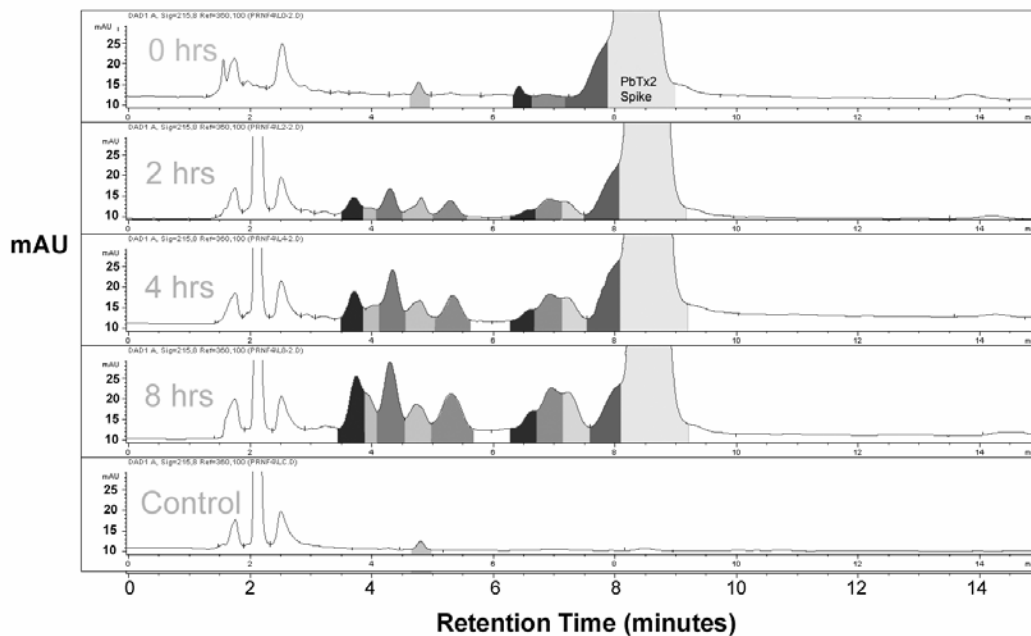


Figure 2: Chromatograms - Effects of Solar Radiation on PbTx2 By-Product Formation

The above 5 chromatograms are from a typical 8 hour solar radiation exposure. In the solar exposed samples above can be seen an increase in by-product formation over time (from 0 to 8 hours) between the retention times (RT) of 3.2 and 7.9 minutes (colored). The PbTx2 spike can be seen at approximately 8.3 minutes (farthest right-gray). Evident in the control is the lack of by-product formation in the absence of PbTx2. The early peaks in the chromatograms, those from 0 minutes to approximately 3.1 minutes are considered insignificant to the purposes of this study, these peaks were common to all samples in all experiments (PbTx2 spiked samples and un-spiked controls under both light and dark conditions). These early peaks (RT's 0 to 3.1 min.) are suspected to be by-products of the methodology employed or by-products not of photochemical origin. Significant is the increase of by-product formation (in the presence of PbTx2) under solar radiation over time, which was found in all solar radiation exposures (n=17).



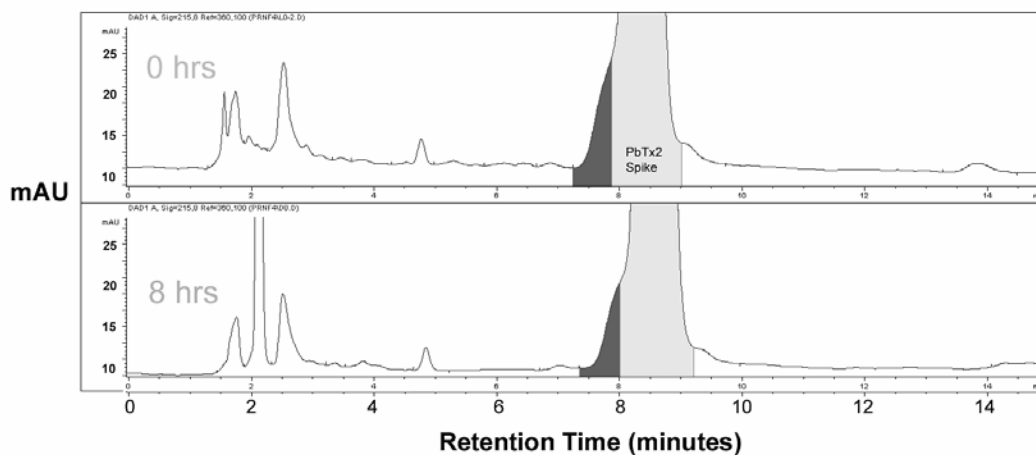


Figure 3: Chromatograms - PbTx2 Spiked Samples Subjected to Dark Conditions

Figure 3 are the chromatograms (same experiment as Figure 2) from samples subjected to dark conditions. Time 0 hours is the time of initial spike. No by-product formation was detected in any of the samples spiked with purified PbTx2 and subjected to dark conditions (n=17). The light gray region is the PbTx2

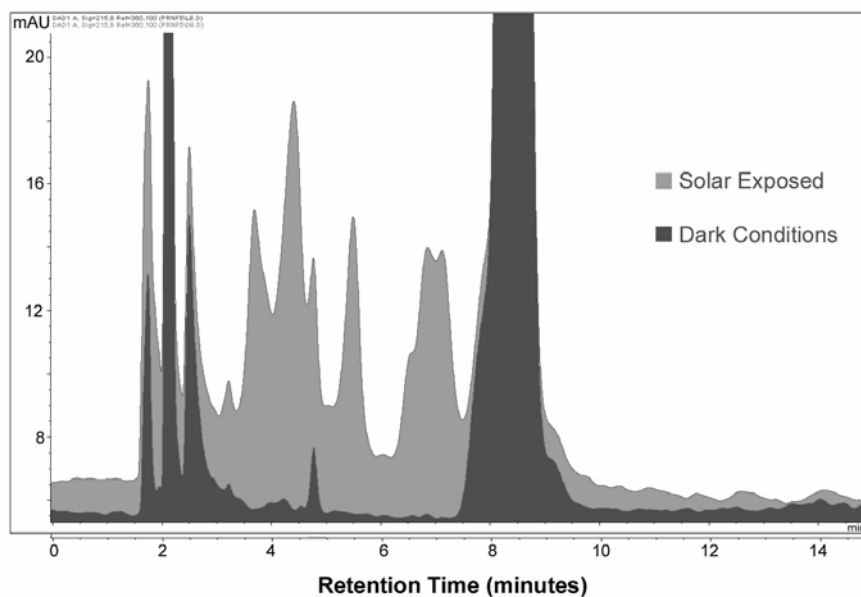


Figure 4: Chromatogram - Solar Radiation vs. Dark Conditions.

Displayed are typical chromatograms from an 8 hour experiment comparing PbTx2 spike samples subjected to solar radiation and PbTx2 spike samples subjected to dark conditions. In the foreground (dark) can be seen the chromatogram from the PbTx2 spiked sample subjected to dark conditions. In the background (light) is the chromatogram from the PbTx2 spiked sample subjected to solar radiation (at 8 hours). Distinct is the formation of by-products unique to the solar exposed samples at RT's of 3.72, 3.91, 4.12, 4.41, 5.32, 5.73, 6.55, 6.88 and 7.20, with no corresponding peaks under dark conditions. The formation of products at RT's of 3.2 and 4.8 were common to both light and dark samples. The unique peaks observed in the solar exposed samples are suggested to be photochemical by-products of PbTx2 origin.

None of the by-products observed in the solar exposed samples were detected in any of the control samples (those samples with no PbTx2 spike applied), these by-products were either not formed (due to the absence of the PbTx2 precursor) or of concentrations below detectable limits.

In summary, significant by-product/derivative formation was observed in samples of DiH<sub>2</sub>O containing a purified PbTx2 spike and subjected to solar radiation. Isolation attempts of the photochemical byproducts/peaks eventually revealed 18 distinct chemical entities, unique to samples exposed to solar radiation. Characterization results suggest some of these by-products may be known brevetoxins or possibly novel brevetoxin derivatives. PbTx2 spiked samples subjected to dark conditions did indicate some by-product formation as seen in the solar exposed samples, however, only in trace concentrations. Hence, significantly less by-product or no by-product was formed in samples subjected to dark conditions. Further, there was little difference between controls (those without a PbTx2 spike applied) and PbTx2 spiked samples subjected to dark conditions. In Figure 5 are chromatograms comparing control samples to those subjected to dark conditions. Apparent is the absence of by-product observed in solar exposed samples, the correlation between controls and dark samples suggests PbTx2 under dark conditions is relatively inert. The observed by-products/derivatives formed in the solar exposed samples appear to be of PbTx2 origin and from photochemical processes. Correlating with the photochemical formation of by-products in PbTx2 spiked samples exposed to solar radiation was a consistent reduction in the PbTX2 spike concentration over time in solar exposed samples, to be discussed in a later section.

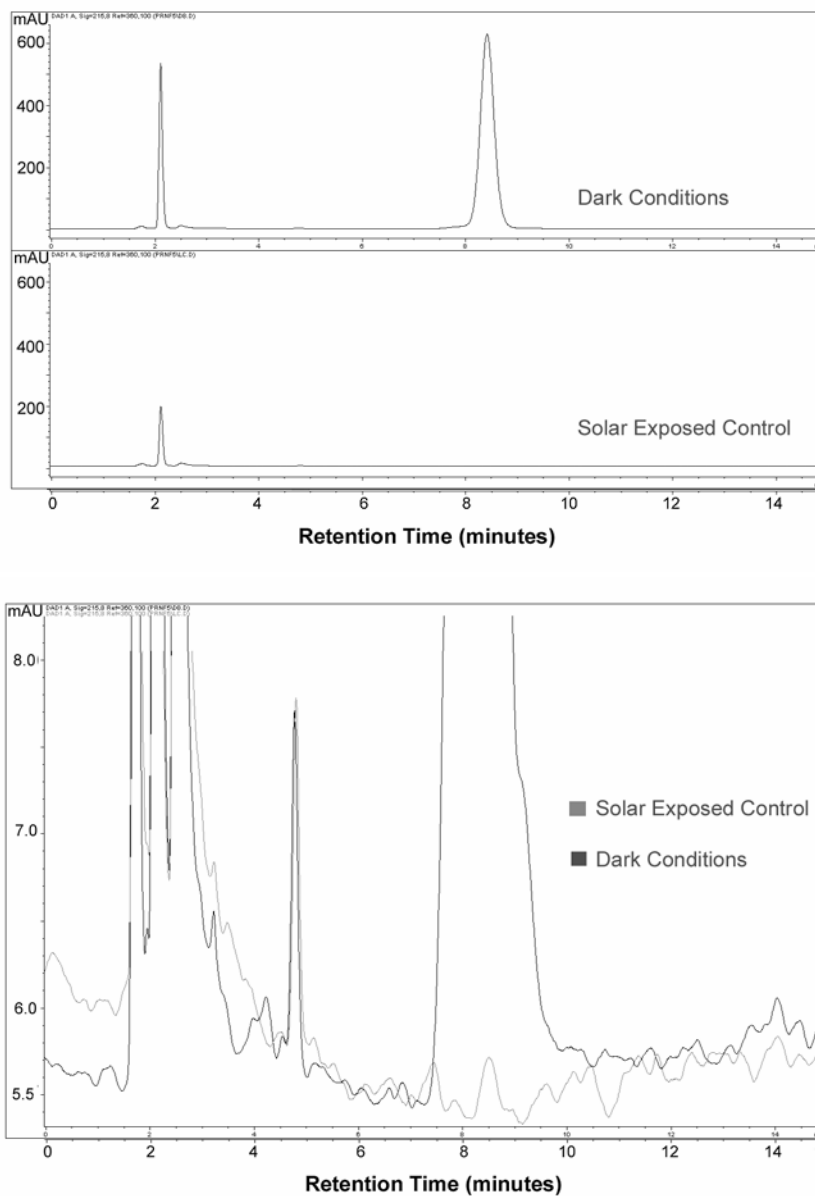


Figure 5: Chromatograms - Control and PbTx2 Spiked Samples

Comparison of a solar exposure control and PbTx2 spiked sample subjected to dark conditions. Top: chromatogram from a PbTx2 spiked sample subjected to dark conditions for 8 hours, and a solar exposed control sample (without PbTx2 spike subjected to solar radiation for 8 hours). PbTx2 spiked samples subjected to dark condition for 8 hours showed little difference from control samples (without PbTx2 spike) subjected to solar radiation for 8 hours, suggesting little reactivity of PbTx2 under dark conditions. Bottom: an overlay of the two chromatograms and exploded view (note mAU's).

## Quantification Overview

While qualitative changes were significant, a thorough quantitative analysis of PbTx2 degradation and derivative/byproduct formation is beyond the scope of the available data collected here (A thorough and accurate quantitative analysis is an area of future research). However, a rough assessment of the quantitative changes can be put forth.

Several factors preclude exact quantification here; 1) Co-elution of by-products prevents ascertaining exact peak area and quantity of material without extensive, conservative purification of all by-products within a given experiment, or a methodology that adequately differentiates peak times. Of the methodologies employed here, those using C18 reverse phase columns with varying ratios of MeOH:H<sub>2</sub>O and ACN: H<sub>2</sub>O, none gave adequate separation of peaks for exact quantitative analysis. 2) Peak area is not indicative of the quantity of material in the media from which it was extracted. PbTx standards prepared using equal quantities of PbTx's 2, 3, 6 and 9 (e.g. 0.1mg), will yield varying peak heights and areas for each toxin upon injection, even though the exact same quantity, by weight, was injected. Figure 6 is a chromatogram of a PbTx2, PbTx3, PbTx6 and PbTx 9 standard solution, prepared using equal quantities of each toxin (0.1mg). As seen, the peak heights and areas for each toxin, though identical quantities, vary. PbTx3 peak area is ~54% of PbTx2, PbTx6 peak area ~56% and PbTx9 ~37%, using the methodology employed. Hence, quantities of PbTx3, PbTx6 and PbTx9 are misrepresented if peak area is used as an indicator of quantity. 3) Exact quantification would entail taking the weights of all materials, PbTx2 spike and all by-products formed, before and after exposures. Inability to isolate peaks of sufficient purity precluded obtaining accurate weight measurements of by-products. 4) Recovery of material, particularly for brevetoxins, varies depending on the solvent used (discussed in the next section – PbTx2 recovery). Hence, peak areas does not necessarily reflect the amount of material actually present, or their ratios one to another, in the media from which they were extracted. Quantitative calculations will need to address these factors if a thorough and precise quantitative

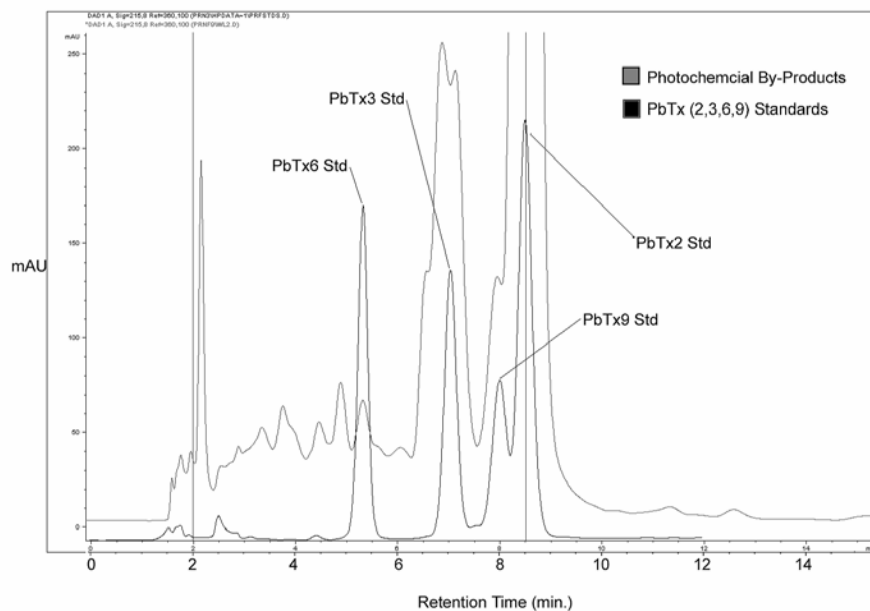


Figure 6: PbTx Standards and By-Products Formed

Chromatogram of PbTx2, PbTx3, PbTx6 and PbTx9 standards with a chromatogram of the by-products from a solar exposed sample (both C18 reverse phase, 85:15 MeOH:H<sub>2</sub>O mobile phase). Co-elution of the PbTx standards was consistent with three peaks in the methanol mobile assessed by both retention time and dual injection.

analysis of degradation and by-product formation is to be done and precise rates of formation of by-product material and PbTx<sub>2</sub> degradation is to be assessed. However, general approximations of by-product formation and PbTx<sub>2</sub> degradation can be offered here. The quantities given here are approximations only and should be considered as such, with the above mentioned factors in mind.

#### Quantification of By-Product Formation

Quantifications were assessed using relative percentages of peak area. Calculations assessed the peak area of by-products as a percent of the peak area of PbTx<sub>2</sub> present in the same sample. PbTx<sub>2</sub> calculations assessed PbTx<sub>2</sub> as a percent of total area of all peaks. All by-products formed were more polar than PbTx<sub>2</sub> using the methodologies employed (Isocratic and gradient 85:15 MeOH: H<sub>2</sub>O and ACN: H<sub>2</sub>O, C18 reverse phase column). In methanol the average retention times (minutes) of significant photochemical by-product peaks were (1) 3.21 (2) 3.72, (3) 3.91, (4) 4.12, (5) 4.41, (6) 5.32, (7) 5.81, (8) 6.55, (9) 6.88, (10) 7.20 and (11) 7.79 as seen in (Figure 7). For the sake of simplicity peaks/by-products will be referenced as numbered in (Figure 7). Unnumbered peaks were not considered significant to this discussion as those peaks were common to both light and dark samples and/or controls, as such they were considered products not of photochemical origin, or artifacts of the methodology, and were not regarded as significant.

A charting of the profile change in PbTx<sub>2</sub> spiked samples from a typical 8hr experiment can be seen in (Figure 8). Distinct is the formation of by-products and degradation of Pbt<sub>x</sub><sub>2</sub> in the solar exposure sample, and the lack of, or marginal formation of by-products in samples subjected to dark conditions. By-product formation and PbTx<sub>2</sub> degradation was observed in all experiments in samples subjected to solar radiation, with exposure times ranging from 4hrs to 24 hrs (n=17). Exposure time and by-product formation, as well PbTx<sub>2</sub> degradation, correlate, with longer exposure times yielding a greater yield of by-product and greater PbTx<sub>2</sub> spike reduction.

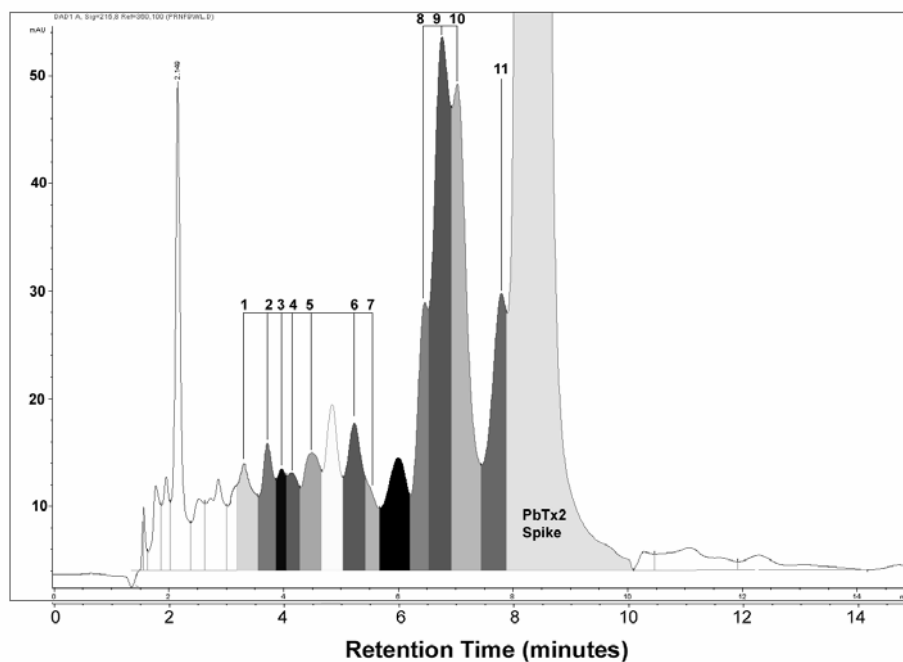


Figure 7: Chromatograms – By-Product Peak Identification

Photochemical by-products were defined as those chemical entities (peaks) unique to solar exposed samples (not found in samples subjected to dark conditions or controls). All by-products formed were more polar than PbTx2 with retention times (RT) between 3.1 and 7.9 using the methodology employed. Average peak times (minutes) of significant photochemical by-product peaks for a typical chromatograms were (1) 3.21 (2) 3.72, (3) 3.91, (4) 4.12, (5) 4.41, (6) 5.32, (7) 5.81, (8) 6.55, (9) 6.88, (10) 7.20 and (11) 7.79. Other peaks seen in the chromatogram in Figure 9 were not considered significant, those peaks not numbered were common to both light and/or dark samples and controls and were not regarded as relevant for the purposes of this study. These materials were considered products not of photochemical origin or artifacts of the methodology and not regarded as significant. [85:15 MeOH: H<sub>2</sub>O - Mobile Phase, C18 Reverse Phase Column].



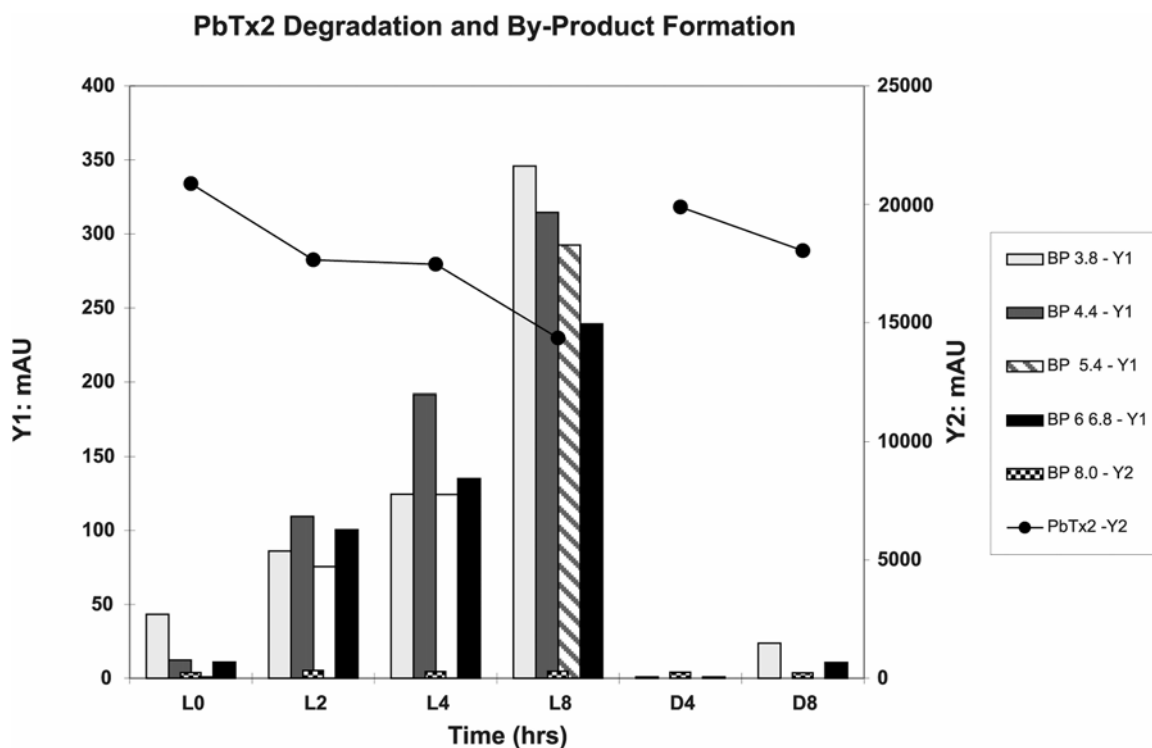


Figure 8: Chromatogram –8hr Exposures

Charting of a typical 8hr experiment of by-product formation in solar exposed samples and samples subjected to dark conditions. Plotted is by-product as a percent of PbTx2. PbTx2 is plotted as a percent of PbTx2 present at time zero, or the time of spike. Suggested is the greater reduction of PbTx2 under light conditions (top line-black), and the formation of by-products not found in samples subjected to dark conditions. L0 through L8 is a PbTx2 spiked sample under solar radiation at 0, 2, 4 and 8 hrs respectively. D4 and D8 are the corresponding PbTx2 spiked samples subjected to dark conditions, D4 and D8 are 4 hours and 8 hours respectively. By-products are listed by their retention times (e.g. BP 5.4), not all byproducts were included for the sake of clarity. The graph is on dual Y-axis. The above is typical of all 8hr exposure experiments (n=6).

Figure 9 plots the average profile change for solar exposed samples and dark condition samples, demonstrating PbTx2 reduction and by-product formation under light and dark conditions, over a 24 hrs period. Table 2 gives the by-product yield from solar exposed samples and samples subjected to dark conditions (average percentages) in samples at 8hrs and 24hrs. Table 3 summarizes average by-product formation for 8hr and 24hr exposures.

#### Quantification of PbTx2 Degradation

Correlating with the photochemical formation of by-products in PbTx2 spiked samples exposed to solar radiation was an apparent and consistent reduction in the PbTx2 spike concentration over time in solar exposed samples. PbTx2 degradation was observed in both light and dark samples, however, degradation in samples subjected to dark conditions was not consistent and marginal, never greater than 9.4% over a 24 hour period. This apparent reduction could be a function of incomplete recovery which could yield an apparent reduction, or it could simply be a product of the variance of peak area data. However, the average reduction of 3% is not statistically significant and ascertaining as to whether PbTx2 reduction under dark conditions occurs will require further investigation. In general, little or no reduction in PbTx2 was observed in PbTx2 spiked samples subjected to dark conditions in all experiments (n=17), with an average reduction in dark samples of 3% (n=6, 8hr exposure; n=2, 24hr exposures).

Quantifications were assessed using relative percentages of peak area, or area under curve. PbTx2 reduction in solar exposed samples was from 24% to 35% (n=6 at 8hr exposures). The greater reduction in PbTx2 concentration in solar exposed versus samples subjected to dark conditions, in conjunction with the formation of what are suggested to be brevetoxin (PbTx2) derivatives suggests the degradation of PbTx2 by photochemical processes. Figure 10 is a typical chromatogram of PbTx2 reduction over an 8hr exposure period under solar simulation (300-700nM). PbTx2 concentrations decreased ranging from 10% to 32% based on calculations using

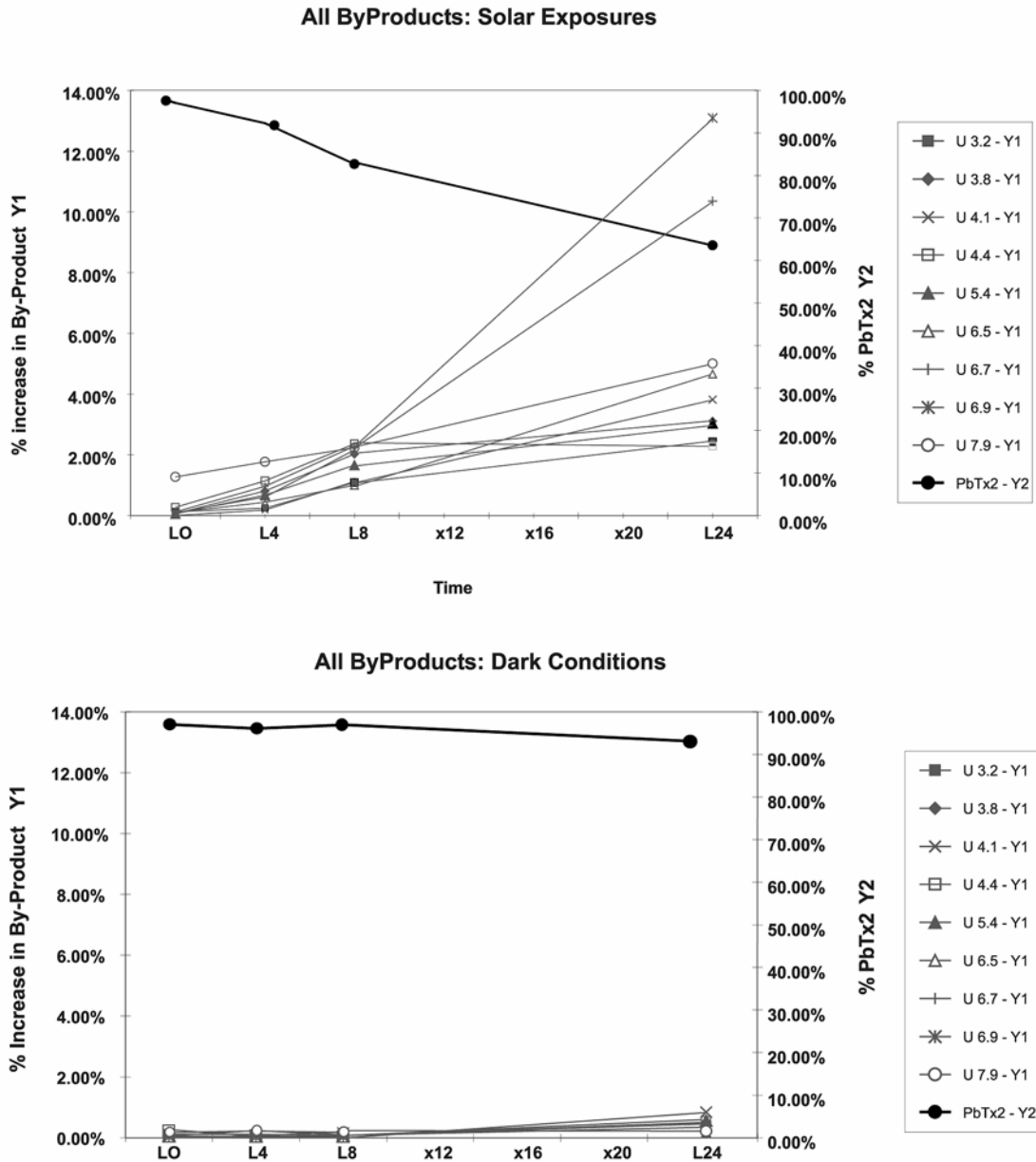


Figure 9: Charting of PbTx2 Profile Changes (24hr Exposures)

Plots comparing by-product formation and PbTx2 spike degradation in solar exposed samples (Top) to samples subjected to dark conditions (Bottom). Displayed are the average increases over time for each byproduct formed (identified by their retention time, eg. U 6.7, etc) and for PbtX2 degradation. L0 and D0 are time zero for both solar exposed and dark samples, L4 and D4 are 4hrs, etc... For (L0,D0 n=6; L4,D4 n=4; L8,D8 n=6; L24,D24 n=3). Plots are based on peak area. By-products are assessed as a percent of PbTx2. PbTx2 calculations reflect PbTx2 as a percent of PbTx2 at time zero, or the time of spike. The averages for by-products and PbTx2 are given below in Table 2.

<b>BY-PRODUCT FORMATION: SOLAR EXPOSURE - 8HRS</b>					
Peak ID	Mean Solar Exp.	AveDev (+,-) Solar Exp.	Mean Dark Cond.	AveDev (+,-) Dark Cond.	n=
B3.2	1.09%	0.54%	0.08%	0.06%	6
B3.7	2.03%	1.02%	0.10%	0.09%	6
B4.1	1.13%	0.88%	0.19%	0.18%	6
B4.3	2.37%	1.01%	0.06%	0.07%	6
B5.3	1.66%	0.61%	0.05%	0.07%	6
B6.7	1.00%	0.34%	0.04%	0.05%	6
B6.9	2.29%	0.57%	0.09%	0.03%	6
B7.2	2.17%	0.96%	0.07%	0.11%	6
B7.9	2.24%	0.24%	1.28%		6
PbTx2	82.64%	4.21%	96.91%	1.22%	6

<b>BY-PRODUCT FORMATION: SOLAR EXPOSURE - 24HRS</b>					
Peak ID	Mean Solar Exp.	AveDev (+,-) Solar Exp.	Mean Dark Cond.	AveDev (+,-) Dark	n=
B3.2	2.42%	0.88%	0.25%	0.06%	3
B3.7	3.11%	0.82%	0.42%	0.15%	3
B4.1	3.82%	0.27%	0.75%	0.06%	3
B4.3	2.29%	0.71%	0.46%	0.25%	3
B5.3	3.04%	0.35%	0.46%	0.16%	3
B6.7	4.66%	0.86%	0.40%	0.35%	3
B6.9	10.35%	1.86%	0.16%	0.06%	3
B7.2	13.09%	5.25%	0.30%	0.05%	3
B7.9	5.01%	0.45%	0.84%	0.84%	3
PbTx2	63.53%	2.55%	93.04%	3.17%	3

Table 2: By-Product Formation

Listed under 'Peak ID' are by-products formed under solar radiation, given by their retention time. Given are the byproducts as a percent of PbTx2 (peak area calculation) and PbTx2 as a percent of total area of all peaks after 8 hr and 24 hr exposures to solar radiation and dark conditions.

**SOLAR EXPOSED SAMPLES: AVERAGE BY-PRODUCT FORMATION AND PBTX2 DEGRADATION**

Peak ID	n=6	n=4	n=6	n=3	AveDev%	AveDev%	AveDev%	AveDev%
	LO	L4	L8	L24	LO	L4	L8	L24
U 3.2 - Y1	0.13%	0.25	1.09%	2.42	0.12%	0.29%	0.54%	0.88%
U 3.8 - Y1	0.07%	0.81	2.03%	3.11	0.07%	0.18%	1.02%	0.82%
U 4.1 - Y1	0.01%	0.19	1.13%	3.82	0.01%	0.19%	0.88%	0.27%
U 4.4 - Y1	0.28%	1.14	2.37%	2.29	0.26%	0.75%	1.01%	0.71%
U 5.4 - Y1	0.06%	0.68	1.66%	3.04	0.07%	0.27%	0.61%	0.35%
U 6.5 - Y1	0.10%	0.44	1.00%	4.66	0.11%	0.12%	0.34%	0.86%
U 6.7 - Y1	0.12%	0.97	2.29%	10.35	0.09%	0.29%	0.57%	1.86%
U 6.9 - Y1	0.10%	0.61	2.17%	13.09	0.14%	0.26%	0.96%	5.25%
U 7.9 - Y1	1.27%	1.77	2.24%	5.01	0.00%	0.40%	0.24%	0.45%
PbTx2 - Y2	97.02	92.2	82.64%	63.53	1.28%	2.07%	4.21%	2.55%

**SAMPLES SUBJECTED TO DARK CONDITIONS: AVERAGE BY-PRODUCT FORMATION AND PBTX2 DEGRADATION**

Peak ID	n=6	n=4	n=6	n=3	AveDev%	AveDev%	AveDev%	AveDev%
	DO	D4	D8	D24	DO	D4	D8	D24
U 3.2 - Y1	0.13%	0.12%	0.08	0.15	0.12%	0.15%	0.06%	0.15%
U 3.8 - Y1	0.07%	0.24%	0.10	0.42	0.07%	0.11%	0.09%	0.15%
U 4.1 - Y1	0.01%	0.07%	0.19	0.75	0.01%	0.09%	0.18%	0.06%
U 4.4 - Y1	0.28%	0.05%	0.06	0.46	0.26%	0.03%	0.07%	0.25%
U 5.4 - Y1	0.06%	0.04%	0.05	0.46	0.07%	0.02%	0.07%	0.16%
U 6.5 - Y1	0.10%	0.05%	0.04	0.40	0.11%	0.06%	0.05%	0.35%
U 6.7 - Y1	0.12%	0.14%	0.09	0.16	0.09%	0.06%	0.03%	0.06%
U 6.9 - Y1	0.10%	0.06%	0.07	0.30	0.14%	0.07%	0.11%	0.05%
U 7.9 - Y1	1.27%	1.59%	1.28	0.84	0.00%	0.70%	0.00%	0.84%
PbTx2 - Y2	97.02%	96.11	96.91	93.04	1.28%	1.82%	1.22%	3.17%

Table 3: Average By-Product Formation and PbTx2 Degradation

Data points based on peak area. Table 3 lists the average by-product formation and PbTx2 degradation over time. The above averages are plotted in Figure 9 . Ratios reflect by-product as percent of PbTx2 and PbTx2 as a percent of PbTx2 spike at time zero. L0 = Solar exposed samples at time zero, D0 = Samples subjected to dark conditions at time zero. L4 and D4 are at 4hrs, L8 and D8 are at 8hrs, L24 and D24 are solar exposed and dark samples at 24hrs,

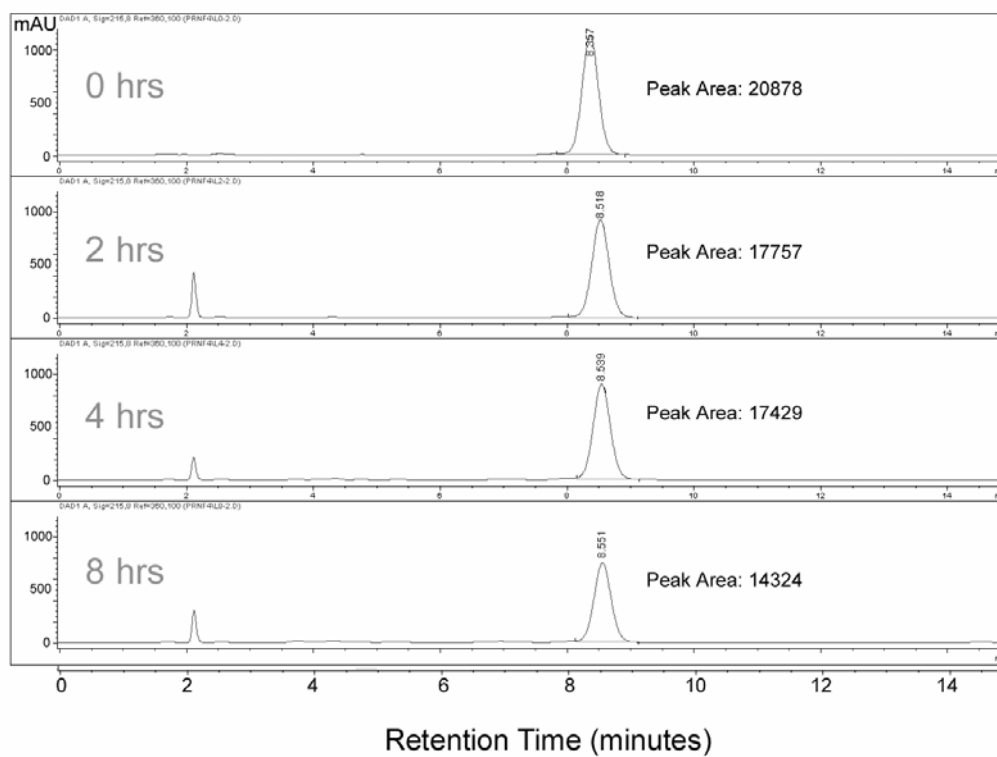


Figure 10: PbTx2 Degradation

In samples subjected to solar radiation PbTx2 spike concentrations were found to diminish with time. The greater reduction in PbTx2 concentration in light versus dark exposed samples suggested photochemical degradation of PbTx2. During an 8 hr exposure period under solar simulation (300-700nM), PbTx2 concentrations decreased ranging from 10% to 32% based on calculations using peak area (n=5 at 8hr exposures). Under dark conditions, PbTx2 concentrations decreased marginally from 0% to 13% (n=5 at 8 hours) with an average reduction of 3% per 8hr period (n=5).

peak area (n=5, 8hr exposures). Figure 11 are plots of PbTx2 reduction in solar exposed samples and samples subjected to dark conditions. Figure 12 illustrates the average reduction of PbTx2 over an 8hr period (n=5) in solar exposed samples and those subjected to dark conditions. The average degradation, based on peak area, of PbTx2 in solar exposed samples over an 8hr period was ~29% (Table 4). Varying concentrations of PbTx2 spike were used in each individual assay to observe for any correlation between concentration and byproduct formation or PbTx2 degradation. Such a correlation between PbTx2 concentration and degradation/byproduct formation may exist if the reactions (degradation, by-product formation) were secondary reactions, dependent on a sensitizer or catalyst.

Whether a correlation between PbTx2 concentration and rates of change, in terms of by-product formation or PbTx2 degradation, exists, is inconclusive. For the data collected here no correlation between PbTx2 concentration and the rate of by-product formation or degradation was observed.

It may be suggested that the reactions taking place are first order reactions, however, this is only a cursory observation, there are limitations to using peak area for quantitative assessments, as were itemized above. A much more thorough investigation into the relationship between concentration and PbTX2 degradation/by-product formation will need to be explored in future experiments designed for quantitative assessment of rates of degradation and by-product formation.

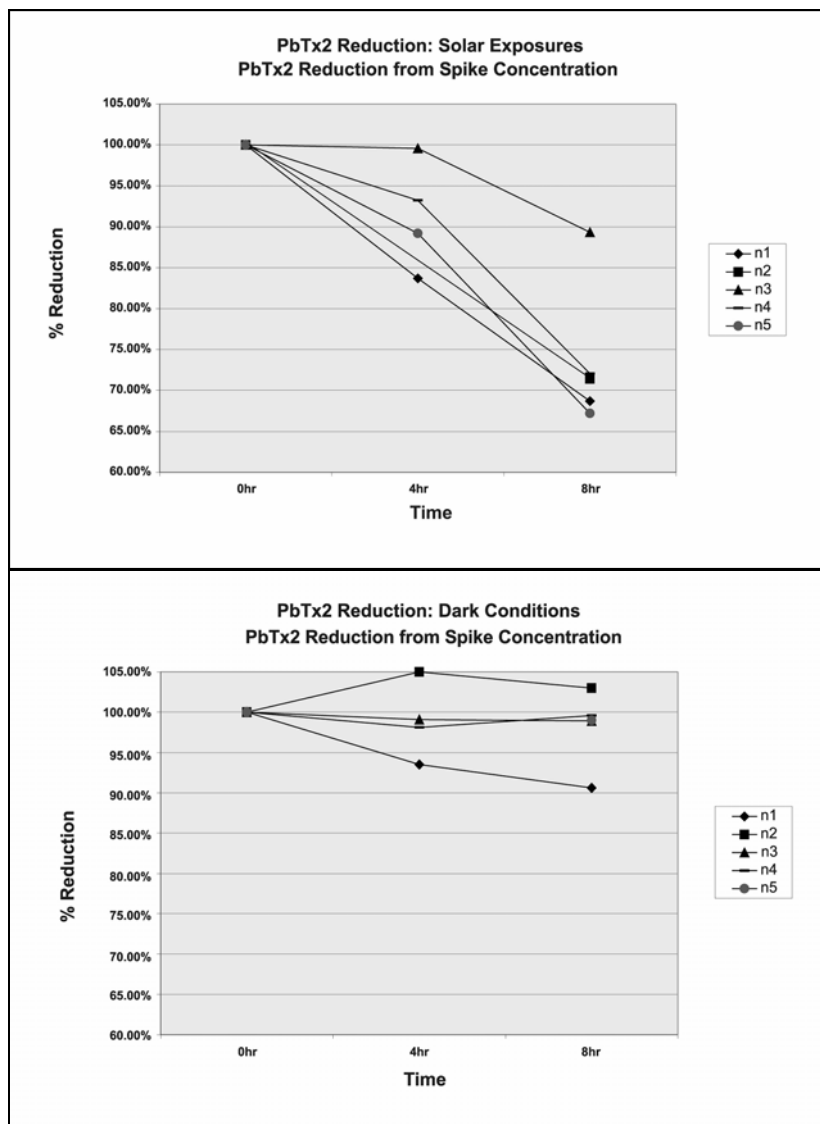


Figure 11: PbTx2 Reduction – Solar Exposed vs. Dark Conditions.

The top Graph plots typical PbTx2 concentrations (peak area) at time 0 (time of spike) against PbTx2 concentrations at 4hrs and 8hrs for solar exposed samples. During 8hr exposures under exposure to solar radiation (300-700nM), PbTx2 concentrations decreased ranging from 10% to 32% based on calculations using peak area (n=5 at 8hr exposure). Bottom: Plots PbTx2 concentration in the samples subjected to dark conditions. Under dark conditions, PbTx2 concentrations may reveal a trend toward a decrease in concentration, though less than that found under solar radiation, from 0% to 13% (n=5 at 8 hours).



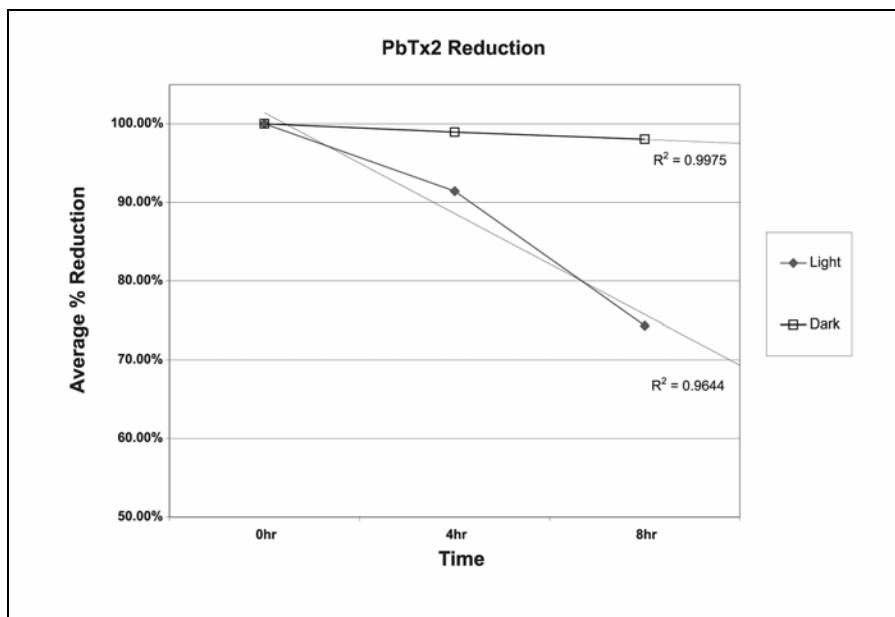


Figure 12: PbTx2 Reduction - Solar Exposed versus Dark Conditions (Averages)

Average reduction of PbTx2 in solar exposed samples and those subjected to dark conditions at 0hrs, 4hrs and 8hrs (n=5). Plots are based on peak area: reduction is assessed by using the ratio of PbTx2 peak area in a sample at time “0”, or time of spike, to peak area after 4hrs and 8hrs of exposure. The average reduction/degradation of PbTx2 in solar exposed samples over an 8hr period was found to be ~29%. Average reduction in samples subjected to dark conditions was ~3%. Reduction of PbTx2 under dark conditions over an 8 hr period is marginal, a 3% reduction is not statistically significant (does not exceed the average deviation). As such further research on PbTx2 degradation under dark conditions should be an area of future study.

<b>PBTX2 DEGRADATION: 8HR EXPOSURES</b>							
<b>N=</b>	<b>1</b>	<b>2</b>	<b>3</b>	<b>4</b>	<b>5</b>	<b>AVE</b>	<b>+/-</b>
Solar	31.30%	10.68%	27.94%	32.80%	28.60%	26.26%	6.23%
Dark	9.4%	** -3.8%	1.1%	0.4%	1.000%	3.0%	3.2%

\*\* (-3.8% represents an increase in PbTx2 based on peak area)

Table 4: Average PbTx2 Reduction

Average PbTx2 reduction on solar exposed samples for 8hr experiments was 26% (+/- 6.3%). Average reduction under dark conditions for the same exposure period was 3% (+/- 3.2%).

## By-Product Characterization

Photochemical by-products were defined as those chemical entities (peaks) unique to solar exposed samples (not found in samples subjected to dark conditions or controls or found in significantly less concentrations). As described earlier, all by-products formed were more polar than PbTx2 using the methodologies employed (Isocratic and gradient 85:15 MeOH: H<sub>2</sub>O) and ACN: H<sub>2</sub>O, C18 reverse phase column). In methanol the average retention time's of significant photochemical by-product peaks were (1) 3.21 (2) 3.72, (3) 3.91, (4) 4.12, (5) 4.41, (6) 5.32, (7) 5.81, (8) 6.55, (9) 6.88, (10) 7.20 and (11) 7.79 as seen in (Figure 7). For the sake of identification peaks will be referenced as numbered in Figure 7. Those peaks not numbered were not regarded as relevant to the purposes of this study as they were common to both light and dark samples and/or controls, as such they were considered products not of photochemical origin or artifacts of the methodology and will not be considered here.

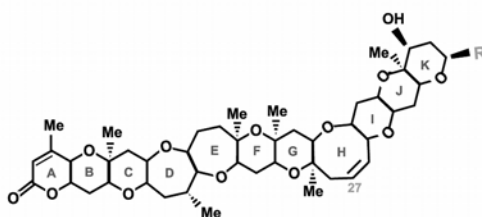
In total, eighteen distinct peaks/by-products were observed suggesting potentially as many individual by-products. Peaks/by-products which co-eluted with brevetoxin standards were given preference for isolation (Figure 6), however, characterization was limited to those by-products which were isolated in sufficient quantity and purity to allow for NMR studies. Of the eighteen by-products four were isolated in sufficient quantities to allow for characterization (Figure 7), peak (6) and the suite of peaks (8), (9) and (10).

Peaks/by-products were isolated via HPLC using a C18 reverse phase column employing both isocratic and gradient mobile phases of MeOH:H<sub>2</sub>O and ACN: H<sub>2</sub>O (each from 85:15 to 70:30) and a Phenyl column (90:10 MeOH:H<sub>2</sub>O). Thin layer chromatography (TLC) plates proved ineffective in isolation attempts, most likely due to an insufficient quantity of by-product material. Characterization of the four isolates was attempted via <sup>1</sup>H-NMR (440 MHz), ELISA, and HPLC-MS.

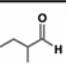
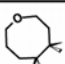
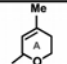
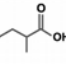
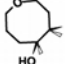
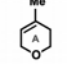
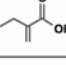
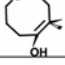
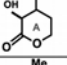
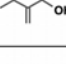

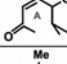
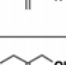
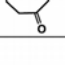
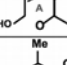
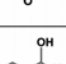
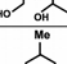
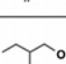
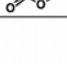
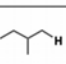
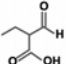

## Analysis of HPLC-MS Peak Ions

HPLC-MS information was obtained for by-product peaks (4), (5), (6), (8) and (11), the results for which can be found in (Table 5). Photochemical modifications to the structure and molecular weight of the PbTx2 spike and the resulting derivative molecular ions can be assumed to result from reaction mechanism based on either oxygen radicals formed by photochemical process in solution or via direct photolysis / photoreduction of active sites on the molecule. Reactive participants in derivative formation are the photochemical intermediates in water which include singlet oxygen ( $^1\text{O}_2$ ), superoxide and hydroperoxide ( $\text{O}_2^-$  and  $\text{HO}_2$ ), peroxide ( $\text{H}_2\text{O}_2$ ) (Zepp et al, 185; Copper, 1989) and hydroxyl ( $\text{OH}$ ). Structural modifications to reactive sites of PbTx2 were considered with these intermediates in mind.

Several possible structural changes resulting from photochemical modifications to the K-ring side chain, H-ring and A-ring lactone are proposed. In (Figure 13) are given twenty theoretical modifications that may occur via photochemical processes, presented are the structures of photochemically modified K-ring, H-ring and A-ring lactone regions, along with the resulting change such modifications would have on the molecular weight of the derivative. The modifications considered were conservative, assessing redox and possible Michael addition reactions to double bonded regions (carbonyl, H-ring and A-ring lactone and methylene). Modifications to C-C bonds or changes involving the rearrangement or relocation of carbons were not considered, such as folding or cleavage. Several HPLC-MS ions yielded masses significantly greater than PbTx2 (m.w. 894), such as ( $m/z$  980), ( $m/z$  961) and ( $m/z$  972), weights that would require considerable hydration.



PbTx Type B

	Side-Chain		H-Ring		A-Ring	
1	 +2	11	 +2	15	 +2	
2	 +18	12	 +18	16	 -14	
3	 +16	13	 +16	17	 +16	
4	 +2	PbTx6	 +14	18	 -14	
5	 -14	14	 +16	19	 +2	
6	 +4			20	 +4	
7	 +2			21	 +2	
8	 +4					
9	 -12					
10	 +32					

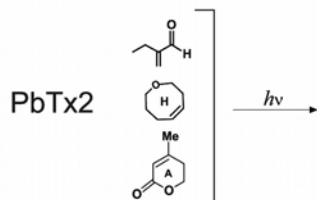


Figure 13: Theoretical Modifications to H-ring, J-ring and K-ring Side Chain.

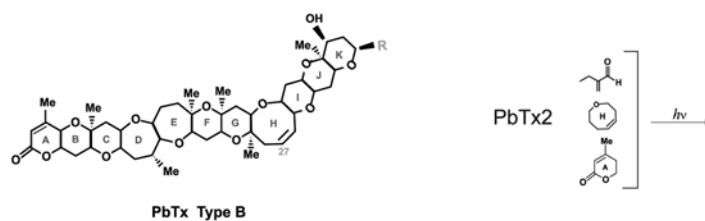
Given are proposed structures resulting from photochemically modified K-ring side chain, H-ring and A-ring lactone regions and the resulting change such modifications would have on molecular weight.

Permutations of possible combinations of the structural modifications given in Figure 13 were assessed (Appendix 1) and the molecular weights resulting from these modifications were compared the weights of molecular ions from the HPLC-MS peak data. Table 5 is a summary of the molecular ions detected for each peak (by-products). Molecular ions in bold are those ions which correspond to the calculated molecular weights from the proposed structural modifications. Molecular ions with an asterisk are those peaks in excess of 50%.

Once molecular ion masses from the HPLC-MS data were correlated to the molecular weights resulting from the proposed modifications, the table in (Appendix 1) was used to assess which structural modifications (Figure 13) yielded masses corresponding to the HPLC-MS ions detected. Not all correlations are given (there were over 400 possible combinations, not all of which yielded molecular weights corresponding to molecular ions from MS data). There were however over 57 possible combinations that would yield molecular weights found as molecular ions from the HPLC-MS data. Figure 14 presents a few of the proposed modifications that yielded molecular weights identical to HPLC-MS molecular ion results. As can be seen, a single modification to the K-ring side-chain, or a combination of modifications to the K-ring, H-ring and A-ring lactone were found to yield relative molecular weights.

Molecular ions below the <40% threshold were not correlated. In total, 3 molecular ions from HPLC-MS results correlated to single K-ring side chain modifications, 3 single H-ring modifications and 2 single A-ring modifications. There were 17 correlations to K-ring/H-ring combination modifications and over 30 combinations of modifications to all three, the H-ring, K-ring and A-ring Lactone.

What can be said is that potentially there are numerous derivatives that may result from photochemical modification(s) to the PbTx2 structure. However, modifications to the A-ring lactone, H-ring and K-ring side chain regions results in altered binding affinities and toxicities (Baden et al, 1994; Gawley et al 1995; Puerkerson-Parker, 2000). The A-ring lactone in particular



Peak ID	Molecular Ions	Modification	Side-Chain	H-Ring	A-Ring	m.w.
Peak 11	876 894 911* 926* 948 980	S5H14				894
		S10				926
		S2H14				926
		S3H13				926
Peak 8	894* 911 926* 943* 957 980* 971	S3Hpbtx6				926
		S3H14A15				926
		S11H13				926
Peak 6	894 912* 919 929* 945 961 976	S2				912
		H11				912
		S1H13				912
		S4H12				912
		S6H14				912
		S3H13A16				912
Peak 4	884 926 928 962* 929* 948 972	S9H11				884
		S5H11A16				884
		S2Hepoxide				928

Figure 14: Correlation of Proposed Structural Modifications to Mass Ions

Given are several of the proposed structures, the molecular weights of which correlate to the mass of molecular ions from HPLC-MS peak data. Not all correlates are listed. Peak 11 contained six molecular ions, two of which correlated to the m.w.'s of theoretical structures. Presented are four possible structures; three combination K-ring/H-ring modifications and a single K-ring side chain modification. Of the seven MS ions in Peak 8 several proposed structures gave correlative molecular weights, three are listed; two K-ring side chain modifications combined with H-ring modifications and one combination of the K-ring side chain, H-ring and A-ring lactone. Peak 6 yielded six molecular ions, and six correlative proposed structures are listed which yield corresponding molecular weights. Peak 4 yielded seven molecular ions and three proposed structures are given which correlate to their molecular weights. Molecular ions (column 2) with asterisk are those ions present in excess of 50%.

seems to play a critical role in binding, loss of the A-ring carbonyl results in a 7 fold loss in binding affinity (Gawley et al, 1995). While the carbonyl reduction affects binding affinity, opening of the ring into an A-ring diol conformation, while diminishing binding affinity, does not significantly alter its ability to affect sodium channel function. Gawley et al (1995) suggested such a modification demonstrated that, while binding affinity was diminished, the saturated A-ring diol (number 19, Figure 13) still retains the ability to populate five conductance states. Similarly, reduction of the H-ring double bond (resulting in a boat-chair to crown conformation) yields ~1000 fold loss in binding affinity (Rein et al, 1994). Conservative modifications to the K-ring side chain have less dramatic effects on binding and toxicity, however, increasing the length of the carbon chain functional group, cyclization and the addition of groups other than aldehydes or alcohols can markedly alter toxicity, even result in antagonistic activity, nulling the toxicity of sister derivatives.

It can be suggested that the number of toxic photochemical derivatives will be limited. A conservative estimate would be those modifications leaving the A-ring carbonyl and H-ring double bond intact (or epoxidized), in conjunction with conservative modifications to the K-ring side chain, as such, significantly toxic derivatives may be limited to less than 5, based on the number of proposed structures that correlate with molecular ions from HPLC-MS results. This assumption has its limits; first, the number of possible theoretical structures exceeds the twenty two that are offered here, secondly, HPLC-MS data exists for only 6 of 17 peaks, the remaining 11 by-products have not been assayed via HPLC-MS, hence, the mass of these ions is unknown.

In summary, the findings here suggest there are at least 18 potential PbTx2 photochemical derivatives, hence, most likely, the total number of photochemical derivatives possible. Whether all of these by-products are toxic is unknown. Of the 16 modifications presented in (Figure 14) only 5, based on the above discussion, present potential significant toxicity, the remaining 11 demonstrate H-ring and A-ring modifications which suggest diminished binding affinities.



HPLC-MS Results: Molecular Ions Present in Given Peaks																				
PbTx Standards					By-Product															
Peak No.	2	3	6	9	4	5	6	6a	8	11	Pb2	8	8a	8b	9	9b	9c	9b	11	
RT HP-HPLC					3.74	4.29	5.41	6	6.55	7.94	8.41	6.55			6.8				7.94	
RT HPLC-MS					5.35	6.87	7.47	8.59	9.51	11.6	12.1	9.51	9.63	9.83	10.0	10.2	10.7	10.8	11.3	
Peak Ions <i>m/z</i> [M+H]					1st Run								2nd Run							
	895	897	911	899	848	*930	<b>895</b>	914	* <b>895</b>	877	*912	*895	895	913	895	895	913	895	899	
					864	*962	* <b>913</b>	930	*912	<b>894</b>	* <b>895</b>	*912	*912	*927	912	*912	*928	912	*912	
					<b>885</b>	* <b>913</b>	920	946	* <b>927</b>	*912	949	*927	*944	*944	927	*927	*944	*927	*927	
					*962	946	*930	*962	*944	<b>927</b>	927	973	*981	957	*944	*944	959	*944	*944	
	Y	N	Y	Y	<b>927</b>	*579	946	977	*981	949		*981	981	981	959	981	961	982		
					929	904	962		958	981					981	981	532			
					978	922	977		972	<b>899</b>										
					<b>948</b>	904														

\*Denotes Ions >50%

Table 5: HPLC-MS Results for Six By-Products

Molecular ions from HPLC-MS results are listed in the columns below each of the by-products assayed. Those values in bold indicate molecular ions which correlate to the molecular weights that exist from the proposed modifications given in Figure 13. [HPLC-MS Information: Source Conditions: ESI+ 4.66kV, 300°C, 25V. Mass Range:500-1100 Da. LC Program:85% MeOH, 10% H<sub>2</sub>O, 5% HOAc (1%) Isocratic. Flow 1.00 ml/min. Reconstituted in 300uL, 10ul Injection]

### Characterization of Peaks 8, 9 and 10

Prior to characterization attempts were made to identify each by-product as a unique chemical entity, to do so, attempts to correlate by-products peaks across mobile phases and columns were made. Initial identification attempts revealed that the three peaks (8), (9) and (10), as seen in (Figure 7, methanol mobile phase) were actually a suite of at least 9 distinct chemical entities when further assayed with an acetonitrile mobile phase (Figure 15). All three peaks (8), (9) and (10) were isolated together using a MeOH:H<sub>2</sub>O mobile phase, dried under vacuum as a collective isolate and further assayed on C18 reverse phase column using an 80:20 ACN:H<sub>2</sub>O mobile phase. The acetonitrile mobile phase apparently yields the best separation revealing 9 distinct peaks chemical entities which apparently co-elute under the MeOH:H<sub>2</sub>O mobile phase. Peak (8) (Figure 7) in the methanol mobile phase appears to correlate to peak (7) in the Acetonitrile mobile phase (Figure 15), peak (9) to (4) and peak (10) to (8), respectively. These are preliminary correlations and should be considered as such, more work will need to be done to verify the correlation of these by-products across mobile phases.

Identification attempts of peak (8), (9) and (10) were also attempted on a phenyl column which yield four fractions with RT's of 1.9, 9.0, 11.1 and 12.3 (90:10 MeOH:H<sub>2</sub>O mobile phase). The material with a RT of 12.3 on the phenyl column was collected and re-assayed via C18 reverse phase column (85:15 MeOH:H<sub>2</sub>O) and was found to co-elute with the PbTx2 standard. When re-assayed there was no product eluting with a RT of those of peaks (8), (9) or (10), the very isolates from which this particular peak (RT 12.3) was collected. It is suspected this particular peak may be an isomer of PbTx2, which peak this correlates to on the C18 reverse phase column (MeOH:H<sub>2</sub>O 85:15) is still a matter of speculation.

An isolate with a RT of 9.0 from the phenyl column yielded 2 distinct peaks when collected and re-assayed on the C18 reverse phase column using the methanol mobile phase. One peak co-eluting with the PbTx2 standard, as the 12.3RT isolate above, and another corresponding to peak (9) in the methanol mobile phase. Hence, isolation attempts of peaks (8), (9) and (10) yielded

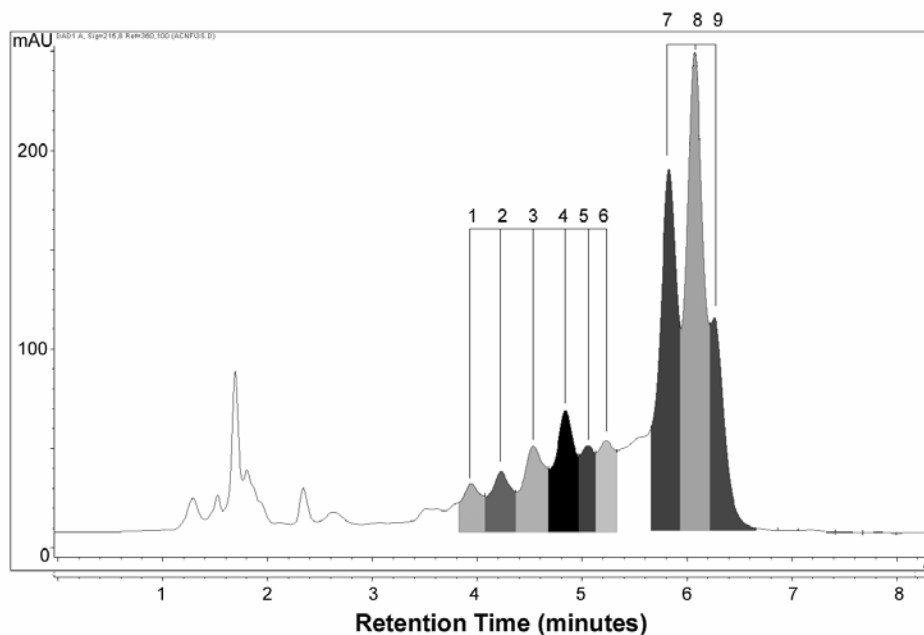


Figure 15: Peaks (8), (9) and (10) [83:17, ACN:H<sub>2</sub>O]

The suite of peaks (8), (9) and (10) were best isolated using an 80:20 mobile phase of ACN:H<sub>2</sub>O, reverse phase C18 column. The suite of peaks were collected together using a C18 reverse phase column, 85:15, MeOH: H<sub>2</sub>O. The collected peaks were dried, resuspended and analyzed using the ACN:H<sub>2</sub>O, 80:20 mobile phase on the same column. The collected peaks (8,9 and 10) yielded the typical chromatogram above, indicating additional chemical entities co-eluting in the methanol mobile phase. The PbTx 3 standard co-elutes with peak (4) above, PbTx2 with the peak (9), the shoulder on the largest peak. However, due to isolation it would be assumed PbTx 2 would not be present. The largest peak with an RT of 6.0 was isolated for NMR.

interesting results under varying mobile phases and columns and Phenyl column work suggested possible isomerization. Two of the nine peaks from the Acetonitrile mobile phase (Figure 15) were eventually isolated in sufficient quantity for <sup>1</sup>H-NMR work and chosen for characterization, these will be called isolate P1 and isolate ACN 5.8 (Peak 8, ACN mobile phase) for the purposes of identification. Isolate P1 was achieved by collecting peaks (8), (9) and (10) together, assaying on a Phenyl column (90:10 MeOH: H<sub>2</sub>O) and collection of the peak with a RT of 9.0. This material was then assayed on a C18 reverse phase column (MeOH:H<sub>2</sub>O) which yielded 2 peaks. The peak with the same RT of peak (9) in the methanol mobile phase was collected for ELISA and <sup>1</sup>H-NMR (Figure 16), and named isolate P1. Isolate ACN5.8 is from the Acetonitrile mobile phase with a RT of 5.8 (Figure 15, peak 8). An overview of the characterization data for all four isolates will be given and the results for each can be found summarized in Table 6.

Isolate P1 yielded a positive ELISA, suggesting a brevetoxin B core structure. The <sup>1</sup>H-NMR spectra (Figure 16) for isolate P1 appears suggestive of a brevetoxin. The spectra suggested 2 aldehyde groups (9.657/9.662, 9.744/9.748 ppm), the typical lactone (2-H) and (27, 28-H) H- ring hydrogens (5.691, 5.682/5.687 ppm) respectively, as well the typical methyl groups associated PbTx2 (1.164-1.329 ppm). Interestingly the <sup>1</sup>H-NMR spectra suggests the presence of 9 methyl groups, one more than PbTx9. Absent in the <sup>1</sup>H-NMR was the indication of the characteristic methylene group of PbTx2. Anomalous is the indication of a second aldehyde group which may suggest isomerization or possibly impurity. The isolate appears similar to the PbTx2 standard in <sup>1</sup>H-NMR spectra, though lacking the characteristic methylene and suggests the presence of an additional proton slightly shifted from the location of the characteristic aldehyde. Given that there are indicated 9 methyl groups and an additional aldehyde it is not impossible that these are the result of impurity.

In summary isolate P1 yields a positive ELISA and suggests a <sup>1</sup>H-NMR spectra resembling the PbTx2 standard. Isolate P1 appears to correspond to peak (9), (Figure 7), however, this is not

a definitive correlation. Given no HPLC-MS data was obtained for peak (9) no comparison to mass ions can be made to the proposed structural modifications discussed earlier.

The second isolate, peak 5.8 from the ACN:H<sub>2</sub>O mobile phase, also yielded a positive ELISA. The <sup>1</sup>H-NMR spectra for peak 5.8 (Figure 17) shares common features with the PbTx3 standard proton spectra (Figure 17). Indicated are the requisite 7 methyl groups (0.996-1.314 ppm), methylene H's (4.383,4.599 ppm), the lactone (2-H) and (27, 28-H) H-ring H's (5.739,5.677/5.705 ppm). This peak/isolate appears to co-elute with the PbTx2 standard in the acetonitrile mobile phase and PbTx3 standard in the methanol mobile phase. As with isolate P1, there is no HPLC-MS data for peak ACN5.8 and no reference to the proposed structures can be made.

While peak (8) from Figure 7 was not isolated in sufficient purity for <sup>1</sup>H-NMR spectra, HPLC-MS data on peak (8) revealed the presence of the characteristic of PbTx2 ion (MH+: *m/z* 895), as well as (MH+: *m/z* 904, 912, 927 and 944), however, it was not observed to co-elute with any PbTx standard. This particular isolate did not yield an adequate <sup>1</sup>H-NMR, however, it did demonstrate a positive ELISA. Several proposed modifications correlated with the HPLC-MS ions (*m/z* 926) and (*m/z* 894) present in peak (8). Figure 13 presents 4 of these modifications which yield masses of 926. Interestingly the characteristic mass of PbTx2 (894.6) is indicated, however, peak (8) does not co-elute with the PbTx2 standard. One proposed modification from Figure 12 (not shown) yields a corresponding mass of 894, this is the combination of (S5H14). The K-ring side chain modification is a simple 5-carbon chain possessing a methylene group and terminal hydrogen. The H-ring modification is a shift of the C-27 double bond to a carbonyl group. Whether such a modification is an accurate correlation and whether the resulting structure is toxic is an interesting consideration.

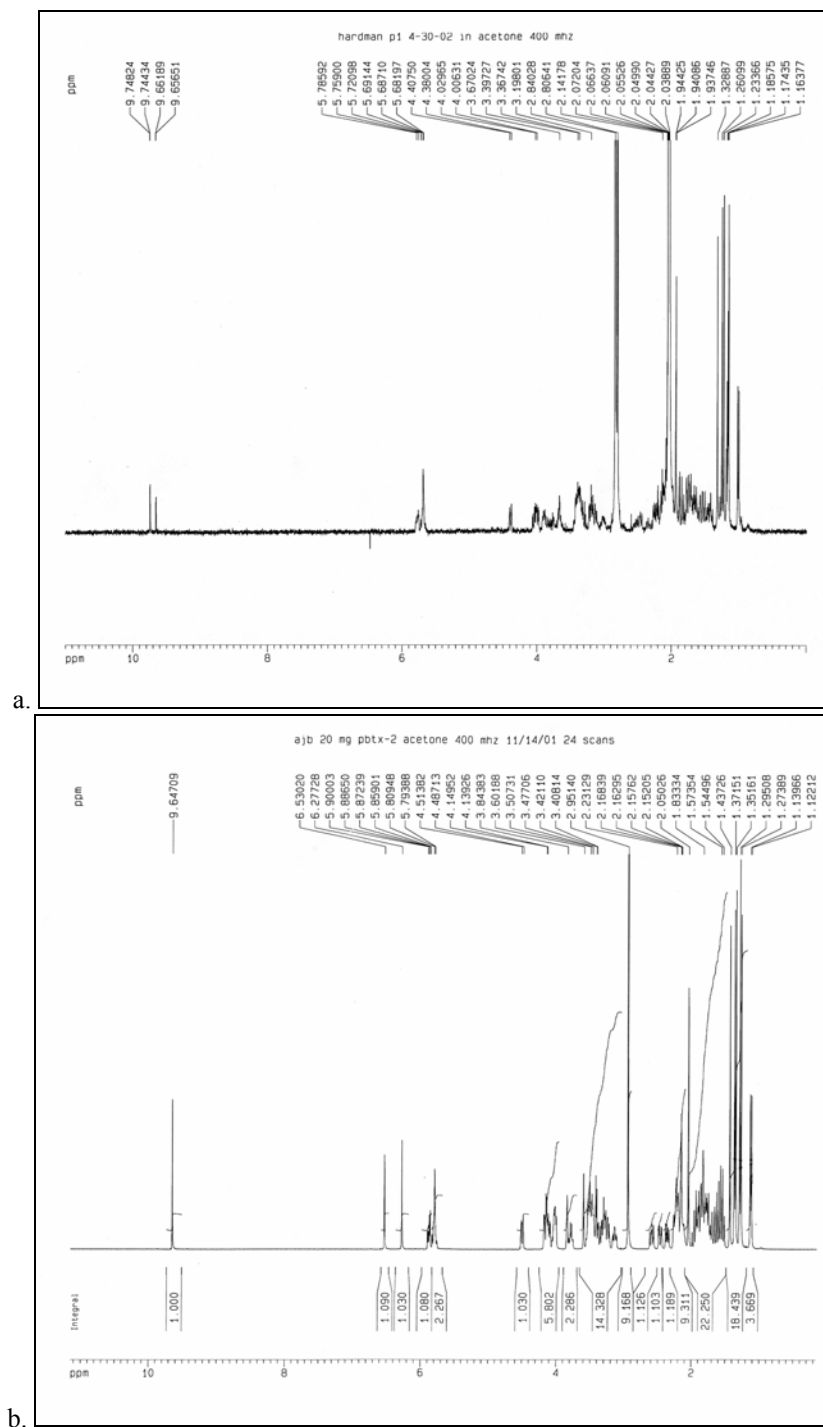


Figure 16:  $^1\text{H-NMR}$  (400 MHz) Spectra - By-Product P1

Isolate P1 appeared similar to the PbTx2  $^1\text{H-NMR}$  spectra (Bottom). The spectra for isolate P1 (Top) revealed 2 aldehyde groups (ppm 9.656, 9.744), the typical (C2-H) lactone and (C27, 28-H) H-ring hydrogens (ppm 5.681, 5.785) as well the typical methyl groups associated brevetoxins (ppm 1.163-1.329). However, absent were the characteristic methylene (C50-H) (ppm 6.277 and 6.530). In essence, Isolate P1 appears similar to PbTx2 yet without the methylene group and an additional aldehyde.

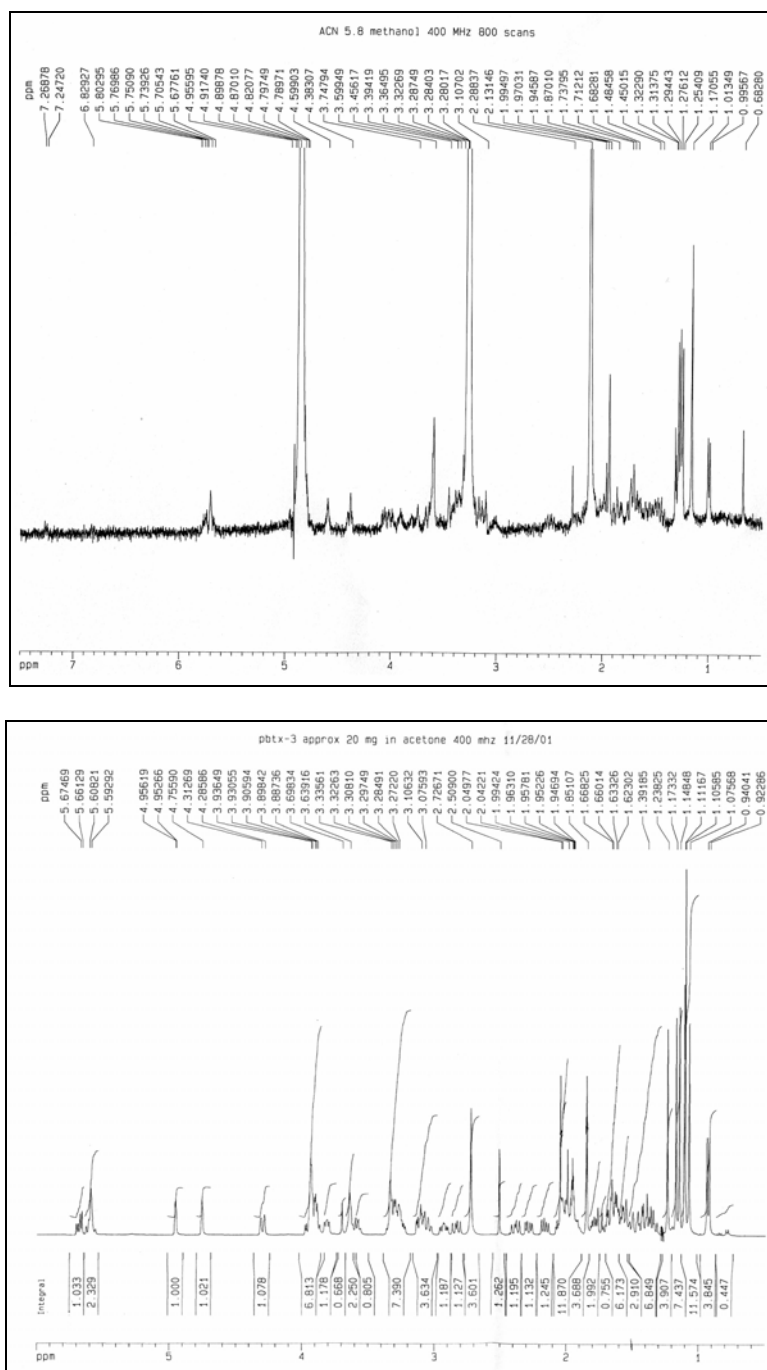


Figure 17: <sup>1</sup>H-NMR (400 MHz) Spectra – Isolate ACN 5.8

Top: <sup>1</sup>H-NMR spectra of the isolate ACN 5.8 indicates characteristic traits of the PbTx3 standard spectra. Present are requisite 7 methyl groups (ppm 0.996-1.323), (C50-H) methylene H's (ppm 4.383, 4.599), the lactone (C2-H) and (C27, 28-H) H-ring H's (ppm 5.678, 5.802). Bottom: PbTx3 standard (in Acetone).

In summary, at least 9 distinct peaks were observed from peaks (8), (9) and (10) upon isolation with an ACN mobile phase (C18 reverse phase column). Two peaks, isolate ACN 5.8 and isolate P1 from phenyl column isolation, were isolated in sufficient quantity to allow for adequate  $^1\text{H}$ -NMR spectra. Both isolates demonstrated positive ELISA, suggesting a brevetoxin B core structure and  $^1\text{H}$ -NMR analysis of the 2 isolates correlate to PbTx2 and PbTx3 standard proton spectra, suggesting these byproducts are possibly brevetoxin derivatives.

#### Characterization of Peak 5

An isolate of peak 5 (RT=5.32) demonstrated a positive ELISA suggesting the presence of the brevetoxin B core structure. As with several isolates, generation of an adequate quantity of material for a clear  $^1\text{H}$ -NMR spectra proved difficult, however, preliminary  $^1\text{H}$ -NMR work suggests similarities between peak (5) and the PbTx6 standard proton spectra. Suggested are the characteristic 7 methyl groups (0.8673 to 1.307 ppm) and (41-H) aldehyde (9.522 ppm), as well the methylene group (6.466, 6.089 ppm) and lactone (2-H) (5.688 ppm). Indistinct and uncertain in the spectra is the characteristic absence of (27,28-H) H-ring hydrogens. The  $^1\text{H}$ -NMR spectra, while more distinct for some of the characteristic protons was inadequate (due to a minimal amount of material) to distinguish between the absence or presence of the (27,28-H).

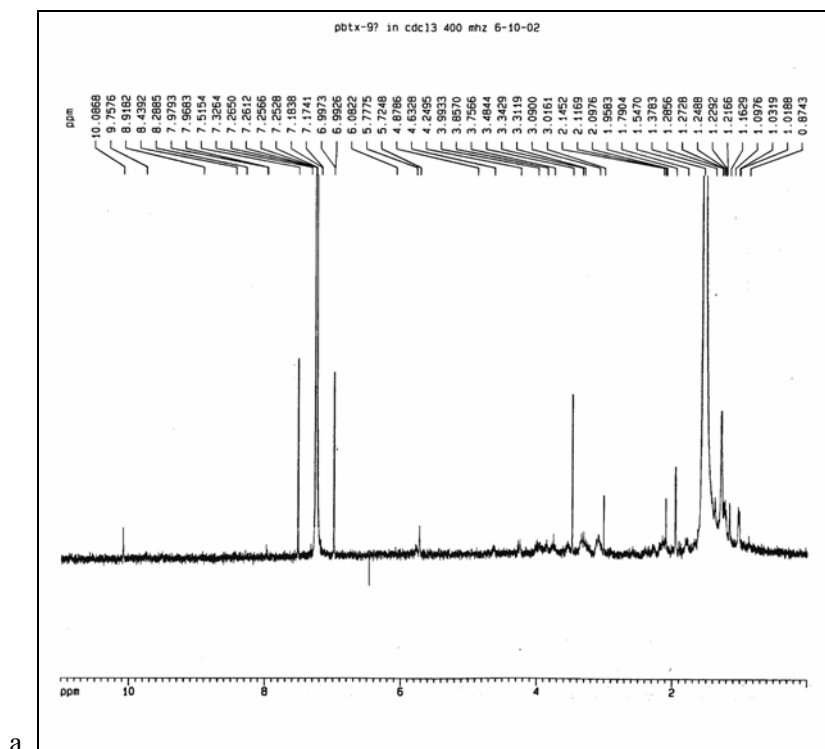
While peak (5) co-elutes with the PbTx6 standard in the methanol mobile phase, HPLC-MS results did not indicate the presence of the PbTx6 brevetoxin ion. Molecular ion masses for peak 5.32 were (MH+:  $m/z$  895), (MH+:  $m/z$  913) and (MH+:  $m/z$  930). Pbtx6 standard is (MH+:  $m/z$  911), Pbtx2 standard (MH+:  $m/z$  895). Structures from the proposed modifications (Figure 13) that correlate to the ion (MH+:  $m/z$  913) bear the characteristic H-ring epoxide with varying K-ring side chain modifications (resulting in a m.w. of 912). Side chains 1, 4 and 7 along with the H-ring epoxide all yield m.w.'s of 912. Of these, K-ring side chains 4 and 7 (Figure 13) possess a methylene group, suggested in the  $^1\text{H}$ -NMR spectra, however, neither of these is an aldehyde,



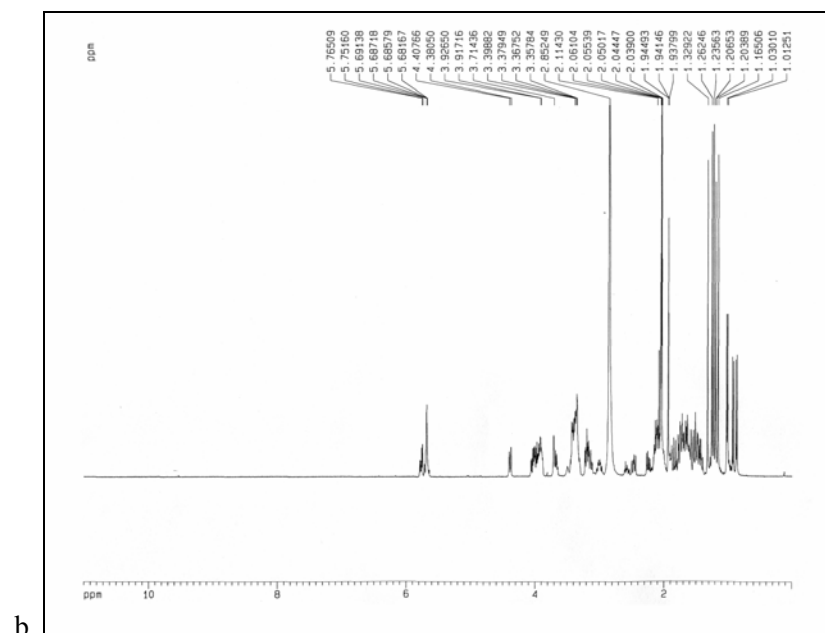
also suggested in the  $^1\text{H-NMR}$  spectra. While it is uncertain, as mentioned, the NMR spectra suggests the presence of the C-27, 28 protons, indicating the lack of the characteristic PbTx6 epoxide. There are also several proposed structures which suit this condition; H-rings 11, 13 and 14 in conjunction with K-ring side chains all result in molecular weights correlative to the HPLC-MS ions present. The combinations are S1H11, S1H13, S4H13, S7H13, S6H14 and S8H14. The proposed modifications which correlate to the molecular ion masses present in peak (5) (Figure 14) are interesting to consider as possible structures for this particular by-product.

#### Characterization of Peak 11

Peak (11), (Figure 7), demonstrated a positive ELISA, suggesting the brevetoxin B core structure. As a by-product the peak was always found to some extent in all samples under light and dark conditions. Its rate of formation appears to be somewhat slower than other peaks and as a by-product only becomes more distinct upon longer exposure times (>24 hrs). Isolation of peak (11) was achieved on a C18 reverse phase column (MeOH:H<sub>2</sub>O 70:30 mobile phase). The  $^1\text{H-NMR}$  spectra is similar to the PbTx9 standard  $^1\text{H-NMR}$  spectra, however, the spectra suggests the presence of an aldehyde (H), which is shifted (ppm =10.086, the PbTx2 standard is 9.514 ppm). Characteristic are the lactone (2-H) (5.725 ppm), (27,28-H) H-ring H's (5.775 ppm) and 8 methyl groups, (0.874-1.286 ppm), (Figure 18). Peak (11) co-elutes with the PbTx9 standard in methanol and HPLC-MS results indicated the presence of a molecular ion mass (MH<sup>+</sup>:  $m/z$  899), characteristic of the PbTx9 brevetoxin ion (MH<sup>+</sup>:  $m/z$  899). Other MS ions for peak (11) were (MH<sup>+</sup>:  $m/z$  877), (MH<sup>+</sup>:  $m/z$  895), (MH<sup>+</sup>:  $m/z$  912), (MH<sup>+</sup>:  $m/z$  927) and (MH<sup>+</sup>:  $m/z$  945). Several proposed modifications, aside from PbTx9 exist whose molecular weights correlate to the molecular ion masses present in peak (11), a summary of these possible structures can be found in (Figure 14).



a.



b.

Figure 18:  $^1\text{H-NMR}$  (400 MHz) Spectra - Peak 11

The  $^1\text{H-NMR}$  spectra (Top) for peak (11) (in  $\text{CDCl}_3$ ), is similar to the  $\text{PbTx}_9$  standard (in acetone)  $^1\text{H-NMR}$  spectra (Bottom), however, the spectra suggests the presence of an aldehyde, shifted to 10.086 ppm ( $\text{PbTx}_2$  standard is 9.514 ppm). Characteristic are the lactone (C2-H) (5.725 ppm) and (C27,28-H) H-ring H's (5.775 ppm) and suggested methyl groups.

## Characterization Summary

Four byproducts were isolated in adequate quantities and purity to allow for preliminary characterization. Each isolate demonstrates a positive ELISA, suggesting a brevetoxin B core structure.  $^1\text{H-NMR}$  spectra for each the by-products suggests similarities to known brevetoxin standards  $^1\text{H-NMR}$  spectra. Hence, the current data suggests these by-products are most likely of brevetoxin (PbTx2) origin and may be known brevetoxins and/or novel brevetoxin derivatives. Similarly, it is suggested that one or more the by-products may be a PbTx2 isomer. A summary table of  $^1\text{H-NMR}$  results for the four isolates can be seen in (Table 6).

Of interest was peak (9), (Figure 7) and its correlate peak (4) of (Figure 15) which was not isolate in a quantity of sufficient purity to allow for NMR work. This particular peak co-eluted with the PbTx3 standard in the both methanol and acetonitrile mobile phases, in varying concentrations. An isolate of this particular by-product demonstrates a positive ELISA, however, the material was found to be impure at the time testing (ELISA) and it cannot be suggested that the ELISA results are valid. However, due to co-elution and the presence of by-products that are suggestive of brevetoxins it is interesting to consider that this particular by-product may be PbTx3.

Correlations of proposed structures (Figure 13) to HPLC-MS molecular ion peak data (Table 5) yielded 57 potential modifications (Appendix 2). Only a select few of these proposed modifications which yielded molecular weights corresponding to HPLC-MS peak ions were presents (Figure 14). Of interest, as seen in (Table 5) are HPLC-MS ions with weights of an odd number (e.g.  $m/z$  911,  $m/z$  943,  $m/z$  957,  $m/z$  971,  $m/z$  919), these could not be accounted for with the proposed modifications. Considered would be carboxyl and carbonyl anions, though they are not favored. The toxicity of these by-products has not yet been determined, precluded by the lack of adequate quantities of by-product in pure form. A more thorough discussion addressing the issue of isolating these by-products will be made in the conclusive remarks ‘Caveats and Recommendations’.

<b><sup>1</sup>H-NMR 400 MHz Spectra By-Products</b>								
	<b>PbTx3</b>	<b>Isolate</b>	<b>PbTx6</b>	<b>Isolate</b>	<b>PbTx2</b>	<b>Isolate</b>	<b>PbTx9</b>	<b>Isolate</b>
	<b>STD</b>	<b>ACN 5.8</b>	<b>STD</b>	<b>Peak(6)</b>	<b>STD</b>	<b>P1</b>	<b>STD</b>	<b>Peak(11)</b>
<b>NMR</b>	Acetone		CDCl <sub>3</sub>		Acetone		Acetone	CDCl <sub>3</sub>
<b>8-Me</b>	0.940	0.0995	1.153	0.867	1.122	1.012	1.023	1.012
<b>13-Me</b>	1.076	1.013	1.159	1.011	1.139	1.029	1.03	1.032
<b>36-Me</b>	1.106	1.171	1.16	1.03	1.274	1.164	1.165	1.097
<b>18-Me</b>	1.112	1.254	1.242	1.157	1.295	1.174	1.204	1.163
<b>22-Me</b>	1.149	1.276	1.245	1.213	1.352	1.186	1.206	1.217
<b>25-Me</b>	1.173	1.294	1.249	1.242	1.371	1.196	1.236	1.229
<b>3-Me</b>	1.238	1.314	1.296	1.281	1.437	1.234	1.262	1.249
<b>41-Me</b>						1.261	1.329	1.273
<b>?-Me</b>						1.329		
<b>27,28 -H</b>	5.593	5.705			5.859	5.759	5.691	5.775
	5.608	5.739			5.873	5.785	5.687	
<b>2-H</b>	5.661	5.750	5.713	5.688	5.793	5.682	5.681	5.725
	5.675	5.769	5.718	5.720	5.809	5.687	5.686	
<b>41- H</b>	4.756	4.383	6.141	6.093/	6.277			
	4.953	4.599	6.396	6.466	6.53			
<b>42-H</b>			9.508	9.522	9.647	9.656		
<b>? - H</b>						9.744		10.68
<b>ELISA</b>	Positive		Positive		Positive		Positive	
<b>HPLC-MS</b>	897*		911	894	895*		899*	876
<b>MH+: m/z</b>	914		928*	912*	912*		910	894
	929		965	919	927		946	911*
	951			929*	949		953	926*
				945				948
				961				980
				976				

Table 6: Summary Characterization Data For Each Isolate

Summarized in Table 6 are the <sup>1</sup>H-NMR 400 MHz spectra [MH+: m/z], ELISA and co-elution results for the four isolates examined.

## PbTx2 Recovery

Assessments of PbTx2 recovery were made using regression analysis and weight measurements of PbTx2 spike material. Regressions were generated using PbTx2, PbTx3, PbTx6 and PbTx9 standards. Quantities of 0.1ug, .25ug, .50ug, 1.0ug, 55ug and 135ug were injected on an HP-HPLC 1100 and regressions generated using quantities correlated to peak area.

Recovery of PbTx2 spiking material from samples was found to be 64% to 71% (n=6), which was considered to be good recovery. Recovery from time zero samples was assessed and correlated with recovery from samples under dark conditions for 8 hours and the PbTx2 spike. Regression analysis of peak areas correlated with weights of spiked and recovered material, supporting the peak areas as a basis for quantitative work.

Several factors can be considered as the source of incomplete recovery of the PbTx2 spike material. One, methodology; the loss of material in the extraction process. Solubility of individual PbTx species varies slightly among organic solvents. While ethyl acetate seems to be a good general solvent for recovering the spectrum of brevetoxins, acetone and methanol appear to be more selective. PbTx2 appears to be better recovered with acetone, PbTx3 with methanol and ethyl acetate. Generally, ethyl acetate appears to be better at extracting the suite of brevetoxins as a whole (hence, employed as the organic solvent in this research).

As reported elsewhere recovery of PbTx3 in ethyl acetate was found to be ~76%, recovery of PbTx2 in ethyl acetate as low as 10% (Whitney and Baden, 2001) and <5% in oyster tissue studies (Plakas et al, 2001). Secondly, the hydrophobicity and non-specific binding of PbTx2 may yield tendencies to bind to glassware where it is simply not dissolved.

A loss of some of the PbTx2 spiking material was most likely due to a combination of all the factors mentioned above. Incomplete recovery cannot be ruled out as a factor that may affect the interpretation of these findings regarding PbTx2 degradation, however, incomplete recovery would not affect findings regarding by-product formation. Across all experiments (n=17) (Figure

9) PbTx2 degradation under dark conditions appeared consistent and in a subset of experiments (n=5) targeting recovery and degradation, degradation of PbTx2 never varied by more than 3.2% (Figure 11).

#### PbTx2 Spike Purity

The two most significant concerns in these experiments were cross contamination between samples via glassware and other equipment and the purity of the PbTX2 spiking solution. Early work revealed cross contamination to be a significant problem and source of error in detecting newly formed photochemical by-products. Hence, the methodology employed in this experiment demanded meticulous cleaning of all materials and equipment throughout the experimental procedure.

Purity of the PbTx2 spike solution was considered to be a critical factor. Purified PbTx2 spiking solution was checked (HPLC) for the presence of other materials and PbTx derivatives immediately upon preparation. Ideal PbTx2 spike solutions would be 100% pure, however, several of the spiking solutions (all spike solutions were assayed via HPLC prior to the application of the spike to samples) were found to contain trace amounts of material which shared a retention time with PbTx3 (Figure 19). Whether this material was a trace quantity of PbTx3 is unknown, however, it's presence was regarded as significant and was checked against by-product formation in solar exposed samples and samples subjected to dark conditions in the experiment in which the spike was used.

Examined were the spiking solutions used for 8 hour experiments (n=9). Trace quantities of material sharing a retention time with PbTx3 were found to be present in four of spike solutions at 0.39%, 0.12%, 0.09%, 0.16% (% of material present, indicated in Figure 19, in respect to total PbTx2 spike). Whether the detected trace quantities in the spike solution were actually present in the spike solution or were residual material in the column is not known, to err on the side of

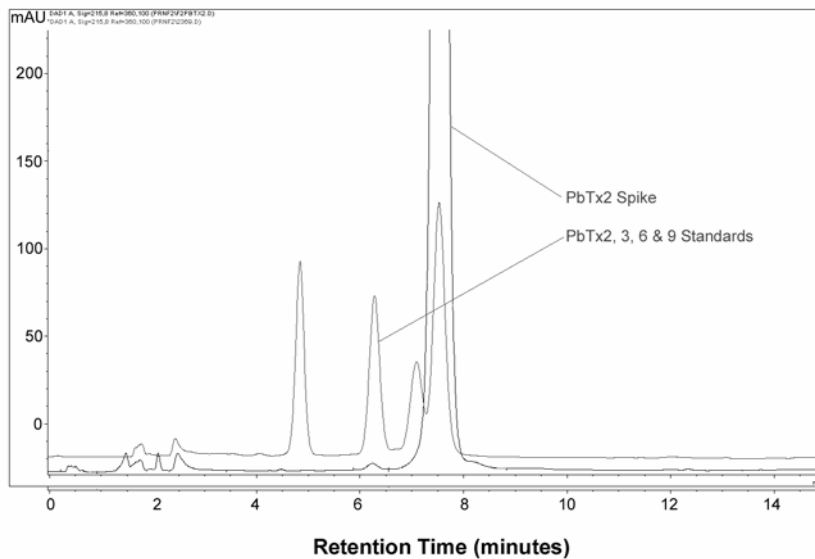
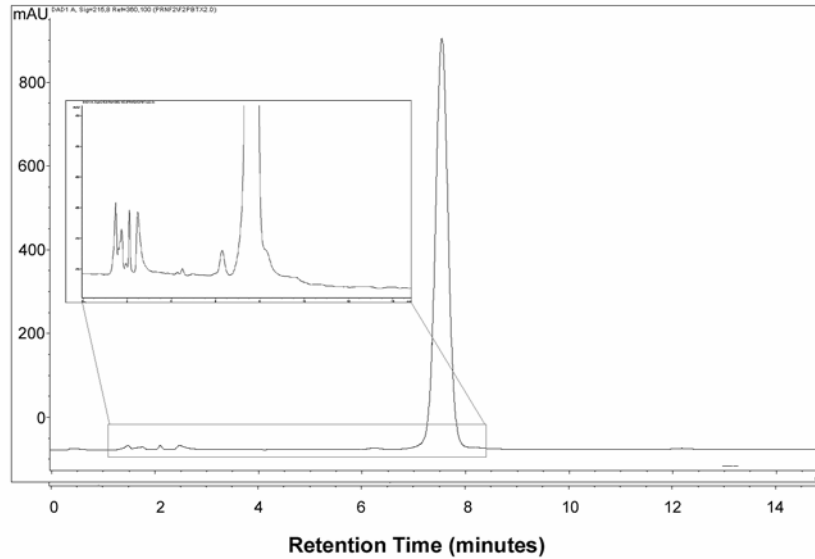


Figure 19: Purity Check of PbTx2 Spike

The chromatograms above are of a PbTx2 spike solution. Bottom: an overlay of a PbTx2 spike chromatogram with PbTx standards. The central significant peak is PbTx2. PbTx standards are indicated, eluting in the order of PbTx6 (RT=4.9), PbTx3 (RT=6.2) PbTx9 (RT=7.3) and PbTx2 (RT=7.9). At a RT of 6.2min can be seen co-eluting with thePbTx3 standard the presence of trace material in the spike. Examined were the spiking solutions used for 8 hour experiments (n=9). Trace quantities of material, possibly trace PbTx3, were found to be present in 4 of the 9 spike solutions at 0.39%, 0.12%, 0.09%, 0.16% (% of PbTx3 present in respect to PbTx2). The peak just left of the PbTx2 spike in the inset (Top) is the trace quantity of PbTx3.

caution it was assumed to be present in the spike solution. As seen in (Figure 20), the concentration of trace material in the PbTx2 spiked samples subjected to dark conditions after an 8 hour period correlates well with the initial percentage of trace material in the spike used for these samples. The ratio of the trace material to PbTx2 found in the spike (prior to spiking of samples) as compared to the ratio found in the dark samples (after 8 hrs) never varied by more than 0.06%.

Hence, there was no change in the trace material/PbTx2 ratio (trace material as a percent of PbTx2) in the spiked dark samples from the moment of spike to the time of extraction 8 hrs later. These findings suggest that the trace material detected in the spike solutions were stable and were not significant in degradation or by-product formation processes. Indirectly these results demonstrate the reproducibility of material recovery and consistency across experiments. A summary of the purity check of the PbTX2 spiking standard is given in Table 7.



	<b>% TRACE MATERIAL IN PBTX2 SPIKE</b>	<b>% TRACE MATERIAL IN DARK SAMPLE</b>	<b>% TRACE MATERIAL IN LIGHT SAMPLE</b>	<b>DARK VS SPIKE Δ</b>	<b>LIGHT VS SPIKE Δ</b>	<b>QTY OF PBTX2 IN SPIKE</b>
n1	0.39%	0.35%	3.35%	-0.04%	2.96%	1.69 mg
n2	0.12%	0.06%	1.67%	-0.06%	1.55%	1.13 mg
n3	0.09%	0.050%	1.37%	+0.04%	1.28%	0.5 mg
n4	0.16%	0.13%	2.82%	+0.03%	2.66%	1.0 mg

Table 7: Spiking Solution Check:

Table 6 is data from four 8hr experiments. This table lists the percent of Trace Material present in the spiking solution, dark samples and light samples. The ratio of Trace Material:Pbtx2 in the spiked dark samples after 8 hrs correlates well with the Trace Material:PbTx2 ratio present in the spike prior to spiking of samples. The variations of the Trace Material:PbTx2 ratios present in the spiking solution vs the dark samples was from +0.03% to -0.06%. In contrast, in the solar exposure samples, the by-product formation of PbTx3 is apparent in the increase over the background levels of Trace Material present in the spike.

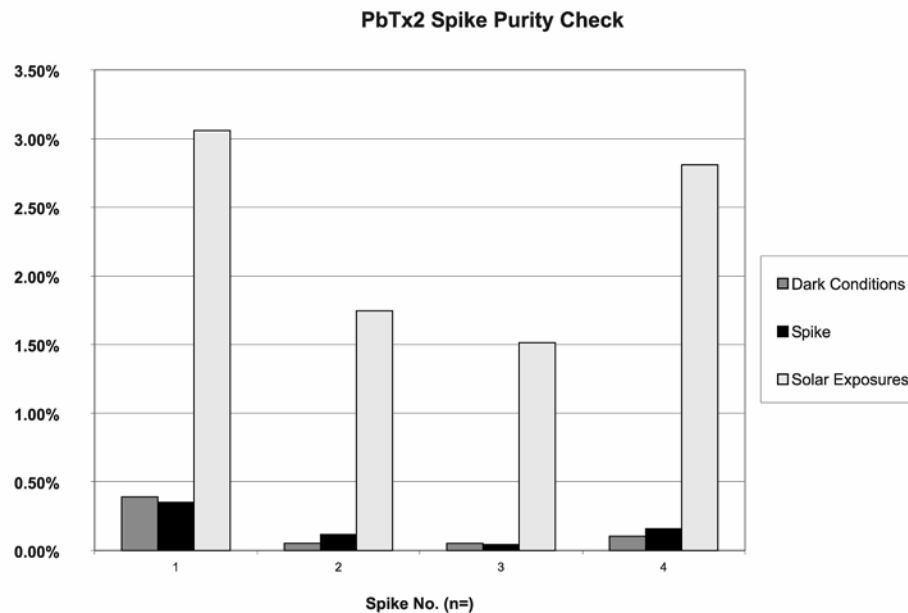


Figure 20: PbTx2 Spike Purity – Comparison Chart

The spiking solution was found to contain trace amounts of material co-eluting with PbTx3, however, this did not affect the results and interpretation of the findings. Examined were 8 hour experiments (n=4), the trace material was found to be present in the spike at 0.39%, 0.12%, 0.09%, 0.16% (% of PbTx3 present in respect to PbTx2) respectively. As can be seen the concentration of trace material detected in the dark samples (receiving the spike indicating the presence of this material) agrees well with the percentages of trace material found in the spike after an 8 hour exposures (Dark Samples=Mid Gray, Spike=Black). The concentration, or ratio of trace material to PbTx2 found in the spike (prior to spiking all samples) as compared to that found in the dark samples after 8 hours never varied by more 0.06%. The increase in solar exposed samples reflects the development of by-product which elutes at the retention time of the trace material (Solar Exposure=Light Gray). The variations in height reflect the different concentrations of PbTx2 spike used in each sample. (n1 spike = 1.69mg; n2 spike=1.13mg; n3 spike=0.5mg; n4 spike=1.0mg). All calculations are based on peak area

## DISCUSSION

### Temperature Effects

Temperature seemed to be insignificant in affecting by-product formation and PbTx2 degradation. Samples were exposed throughout the year with temperature ranges from ~40F to 95F for solar exposed and dark samples. Throughout this range negligible effect on rates of formation or degradation were observed. It should be kept in mind this study was more of a qualitative approach, as such, the observations of temperature effect were crude. Temperature may effect rates of change here as in many other reactions, however, the effects on this particularly reaction appear to be minimal.

### Mass Balance

Generally speaking it can be said that a mass balance between the PbTx2 spike, derivative formation and the total amount material in solution after a given exposure was conserved. While by-product peak area increased and PbTx2 spike area decreased and the total area for all peaks, from time 0 to 24hrs never varied by more than 30% and typical variance of total peak area in a given experiment was found to be less than 10% (n=5). The general trend was that total peak area seemed to declined with greater exposure time. Overall total peak area, which equates to mass balance, was conserved in experiments. Variance will be due to the fact, as discussed earlier, that peak area is not indicative of the quantity of material present ion solution. With 18 by-products, it is likely that, as with brevetoxin standards, some of these compounds exhibit different peak areas in reference to the amount the compound present by mass.

## Theoretical Considerations

The results here suggest the formation of brevetoxin derivatives via photochemical processes, if such derivatives are found to be known brevetoxins, such as PbTx3 and PbTx6, it is interesting to hypothesize that the some or many of the known brevetoxins may be photochemical by-products, produced from a parent structure such as PbTx2.

### *K. brevis* Production- Polyketide Synthesis of Brevetoxins

From a theoretical standpoint the findings here may raise questions as to what the organism (*K. brevis*) is producing in vivo as a secondary metabolite. Intuition would dictate the organism would prefer to be conservative in terms of the synthesis of brevetoxin given the expenditures needed to produce compounds of brevetoxins size and complexity (m.w.894). It may be hypothesized the organism is synthesizing only the one or two structural backbones, PbTx1 and/or PbTx2 for instance, in vivo, while many, or possibly all of the derivatives (PbTx's 3, 6, 7, 9, 10, etc...) may be environmental (photochemical) byproducts.

To test this hypothesis some preliminary experiments were done employing a *K. brevis* culture room (Center for Marine Science Research/UNCW) to observe for the formation of 'grow light' induced by-products which could only be formed under 'culture' conditions. The methodology employed was the same as described earlier in this paper. A sample of deionized water was spiked with purified PbTX2, placed under the artificial grow lights alongside carboys of *K. brevis* cultures and exposed for 8 hrs, 24 hrs and 120 hrs (n=3). A control sample was run in tandem (deionized water spiked with PbTx2, subjected to dark conditions). All samples were extracted after 8 hrs, 24hrs and 120 hrs with ethyl acetate, dried under vacuum and analyzed for by-product formation.

Interestingly, the purified PbTx2 spiked sample exposed under culture conditions (grow lights) alongside the *K. brevis* cultures seemed to reveal modest byproduct formation. Those

samples subjected to grow lights, as opposed to solar radiation, revealed by-products with RT's of 3.2, 3.7 and 4.0 (in the methanol mobile phase), which correspond to the by-products (2), (3) and (4) formed under solar radiation (Figure 7). Other by-products formed under solar radiation, (5), (6), (7), (8) were detected in the culture room samples (grow lights) but not in statistically significant quantities (Figure 21). The results from culture condition experiments seem to suggest the formation of some of the by-products observed under solar radiation, however, the rate of formation was significantly slower.

Historically it has been found that the major brevetoxin produced by *K. brevis* is PbTx2 with lesser amounts of PbTx1, PbTx3, and hemolytic components. Most isolates procured from cultured or environmental samples of *K. brevis* suggested that the organism produced primarily PbTx2, PbTx1 and PbTx3 in the ratio of 20:4:1 respectively, with lesser amounts of the remaining derivatives, ratio's not dissimilar from the ratios of the observed in the photochemical by-product formation seen here (Table 2).

Similarly, past studies indicated that cultures of *K. brevis* yielded different toxin profiles depending upon the growth phase of the organism. It has been observed that the total amount of toxin from culture does not vary, regardless of growth phase, that the 2 aldehyde toxins, PbTx1 and PbTx2 predominate in logarithmic growth phase (Rozell et al, 1989) while stationary growth phase yields profiles composed of 6 toxins including the PbTx1 and PbTx2 as well as the C-27,28 epoxide (PbTx6), the C37 O-acetate (PbTx5), the C42 primary alcohol forms of PbTx2 (PbTx3, PbTx9) and the C43 primary alcohol of PbTx1 (PbTx7) (Rozell et al, 1989). It may be possible these past observations reflect toxin profiles due to degradation of a parent structure, such as PbTx2, due to photochemical transformations of brevetoxin (PbTx2) in solution under a light source, rather than variations in toxin synthesis by the organism itself during different phases of growth.

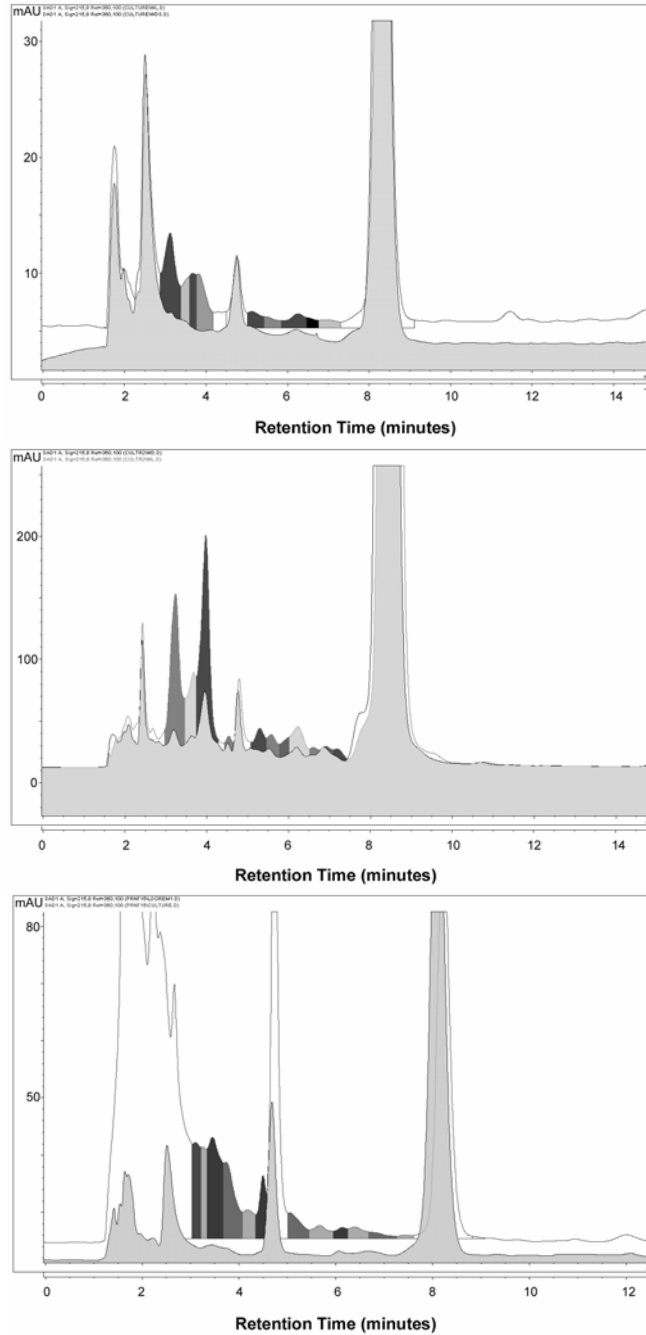


Figure 21: *Karenia brevis* Culture Room Experiments

Chromatograms from preliminary experiments looking by-product formation under ‘grow lights’ (culture) conditions. By-product formation was similar to that found in the solar exposed samples, but not identical. Culture room samples are the background chromatograms with colored shaded peaks. Foreground solid peaks are the samples subjected to dark conditions. Most clear were by-products forming with RT’s between 3 and 3.8 minutes. By-products found in the solar exposed samples with RT’s of 5.4 minutes and higher were detected in the culture room samples, however, not in statistically significant quantities over the samples subjected to dark conditions. Top: 8hr, Middle: 24hrs, Bottom: 120hr Exposures.

Likewise, early investigations into *K. brevis* toxins revealed a perplexing number of isolates (Kim and Padilla et al, 1977; Baden et al, 1981; Alam et al, 1975). Kim and Padilla described the natural decomposition of their isolate, GBTX, into a more polar toxic fraction known as 2b, which ultimately decomposed to nontoxic fractions 2c, and 2d. This decomposition took place at room temp in an ethanol solution. Baden et al (1983) later found that the GBTX was BTX-B, a structure used synonymously with and commonly referenced as PbTx2.

In summary the results from this preliminary work are inconclusive, but interesting. What these preliminary tests (n=3) would suggest is that there may be activity in samples under grow light conditions and this initial observation may merit further research. The findings from the solar radiation experiments suggest that the toxin profiles procured in the past from cultured or environmental samples of *K. brevis* may reflect environmental conditions, that the observed derivatives may not be products of *K. brevis* synthesis, but instead photochemical by-products of a parent structure, such as PbTx2. Or, they may be natural degradatory (reduction) products, however, the findings here suggest degradation and by-product formation under dark conditions is minimal if it occurs at all. As discussed, intuitively the organism would most likely prefer to be conservative in PKS expenditures, particularly when generating a structure as large and complex as brevetoxin (m.w. 894). It is interesting to suggest that *K. brevis* is synthesizing only one or two toxins, possibly only PbTx2 (Type B backbone) or both PbTx2 and PbTx1 (both Type B and Type A backbones), and that the remaining derivatives observed in culture and environmental samples are derivatives due to photochemical transformation of parent type A or type B brevetoxin structures, such as PbTx2.

While extensive work was done employing natural sunlight and solar simulation in the experiments described in the bulk of this paper, the small experiments subjecting a PbTx2 spiked sample to culture conditions was a cursory look (n=3) due to the results of solar radiation experiments. While the samples subjected to culture conditions revealed some correlation with all prior work (same methodology and possible similar by-product formation), more work will

need to be done to further investigate the effects of grow lights and any related photochemical changes to PbTx2 profiles under grow light conditions. Certainly a more thorough look at the effects on by-production formation under grow light conditions is called for.

#### Metabolites

Studies by Plakas et al (2001) have shown that while both PbTx2 and PbTx3 are assimilated by eastern oysters, PbTx2 is rapidly metabolized by the organism where PbTx3 is not. Metabolites of PbTx2 were shown to be PbTx3 and a cystein conjugate. The PbTx3 persisted in tissues and while largely depurated after two weeks was found to remain in tissue at minimal levels after a period of 8 weeks. Hence, PbTx3, once formed metabolically from PbTx2, was not metabolized any further. These results suggest the inherent metabolic stability/instabilities of the two structures and allude to the idea that PbTx2 is readily susceptible to metabolic processes such as reduction of the aldehyde group, a metabolic process not dissimilar from photochemical processes.

#### Photochemistry

The photochemical processes at work here are suggests direct photoreduction/photolysis of the methylene and aldehyde carbonyl's. As discussed earlier, varying concentrations of PbTx2 spike were applied to samples and there was no apparent correlation between PbTx2 concentration and by-product formation or degradation. However, whether the degradation and by-product formation processes are due to direct or indirect photochemical processes remains to be elucidated. Similar studies of microcystins, while not chemically identical, although possessing methylene, carbonyl and carboxyl groups, found that degradation of the toxin was due to indirect, as opposed to direct, photolysis, with degradation occurring in the presence of humic substances (Welker and Steinberg, 1999).



<sup>1</sup>H-NMR spectra suggest changes to primarily to the K-ring side chain carbonyl group and H-ring double bond. Carbonyl's are well known chromophores, however, typically absorbing at lower wavelengths <300nm. Photochemically it is possible the aldehyde functional group is activated by wavelengths in the UVB region.

A subset of experiments were run to assess the effects of UV and PAR on by-product formation. The experimental procedure was identical to that describe earlier in this paper under "Procedure", though the samples were subjected to a variety of light sources; (1) Sunlight, (2) Simulated Solar Radiation, (3) Greenhouse, (4) Laboratory Fluorescent Lighting and (5) Grow Lights in *K. brevis* Culture Room. Light measurements were taken in the each of the exposure areas (Table 8). As is seen, natural sunlight, solar simulated sunlight and greenhouse conditions were those that suggested a full spectrum (Figure 22) of PAR, UVA and UVB. Greenhouse conditions, measuring significantly less available energy across the spectrum, interestingly, yielded similar results as those reported here were under natural and simulated solar radiation. However, the rate of by-product formation was significantly less per unit time as what was observed under natural and simulated solar radiation. The culture room grow lights registered minimal levels of PAR and UVA, no UVB was detected. The energy available from grow light conditions (Figure 22) was a fraction of natural sunlight (0.03% UVA, UVB undetected).

As expected, greatest by-product formation and PbTx2 reduction occurred in those environments with greatest available energies in the UVA and UVB spectrum. Having observed similar by-product formation in greenhouse experiments under significantly lower levels of UV light (UVA 18% of natural sunlight, UVB 3%) it may be inferred that even under lower intensities of energy, as long the appropriate wavelength (energy) is available, by-product formation and degradation will occur, albeit at a corresponding rate.

<b>ELECTROMAGNETIC SPECTRUM</b>			
	<b>PAR</b>	<b>UVA</b>	<b>UVB</b>
	uE/m2/sec	uW/cm2	uW/cm2
Outdoors	1670	3060	290
Culture Room	36.4	11.51	0
Greenhouse	1248	558	9
Lab	9.69	1.55	0
Solar Simulator	1830	4590	820
<i>*Solar Noon: 6.4.2002 Slightly Hazy</i>			

Table 8: Electromagnetic Spectrum Measurements

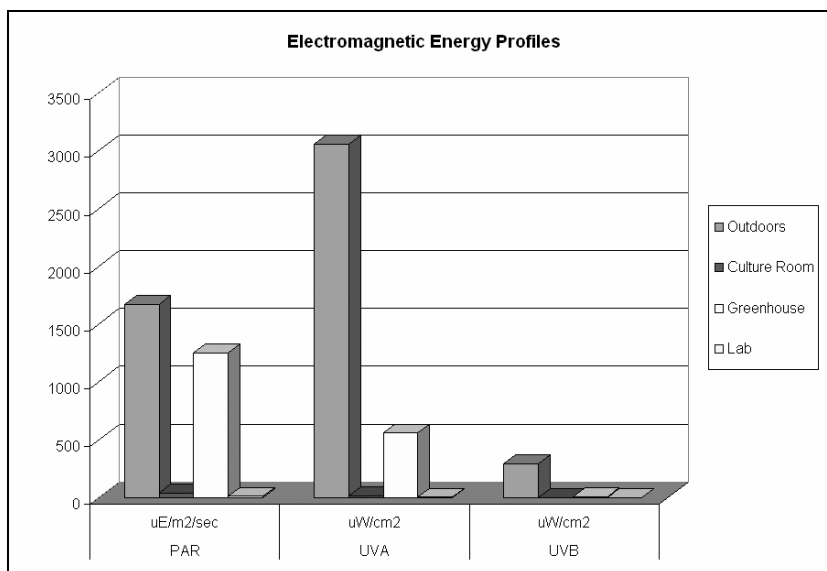


Figure 22: Electromagnetic Energy Profiles

Profiles of the electromagnetic energy available at locations under which samples were exposed. Four locations were measured, (1) Noontime sun at the location where solar exposures were made, (2) The culture room grow lights under which *Karenia brevis* cultures are grown, (3) The greenhouse at CMSR and (4) The fluorescent light output in the laboratory under which these experiments were conducted. PbTx2 degradation and derivative formation was definitively observed only in outdoor sunlight or solar simulated exposures (up to 36 hr exposures). However, preliminary experiments suggest there may be by-product formation under greenhouse and culture room conditions, though these results are inconclusive and more experiments are called for. Given the PAR, UVB and UVA available under each condition and the conditions under which degradation and by-product formation were observed, it suggests, as would be assumed, that energy in the UV part of the spectrum, as opposed to PAR, is driving photochemical process. (Solar simulation output is 1.5 times that of noontime Sun during June at 45 degrees latitude – see Appendix 2).

Interesting to note in culture room samples is the suggestion of the formation of the more polar by-products, corresponding to peaks (2), (3) and (4) from the solar radiation exposures (Figure 6), and the absence of the remaining peaks. If such by-products that seem to be present in the culture room samples are due to light energy, which can be assumed as they were not detected in samples subjected to dark conditions, the only variance between the solar exposed samples and culture room samples is the presence UVB. Whether UVB is more involved in generating peaks (5) through (11), (Figure 6), and UVA more involved in generating other by-products detected is unknown and an interesting consideration.

#### The Environment

Given the results and discussion above, it could be suggested that the transport and fate of brevetoxins in the natural environment is significantly mediated by solar radiation. When there is a release of toxin into the water column upon cell death/lysis, photochemical processes may play a significant role in regulating environmental toxin profiles. The energy of solar radiation at GOM latitudes equals or exceeds solar energy levels employed (both natural and solar simulated radiation) in these experiments, hence, solar energy at GOM latitudes is be more than sufficient to drive the processes at work in these findings. In addition it has been observed that UV-B radiation (290–320nm) penetrates to a depth of 30m in offshore tropical waters (Smith and Baker, 1979).

Natural sunlight exposures in these experiments were made at latitudes of ~45° N, *K. brevis* blooms at typical latitudes of 20° N to 30° N. The solar energy output of simulated sunlight used here in these experiments correlates to a 45°N noon day sun (Appendix 3). Preliminary work, as discussed earlier, revealed no difference between saltwater samples and distilled water samples, as such, it can be inferred from these findings that the observations made here demonstrate what is most likely occurring in the natural environment.

However, the environmental variables affecting PbTx2 by-product formation (speciation) are dynamic, complex and further work will need to be done to elucidate the effects of these variables on brevetoxin chemistry in the natural environment to quantify with some degree of certainty how PbTx2 degrades and its byproducts/derivatives form under environmental conditions. Light attenuation with depth, available PAR/UVA/UVB, free versus intracellular PbTx2 in the environment and the water chemistry of open ocean and estuarine systems are significant variables if the need to thoroughly understand the dynamics of environmental degradation and by-product formation of PbTx2 are needed. These findings may raise more questions than they answer. Certainly work remains to be done on by-product characterization, the photochemical processes at work and quantitative analysis of the rates of formation and degradation.

#### Aerosolized Brevetoxin

One of the more significant aspects of these findings are the implications for the profiles of aerosolized brevetoxin. Past studies have suggested the predominate species of brevetoxin in aerosols were PbTx1, PbTx1, PbTx3 and PbTx6 (Pierce et al, 1990). The findings here suggest that aerosols of brevetoxin may be enriched in other brevetoxin species as well, the by-products detected here, and may have gone undetected in past studies simply due to the fact that these by-products had not yet been observed. Certainly these findings raise questions as to whether these by-products are enriched in aerosols as well.

#### Caveats and Recommendations

Purification of by-products proved difficult using the methodologies employed. Mobile phases (isocratic and gradient MeOH:H<sub>2</sub>O and ACN: H<sub>2</sub>O) from 85:15 to 70:30 proved ineffective in sufficiently isolating peaks for purification. Similarly, thin-layer chromatography (TLC) plates yielded poor results, most likely due to low concentrations of by-product. Future

attempts to purify by-products will need to explore alternative methodologies, such as different columns and/or mobile phases. Further, generation of an adequate quantity of by-product requires sufficient quantities of PbTx2 spike, recommended would be a 5mg spike in 100mls media (Di H<sub>2</sub>O, Seawater, SSML) with extended exposure times (>24hrs). Exposures employing natural sunlight and artificial sunlight yield similar results, however, a greater yield of by-product per unit time may be had employing a solar simulator. Ideally experimental design would incorporate two HPLC setups, one for crude processing of exposed media, fractioning post exposure samples, their by-products and PbTx2 spike remaining, the second HPLC for analytical and/or isolation work. TLC plates may prove useful if an adequate quantity of by-product is generated.

#### Sea Surface Microlayer

The results here do not imply brevetoxin chemistry is not dissimilar in the sea surface microlayer (SSML). More research on brevetoxin photochemistry in the SSML is called for, as discussed, the microlayer concentrates a variety chemical substances, both anthropogenic and biotic; amino acids, proteins, fatty acids, lipids, phenols, halogens, anthropogenic chemicals and pollutants and an array of other organics accumulate in the surface layer. The photochemical intermediates; singlet oxygen (<sup>1</sup>O<sub>2</sub>), superoxide and hydroperoxide (O<sub>2</sub><sup>-</sup> and HO<sub>2</sub>), peroxide (H<sub>2</sub>O<sub>2</sub>) and hydroxyl (OH<sup>•</sup>) and peroxy radicals (RO<sub>2</sub>), as well as halogens, metals, ketones, amines and phenoxy radicals are all known to be present. Given the results of this research, it suggested that additional derivatives may be found occurring in such a matrix, derivatives unable to be formed in a sterile DiH<sub>2</sub>O environment.

## CONCLUSION

The findings here suggest solar radiation has a significant effect on the brevetoxin profile present in the natural environment and allude to what may be occurring during the course of *K. brevis* HAB events in the Gulf of Mexico. These results suggest solar radiation mediates brevetoxin (PbTx<sub>2</sub>) degradation and brevetoxin derivative formation, information vital to understanding the transport and fate of brevetoxin(s) in coastal waters. Undoubtedly photochemical processes will prove valuable in further understanding bloom dynamics and lend insight into the molecular mechanisms of brevetoxin speciation in natural waters.

Further, these results may raise more questions than they answer. Suggested are, potentially, 18 photochemical by-products of PbTx<sub>2</sub> origin; whether these photochemical by-products prove to be known brevetoxin derivatives or are discovered upon full characterization to be novel brevetoxins should be of special interest given their toxicity is not yet known. Of particular concern is the toxicity/pharmacological activity of the photochemical by-products. The presence of such derivatives, if toxic, implies an expanded range of exposure for humans and marine wildlife to brevetoxins which may pose adverse health risks and pose new challenges in assessing the risks of brevetoxin exposure.

If such by-products are indeed brevetoxin derivatives, it may be suggested these particular derivatives are more environmentally stable than the parent compound, PbTx<sub>2</sub>, which would imply longer lifetimes in the environment. These findings suggest that under environmental conditions, PbTx<sub>2</sub> degrades, while the (potential) derivatives detected here increase in concentration. In terms of both acute and chronic exposure, though particularly for chronic exposures, such derivatives/by-products may be of special concern. As such, they may be of significance to public health and marine wildlife as they may pose the known (and possibly greater if such by-products are more environmentally stable) risks associated with brevetoxin exposure.

The results of this work also have implications for aerosolized brevetoxin profiles. Given that brevetoxin tends to accumulate in the surface layer of the ocean (sea surface microlayer) and it is the surface layer most abundant in sea spray aerosols, these results raise interesting questions as to the PbTx profile of aerosolized brevetoxin, common in HAB events in the Gulf of Mexico. Little research has been conducted on the brevetoxin profiles of sea-spray aerosols, these findings may yield new insights and raise interesting questions for this particular area of research.

Lastly, an interesting consideration is the potential these by-products may have as molecular probes. Numerous synthetic brevetoxin derivatives have been generated, a few of which have been employed as molecular probes to elucidate ion channel architecture and function. The possibility exists that one or more of these by-products may promise to serve as such a tool, if so, generation of such a molecular probe via photochemical processes offers to provide an effective and cost effective way to generate derivatives of great value to future investigations into ion channel function and architecture.

These findings yield insight to the transport and fate of brevetoxin in the environment. We have seen that the transport and fate of brevetoxin in the environment may not be a simple matter, the results of this work suggest solar radiation has a significant effect on the brevetoxin profiles present in the natural environment, mediating brevetoxin (PbTx<sub>2</sub>) degradation and brevetoxin derivative formation. Whether some of these photochemical by-products prove to be known brevetoxins or are discovered upon full characterization to be novel brevetoxin derivatives, and more importantly, the determination of their binding affinities and agonistic or antagonistic activity, is an area for future research. Their presence in the environment may be of significance as they may pose the known (and possibly greater if such by-products are more environmentally stable) exposure risks associated with the currently identified brevetoxins.





## REFERENCES

- Alam, M., Trieff, N.M., Ray, S.M., Hudson, J.E. Isolation and partial characterization of toxins from the dinoflagellate *Gymnodinium breve* Davis, *Journal of Pharmaceutical Sciences*, Volume 64, Issue 5, 865-867 (1975)
- Anderson, D. M., Garrison, D.J. The ecology and oceanography of harmful algal blooms. *Limnol. Oceanogr.*, 42, (5). part 2. (1997)
- Anderson, D. M., Toxic algal blooms and red tides: a global perspective. In: *Red Tides : Biology Environmental Science and Toxicology* , T. Okaichi, D. M. Anderson and T. Nemoto (Eds.) Elsevier, NY, pp. 11-16. (1989)
- Anderson, D. M., Hoagland, P., Kaoru, Y., White A., Estimated Annual Economic Impacts from Harmful Algal Blooms (HABs) in the United States. PUB. WHOI-2000-11, Woods Hole Oceanographic Institution. (2000)
- Baden, D. G., Mende, T. J., Amino acid utilization by *Gymnodinium breve*. *Phytochemistry*, 18, 247-251. (1979)
- Baden, D. G., Marine food-borne dinoflagellate toxins, *International Review of Cytology*, Volume 82, Pages 99-150 (1983)
- Baden, D. G., Mende, T. J., Szmant, A. M., Trainer, V. L., Edwards, R. A., Roszell, L. E., Brevetoxin binding: molecular pharmacology versus immunoassay. *Toxicon*, 26, 1. 97-103. (1988)
- Baden, D. G., Brevetoxins: unique polyether dinoflagellate toxins. *Faseb*, 3, 7. 1807-17. (1989)
- Baden, D. G., Bikhazi, G., Decker, S. J., Foldes, F. F., Leung, I., Neuromuscular blocking action of two brevetoxins from the Florida red tide organism *Ptychodiscus brevis*. *Toxicon*, 22, 1. 75-84. (1984)
- Baden, D. G., Rein, K. S., Gawley, R. E., Jeglitsch, G. and Adams, D. J., Is the A-ring lactone of brevetoxin PbTx-3 required for sodium channel orphan receptor binding and activity? *Natural Toxins*, 2, pp. 212-221. pp. 212-221. (1994)
- Baden, D. G., Melinek, R., Sechet, V., Trainer, V. L., Schultz, D. R., Rein, K. S., et al., Modified immunoassays for polyether toxins: implications of biological matrixes, metabolic states, and epitope recognition. *J AOAC Int*, 78, 2. 499-508. (1995)
- Baden, D. G., Rein, K.S., Gawley, R.E., Jeglitsch, G. & Adams, D.J., Marine toxins: scientific approaches, synthetic transformations and molecular mechanisms. T. Yasumoto, Oshima, Y. & Fukuyo, Y., eds. In *Harmful and Toxic Algal Blooms*. (International Oceanographic Commission ICO, UNESCO, Paris, 1996).

- Baden, D.G., and Bourdelais, A.J., Center for Marine Science Research, University of North Carolina at Wilmington [verbal communication]
- Benson, J. M., Tischler, D. L., Baden, D. G., Uptake, tissue distribution, and excretion of brevetoxin 3 administered to rats by intratracheal instillation. *J Toxicol Environ Health A*, 57, 5. 345-55. (1999)
- Berman, F. W., Murray, T. F., Brevetoxins cause acute excitotoxicity in primary cultures of rat cerebellar granule neurons. *J Pharmacol Exp Ther*, 290, 1. 439-44. (1999)
- Blough, N. V., Photochemistry in the sea-surface microlayer. P.S. Liss and R.A. Duce, Ed., In *The Sea Surface and Global Change* (Cambridge University Press., 1996).
- Boesch, D., Donald A. Anderson, Rita A. Horner, Sandra E. Shumway, and, P. A. T., Whittedge, T. E. Harmful Algal Blooms in Coastal Waters: Options for Prevention, Control and Mitigation. NOAA Coastal Ocean Program, Decision Analysis Series., No. 10, Special Joint Report with the National Fish and Wildlife Foundation. (1997)
- Borison, H. L., Ellis, S. and McCarthy, L.E., Central respiratory and circulatory effects of Gymnodinium breve toxin in anesthetized cats. *Br. J. Pharmacology*, 70, 249-256. (1980)
- Bossart, G. D., Baden, D. G., Ewing, R. Y., Roberts, B., Wright, S. D., Brevetoxicosis in manatees (*Trichechus manatus latirostris*) from the 1996 epizootic: gross, histologic, and immunohistochemical features. *Toxicol Pathol*, 26, 2. 276-82. (1998)
- Brousseau, J. L. V., N., Leblanc, R.M., Rein, K.S., Baden, D.G., UV-visible and inelastic electron tunneling spectroscopies of brevetoxins. *Applied Spectroscopy*, 52, 4. 523-527. (1998)
- Capone, D. G., Zehr, J.P., Trichodesmium, a globally significant marine cyanobacterium. *Science*, 276, 5316. 1221-1230. (1997)
- Catterall, W. A., Risk, M., Toxin T46 from *Ptychodiscus brevis* (formerly *Gymnodinium breve*) enhances activation of voltage-sensitive sodium channels by veratridine. *Molecular Pharmacology*, 19, 345-348. (1981)
- CENR, In: National Assessment of Harmful Algal Blooms in US Waters. National Science and Technology Council Committee on Environment and Natural Resources, Washington, D.C. <http://www.habhrca.noaa.gov>. (2000)
- Cestèle, S., and Catterall, W.A., Molecular mechanisms of neurotoxin action on voltage-gated sodium channels. *Biochimie*, 82, 883-892. (2000)
- Clare, J., Tate, S., Nobbs, M., Romanos, M., Voltage-gated sodium channels as therapeutic targets. *Drug Discovery Today*, 5, 11. 506-520. (2000)
- Copper, W. J., Sunlight induced photochemistry of humic substances in natural waters: Major reactive species: I. H. S. a. P. M. eds., Ed., *Aquatic Humic Substances: Influence on Fate and Treatment of Pollutants* (American Chemical Society, 1989), vol. Chemistry Series no. 219.

- Davis, C.C. 1948. *Gymnodinium brevis* sp. nov., a cause of discolored water and animal in the Gulf of Mexico. Bot. Gaz.: 358-360.
- Deshpande, S. S., Adler, M., Sheridan, R. E., Differential actions of brevetoxin on phrenic nerve and diaphragm muscle in the rat. *Toxicon*, 31, 4. 459-70. (1993)
- Dickey, R., Jester, E., Granade, R., Mowdy, D., Moncreiff, C., Rebarchik, D., et al., Monitoring brevetoxins during a *Gymnodinium breve* red tide: comparison of sodium channel specific cytotoxicity assay and mouse bioassay for determination of neurotoxic shellfish toxins in shellfish extracts. *Nat Toxins*, 7, 4. 157-65. (1999)
- ECOHAB, The ecology and oceanography of harmful algal blooms. A national research agenda. ECOHAB workshop Rep., Woods Hole Oceanographic Inst. 66pgs (1995)
- Ellis, S., Introduction to symposium-PbTx's: Chemistry and pharmacology of 'red tide' toxins from *Ptychodiscus brevis* (*Karenia brevis*). *Toxicon*, 23, 469-472. (1985)
- Ewert, L., Frank, D., Shumway, S. E., Ward, J. E., Effect of clay suspensions on clearance rate in six species of benthic invertebrates, Symposium on Harmful Marine Algae in the U.S., Marine Biological Laboratory, Woods Hole, Massachusetts (Symposium Agenda, Abstracts and Participants, 2000).
- Fairey, E. R., Edmunds, J. S., Ramsdell, J. S., A cell-based assay for brevetoxins, saxitoxins, and ciguatoxins using a stably expressed c-fos-luciferase reporter gene. *Anal Biochem*, 251, 1. 129-32. (1997)
- Fleming, L. E. and Baden, D.G. Neurotoxic Shellfish Poisoning: Public Health and Human Health Effects., White Paper for the Proceedings of the Texas Conference on Neurotoxic Shellfish Poisoning, Corpus Christi, Texas. (Proceedings of the Texas NSP Conference, 1998)
- Forrester, D. J., An epizootic of waterfowl associated with a red tide episode in Florida. *Journal of Wild. Dis.*, 13, 160-167. (1977)
- Franz, D. R., LeClaire, R. D., Respiratory effects of brevetoxin and saxitoxin in awake guinea pigs. *Toxicon*, 27, 6. 647-54. (1989)
- FMRI, Florida Marine Research Institute, [<http://www.fmri.edu>]
- Gawley, R. E., Rein, K. S., Kinoshita, M., Baden, D. G., Binding of brevetoxins and ciguatoxin to the voltage-sensitive sodium channel and conformational analysis of brevetoxin B. *Toxicon*, 30, 7. 780-5. (1992)
- Gawley, R. E., Rein, K. S., Jeglitsch, G., Adams, D. J., Theodorakis, E. A., Tiebes, J., et al., The relationship of brevetoxin 'length' and A-ring functionality to binding and activity in neuronal sodium channels. *Chem Biol*, 2, 8. 533-41. (1995)
- Geesey, M., Tester, P. A., *Gymnodinium breve*: ubiquitous in Gulf of Mexico waters?: , *Dev. Mar. Biol.*, (Elsevier, Amsterdam (Netherlands), ed. Toxic Phytoplankton Blooms In The Sea, 1993), vol. 3.

GEOHAB, "A Plan for Co-ordinated Scientific Research and Co-operation to Develop International Capabilities for Assessment, Prediction and Mitigation" For Presentation to SCOR on 3 November 1998 (Report from a Joint IOC / SCOR Workshop, 1998)

GESAMP, The sea-surface microlayer and its role in global change, Rep.Stud.GESAMP, vol. 59. (IMO/FAO/UNESCO/WMO/WHO/IAEA/United Nations/UNEP., 1995)

Gordon, C. J., Kimm-Brinson, K. L., Padnos, B., Ramsdell, J. S., Acute and delayed thermoregulatory response of mice exposed to brevetoxin. *Toxicon*, 39, 9. 1367-74 (2001)

Greene, R. M., Kurtz, J. C., Stanley, R. S., Chancy, C. A., Murrell, M. C., Genter, F. J., et al., Variable brevetoxin production in *Gymnodinium breve* attributable to growth conditions and strain differences (abstract). Presented at the symposium on Harmful Marine Algae, 2000, Woods Hole, Mass., <http://www.epa.gov/ged/publica/c2446.htm>, (2001)

Haddad, K. D., Hydrographic factors associated with west Florida toxic red tide blooms: An assessment for satellite prediction and monitoring. M.S. Thesis, Univ. of South Florida, 161 p. (1982)

Lovejoy, C; Bowman, J P; Hallegraeff, G. M., Algicidal effects of a novel marine pseudoalteromonas isolate (class Proteobacteria, gamma subdivision) on harmful algal bloom species of the genera *Chattonella*, *Gymnodinium*, and *Heterosigma*, *Applied and Environmental Microbiology*, Volume 64, Issue 8, Pages 2806-2813 (1998)

Hallegraeff, G. M., Munday, B.L., Baden, D.G., Whitney, P.L., *Chattonella marina* raphidophyte bloom associated with mortality of cultured bluefin tuna (*Thunnus maccoyii*) in south Australia.: J. B. B Reguera, ML Fernandez, T Wyatt, eds. :, Ed., In: *Harmful Algae*. (IOC, 1998).

Hardy, J. T., Apts, C. W., Crecelius, E. A., & Bloom, N. S. Sea-surface microlayer metals enrichments in an urban and rural bay. *Estuarine Coastal Shelf Sci.*, 20, 299-312 (1985)

Harvell, C. D., Kim, K., Burkholder, J. M., Colwell, R. R., Epstein, P.R., Grimes, D. J., Hofmann, E. E., Lipp, E. K., Osterhaus, A. D.M. E., Overstreet, R. M., Porter, J. W., Smith G. W. and Vasta, G.R., Emerging marine diseases-Climate links and anthropogenic factors. *Science*, 285, 1505-1510. (1999)

Hayes, M. L., J. Bonaventura, T. P. Mitchell, J. M. Prospero, E. A. Shinn, F. Van Dolah and R. T. Barber (2001) How are climate and marine biological outbreaks functionally linked? *Hydrobiologia* 460: 213-220. (2001)

HEED, Health Ecological and Economic Dimensions of Global Change Program: Epstein, E. S. Siegfried, A. Langston, S. Prasad and B. McKay., Ed., In *Marine Ecosystems: Emerging Diseases as Indicators of Change*. Year of the Ocean Special Report on Health of the Oceans from Labrador to Venezuela. (The Center for Health and the Global Environment, Harvard Medical School., Cambridge, 1998), vol.

Hua, Y., Cole, R. B., Electrospray ionization tandem mass spectrometry for structural elucidation of protonated brevetoxins in red tide algae. *Anal Chem*, 72, 2. 376-83. (2000)

- Huang, J. M., Wu, C. H., Baden, D. G., Depolarizing action of a red-tide dinoflagellate brevetoxin on axonal membranes. *J Pharmacol Exp Ther*, 229, 2. 615-21. (1984)
- Huh, O. K., Wiesman, W. J., Rouse, L. J., Intrusion of the Loop Current waters onto the west Florida continental shelf. *J. Geophys. Res.*, 86, 4186-4192. (1981)
- Ishida, Y., Shibata, S., Brevetoxin-B of *Gymnodinium breve* toxin-induced contractions of smooth muscles due to the transmitter release from nerves. *Pharmacology*, 31, 4. 237-40. (1985)
- Ishida, H., Muramatsu, N., Nukaya, H., Kosuge, T., Tsuji, K., Study on neurotoxic shellfish poisoning involving the oyster, *Crassostrea gigas*, in New Zealand. *Toxicon*, 34, 9. 1050-3. (1996)
- Jeglitsch, G., Rein, K., Baden, D. G., Adams, D. J., Brevetoxin-3 (PbTx-3) and its derivatives modulate single tetrodotoxin-sensitive sodium channels in rat sensory neurons. *J Pharmacol Exp Ther*, 284, 2. 516-25. (1998)
- Johnson, G. L., Spikes, J. J., Ellis, S., Cardiovascular effects of brevetoxins in dogs. *Toxicon*, 23, 3. 505-15. (1985)
- Kerr, D. S., Briggs, D.M., and Saba, H.I, A neurophysiological method of rapid detection and analysis of marine algal toxins. *Toxicon*, 37, 1803-1825. (1999)
- Khan, S., Arakawa, O., and Onoue, Y., Neurotoxins in a toxic red tide of *Heterosigma akashiwo* (Raphidophyceae) in Kagoshima Bay, Japan. *Aquacul. Res.*, 28, 9-14. (1997)
- Kim, Y S; Padilla, G M Hemolytically active components from *P. parvum* and *G. breve* toxins, *Life Sciences*, Volume 21, Issue 9, 1977, 1287-1292 (1977)
- Kimm-Brinson, K. L., Ramsdell, J. S., he Red tide toxin, brevetoxin, induces embryo toxicity and developmental abnormalities. *Environ Health Perspect*, 109, 4. 377-81. (2001)
- Koley, J., Sinha, S., Basak, A.K., Das, M., Dube, S.N., Majumder, P.K., Gupta, A.K., Dasgupta, S., Koley, B., Cardiovascular and respiratory changes following exposure to a synthetic toxin of *Ptychodiscus brevis*. *European Journal of Pharmacology*, 293, Environmental Toxicology and Pharmacology Section 293. 483-486. (1995)
- Krueder, C., Bossart, G.D., Elle, M., Clinicopathologic features of an epizootic in the double-crested cormorant (*Phalacrocorax auritus*) along the Florida Gulf Coast. *Proc. Wildlife Dis. Assoc.*, (1998)
- Liu, G., Janowitz, G.S., Kamykowski, D., Influence of environmental nutrient conditions on *Gymnodinium breve* (Dinophyceae) population dynamics: a numerical study. *Marine Ecology Progress, MEPS* 213, 13-37. (2001)
- Lenes, J. M., Darrow, B.P., Cattrall, C., Heil, C., Vargo, G.A., Callahan, M., Byrne, R.H., Prospero, J.M., Bates, D.E., Walsh, J. J., Iron fertilization and the *Trichodesmium* response on the West Florida shelf. *Limnology and Oceanography*, (2001)

- Lin, Y.-Y., Risk, M., Isolation and structure of brevetoxin B from the red tide dino<sup>-</sup>agellate *Ptychodiscus brevis* (*Gymnodinium breve*). *J. Am. Chem. Soc.*, 103, 6773-6775. (1981)
- Martin DF, Martin BB. Red tide terror: effects of red tide and related toxins. *J Chem Ed.*, 53:614-7. (1976)
- Mbourou, G.N., J.J. Bertrand and S.E. Nicholson, The diurnal and seasonal cycles of wind-borne dust over Africa north of the Equator. *J. Appl. Meteor.* 36: 265-273. (1997)
- Murate, K., Sataki, M., Naoki, H., Kaspar, A., Oshima, Y., Yasumoto, T., Isolation and structure of a new brevetoxin analog, brevetoxin B<sub>2</sub>, from greenshell mussels in New Zealand. *Tetrahedron*, 54, 735-742. (1998)
- Naar, J., Branaa, P., M-Y. Bottein-Déchraoui, Chinain, M., Legrand, A.-M., S. Pauillac 1, Polyclonal and monoclonal antibodies to PbTx-2-type brevetoxins using minute amount of hapten<sup>-</sup> protein conjugates obtained in a reversed micellar medium. *Toxicon*, 39, 6. 869-878. (2001)
- O'Shea, T. J., An epizootic of Florida manatees associated with a dinoflagellate bloom. *Marine Mammal Sci.*, 7, 2. 165-179. (1991)
- Perry, K.D., T.A. Cahill, R.A. Eldred and D.D. Dutcher. Long-range transport of North Atlantic dust to the eastern United States. *J. Geophys. Res.* 102D: 11,225-11,238 (1997)
- Pierce, R.H., M.S. Henry, L.S. Proffitt and P.A. Hasbrouck. Red tide toxin (brevetoxin) enrichment in marine aerosol. *Toxic Marine Phytoplankton*. (E. Graneli, S. Sundström, L. Elder and D.M. Anderson, eds.) pp. 397-402. (1990)
- Plakas, S., Said, K., Jester E., Grande H., Musser S., Dickey R., Confirmation of Brevetoxin metabolism in the Eastern Oyster (*Crassostrea virginica*) by controlled exposures to pure toxins and to *Karenia brevis* cultures. *Toxicon*, 1686. (2001)
- Pierce, R. H., Henry, M.S., Proffitt, L.S., and Hasbrouck, P.A., Red tide toxin (brevetoxin) enrichment in marine aerosol.: S. S. ( E. Graneli, L. Elder and D.M. Anderson, eds.), Ed., *Toxic Marine Phytoplankton*. (1990).
- Pierce, R. H., Henry, M., Boggess, S. and Rule, A., Marine toxins in bubble-generated aerosol.: e. E. Monahan and P. van Patton, Ed., In: *The Climate and Health Implications of Bubble-Mediated Sea-Air Exchange* (Connecticut Sea Grant Publications:, 1989)
- Plumely, F. G., Marine Algal Toxins: Biochemistry, Genetics and Molecular Biology. *Limnology and Oceanography*, 42, 5. 1252-1264. (1997)
- Poli, M. A., Mende, T. J., Baden, D. G., Brevetoxins, unique activators of voltage-sensitive sodium channels, bind to specific sites in rat brain synaptosomes. *Mol Pharmacol*, 30, 2. 129-35. (1986)

- Poli, M. A., Templeton, C. B., Thompson, W. L., Hewetson, J. F., Distribution and elimination of brevetoxin PbTx-3 in rats. *Toxicon*, 28, 8. 903-10. (1990)
- Poli, M. A., Rein, K. S., Baden, D. G., Radioimmunoassay for PbTx-2-type brevetoxins: epitope specificity of two anti-PbTx sera. *J AOAC Int*, 78, 2. 538-42. (1995)
- Poli, M. A., Musser, S. M., Dickey, R. W., Eilers, P. P., Hall, S., Neurotoxic shellfish poisoning and brevetoxin metabolites: a case study from Florida. *Toxicon*, 38, 7. 981-93. (2000)
- Prospero, J.M. and R.T. Nees, 1986. Impact of the North African drought and El Niño on mineral dust in the Barbados trade winds. *Nature* 320: 735-738. (2001)
- Purkerson-Parker, S. L., Fieber, L. A., Rein, K. S., Podona, T., Baden, D. G., Brevetoxin derivatives that inhibit toxin activity. *Chem Biol*, 7, 6. 385-93. (2000)
- Rein, KS, DG Baden, RE Gawley. Conformational analysis of the sodium channel modulator, brevetoxin A, comparison with brevetoxin B conformations, and a hypothesis about the common pharmacophore of the "site 5" toxins. *J Org Chem* 59: 2101-2106, (1994)
- Rein, K. a. B., J., Polyketides from dinoflagellates: origins, pharmacology and biosynthesis. *Comparative Biochemistry and Physiology Part B: Biochemistry and Molecular Biology*, Vol. 124, 2. 117-131. (1999)
- Rodgers, R. L., Chou, H. N., Temma, K., Akera, T., Shimizu, Y., Positive inotropic and toxic effects of brevetoxin-B on rat and guinea pig heart. *Toxicol. Appl. Pharmacol.*, 76, 2. 296-305. (1984)
- Roszell, L. E., Schulman, L. S., Baden, D. G., Toxin profiles are dependent on stages in cultured *Ptychodiscus brevis*.: E. G. e. al, Ed., In: *Toxic Marine Phytoplankton* (Elsevier, New York, 1989).
- Rumbold, D., Snedaker, S., Sea-surface microlayer toxicity off the Florida Keys. *Marine Environmental Research*, 47, 5. 457-472. (1999)
- Sagir, A., Arakawa, O., Onoue, Y.,, Toxicity of cultured *Chatonella marina*.: G. A. P. Lassus, E. Erhard, P. Gentien, and C. Marcaillou, eds., Ed., In: *Harmful Marine Algal Blooms*. (Paris: Lavoisier, 1995)
- Schreibmayer, W., Jeglitsch, G. A., The sodium channel activator brevetoxin-3 uncovers a multiplicity of defferent open states of the cardiac sodium channel. *Biochem. & Biophys. Acta*, 1104, 223-242. (1992)
- Shanley, E., Vargo, G. A., Cellular composition, growth, photosynthesis, and respiration rates of *Gymnodinium breve* under varying light levels.: T. J. Smayda, Shimizu, Y., (Eds.), Eds., In: *Toxic Phytoplankton Blooms in the Sea*. (Elsevier, Amsterdam,, 1993).
- Sherman, B. H., Marine ecosystem health as an expression of morbidity, mortality and disease events. *Marine Pollution Bulletin*, 41, Nos. 1-6. pp. 232-254. (2000)



- Shimizu, Y., Wrensford, G., Peculiarities in the biosynthesis of brevetoxins and metabolism of *Gymnodinium breve*: T. J. Smayda, Shimizu, Y. (Eds.), Ed., In: Toxic Phytoplankton Blooms in the Sea. (Elsevier, Amsterdam, 1993)
- Singh, J., Gupta, S., Gupta, A., Dube, S., Deshpande, S., Relative potency of synthetic analogs of *Ptychodiscus brevis* toxin in depressing synaptic transmission evoked in neonatal rat spinal cord in vitro. *Toxicology Letters*, 000, Uncorrected proof at time of citing. (2002)
- Shumway, S. E. A review of the effects of algal blooms on shellfish and aquaculture. *Journal of the World Aquaculture Society* 21, no. 2: 65-104 (1990)
- Singer, L. J., Lee T., Rosen, K.A., Baden, D.G. and Abraham, W.M., Inhaled Florida red tide toxins induce bronchioconstriction (BC) and airway hyperresponsiveness (AHR) in sheep. *Am. J. Respir. Crit. Care Med.*, 157, 3. (1998)
- Smayda, T., Novel and nuisance phytoplankton blooms in the sea: Evidence for a global epidemic. In: Toxic Marine Phytoplankton, Graneli, E., Sundstrom, B., Edler, L. and Anderson, D.M. (Eds.), Elsevier, New York. p 29-40. (1990)
- Smayda, T., Y. Shimizu, e., Toxic phytoplankton blooms in the sea.: , *Dev. Mar. Biol.*, (1993), vol. 3.
- Smith, R. C., Baker, K. S., Penetration of UV-B and biologically effective dose-rates in natural waters. *Photochemistry and Photobiology*, 29. 311-323. (1979)
- Steidinger, K.A., Joyce E.A., Florida Red Tides. Florida Department of Nat. Resources, Marine Research Laboratory Edu. Ser. 17 (1973)
- Steidinger, K.A, Haddad, K., Biological and Hydrographic Aspects of Red Tides. *Bioscience*. Vol. 31, pp 814-819 (1989)
- Steidinger, K. A., Vargo, G. A., Tester, P. A., Tomas, C. R., In: Bloom dynamics and physiology of *Gymnodinium breve* with emphasis on the Gulf of Mexico.: D. M. Anderson, A. D. Cembella, Hallegrae., G.M. (Eds.), Eds., *Physiological Ecology of Harmful Algal Blooms*. (Springer, Berlin, 1998).
- Steidinger, K. A., Tomas, C. R., Harmful microalgae and associated public health risks in the Gulf of Mexico.: K. A. a. P. Steidinger, H.L.M, Ed., United States Environmental Protection Agency Gulf of Mexico Program (Publication by: Florida Marine Research Institute Department of Environmental Protection, St. Petersburg, Florida, 1999)
- Templeton, C. B., Poli, M. A., LeClaire, R. D., Cardiorespiratory effects of brevetoxin (PbTx-2) in conscious, tethered rats. *Toxicon*, 27, 9. 1043-9. (1989)
- Templeton, C. B., Poli, M. A., Solow, R., Prophylactic and therapeutic use of an anti-brevetoxin (PbTx-2) antibody in conscious rats. *Toxicon*, 27, 12. 1389-95. (1989)
- Tester, P. A., Steidinger, K. A., *Gymnodinium breve* red tide blooms: Initiation, transport and consequences of surface circulation. *Limnology and Oceanography*, 42, 5. 1039-1051. (1997)

- Tester, P. A., Stumpf, R.P., Vukovich, F.M., Folwer, P.K., Turner, J.T. , An expatriate red tide bloom: Transport, distribution, and persistence. *Limnology and Oceanography* [LIMNOL. OCEANOGR.], 36, 5. 1053-1061. (1991)
- Trainer, V. L., Moreau, E., Guedin, D., Baden, D. G., Catterall, W. A., Neurotoxin binding and allosteric modulation at receptor sites 2 and 5 on purified and reconstituted rat brain sodium channels. *J Biol Chem*, 268, 23. 17114-9. (1993)
- Trainer, V. L., Baden, D. G., Catterall, W. A., Identification of peptide components of the brevetoxin receptor site of rat brain sodium channels. *J Biol Chem*, 269, 31. 19904-9. (1994)
- Usup, G., R.V., A., In: *Physiological Ecology of Harmful Algal Blooms*: D. M. Anderson, A. D. Cembella, G. M. Hallegraph, Eds., vol. G41 (Springer, Berlin, 1998)
- Van Dolah, F. M., Leighfield, T. A., Haynes, B. L., Hampson, D. R., Ramsdell, J. S., A microplate receptor assay for the amnesic shellfish poisoning toxin, domoic acid, utilizing a cloned glutamate receptor. *Analytical Biochemistry*, 245, 102-105. (1997)
- Vargo, G. A., Heil, C.A., Walsh, J.J., Fanning, K. , Tomas, C.R., Steidinger, K.A., Ault, D., Neely, B.M., Lester, K., and Merkt, R., Hydrography and nutrient characteristics within the ECOHAB: Florida control volume on the west Florida shelf;, *Symposium on Harmful Marine Algae in the U.S.*, Woods Hole, Mass. (2000).
- Viviani, R. Eutrophication, marine biotoxins, and human health. *Sci Total Environ*, 631-62 (1992)
- Walsh, J., Haddad KD, Dieterlea DA, Weisberga RH, ZhenjiangLi a, Huijun Yanga, et al., A numerical analysis of landfall of the 1979 red tide of *Karenia brevis* along the west coast of Florida. *Continental Shelf Research*, 22, 15-38. (2002)
- Welker, M., Steinberg, C., Indirect photolysis of cyanotoxins: one possible mechanism for their low persistence. *Wat. Res.*, Vol. 33, No. 5. pp. 1159-1164. (1999)
- Wilson, B., Arnold, H., Bearzi, G., C. Fortuna, M. , Gaspar, R. , Ingram, S. , Liret, C., Pribani, S. , Read, A. J. , Ridoux, V. , Schneider, K. , Urian, K. W. , Wells, R. S., Wood, C. , Thompson, P. M. , Hammond, P. S., Epidermal diseases in bottlenose dolphins: impacts of natural and anthropogenic factors. *Proc. R. Soc. Lond. B*, 266, Accepted 5 February 1999. 1077-1083. (1999)
- Whitney, P. L., Baden, D. G., Recoveries of PbTx2 type brevetoxins added to homogenates of clam tissue. In Review, (2001)
- Zepp, R. G., P. Schlotzhauer, a., Sink., M. R., Photosensitized transformations involving electronic energy transfer in natural waters: Role of humic substances. *Environ. Sci. Technol.*, 19, 74-81. (1985)
- Zingone, A., Enevoldsen, H. O., The diversity of harmful algal blooms: a challenge for science and management. *Ocean & Coastal Management*, 43, 725-748. (2000)

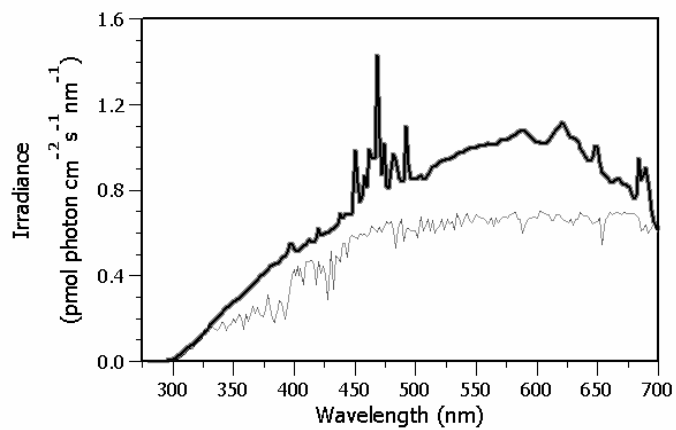


Correlations								
Peak ID	BP 11		BP 8		BP 6		BP 5	BP 4
HPLC-MS ion	894	926	894	926	894	912	912	884
Correlates to Proposed Structures	S5H14	S10	"	"	"	S2	"	S9H11
		S2H14				H12		S5H11A15
		S3H13				S3H11		S1H11A15
		S3Hepoxide				S11H11		S4H11A15
		S11H13				S4H13		S7H11A15
		S11Hepoxide				S7H13		S9H13A16
		S3H14A15				S1Hepoxide		S9HepoxideA16
		S10H14A16				S4Hepoxide		S4H11A18
		S1H14A17				S7Hepoxide		S7H11A18
		S4H14A17				S6H14		S5H12A18
		S7H14A17				S8H14		S9H13A18
		S10H14A16				S1H14A15		S9HepoxideA18
		S3H14A19				S4H14A15		S5H11A19
		S11H14A19				S7H14A15		
						S3H13A16		
						S11H13A16		
						S3HepoxideA16		
						S11HepoxideA16		
						S2H14A16		
						S5H13A17		
					S5HepoxideA17			
					S9H14A17			
					S3H13A16A18			
					S3HepoxideA18			
					S11H13A18			
					S11HepoxideA18			
					S1H14A15A18			
					S2H14A18			
					S1H14A20			

\*57 Total Correlates

## Appendix 2: Correlation of Proposed Structures to HPLC-MS Molecular Ions

Listed are the HPLC-MS molecular ion masses for each peak and the proposed structural modifications which correlate to the mass of the ions. Referencing Figure 13 will give the structures listed. (e.g. S2H14A16 indicates K-ring side chain 2, H-ring 14 and A-ring 16 modifications, combined).



### Appendix 3: solar simulator spectral irradiance

A comparison of the spectral irradiance of the solar simulator AM1 filtered (black line) with noon time clear sky irradiance 47°N (gray line) is shown below. Integrated irradiance of the solar simulator is  $\sim 1.5$  x noon time sun.

<b>COMPARATIVE TOXICITY OF NATURAL TOXINS</b>	
<b>Toxin</b>	<b>* Lethal Dose (moles/kg)</b>
Botulism Toxin (Botulinum A)	$10^{-16}$
Brevetoxin (BTX-B)	$10^{-9 \text{ to } -12}$
Currarae (d-Tubocurarine)	$10^{-7}$

\*Subcutaneous Injection (Baden,1983)

Appendix 4: Relative Toxicity of Brevetoxins